NASA-DoD LEAD-FREE ELECTRONICS PROJECT: JOINT TEST REPORT

Kurt Kessel
ITB, Inc.
NASA Technology Evaluation for Environmental Risk Mitigation (TEERM) Principal Center
Kennedy Space Center, FL, USA
kurt.r.kessel@nasa.gov
{On behalf of the NASA-DoD Lead-Free Electronics Project Consortium}

ABSTRACT
The use of conventional tin-lead (SnPb) in circuit board manufacturing is under ever-increasing political scrutiny due to increasing regulations concerning lead. The "Restriction of Hazardous Substances" (RoHS) directive enacted by the European Union (EU) and a pact between the United States National Electronics Manufacturing Initiative (NEMI), Europe's Soldertec at Tin Technology Ltd. and the Japan Electronics and Information Technology Industries Association (JEITA) are just two examples where worldwide legislative actions and partnerships/agreements are affecting the electronics industry. As a result, many global commercial-grade electronic component suppliers are initiating efforts to transition to lead-free (Pb-free) in order to retain their worldwide market. Pb-free components are likely to find their way into the inventory of aerospace or military assembly processes under current government acquisition reform initiatives. Inventories "contaminated" by Pb-free will result in increased risks associated with the manufacturing, product reliability, and subsequent repair of aerospace and military electronic systems. Although electronics for military and aerospace applications are not included in the RoHS legislation, engineers are beginning to find that the commercial industry's move towards RoHS compliance has affected their supply chain and changed their parts. Most parts suppliers plan to phase out their non-compliant, leaded production and many have already done so. As a result, the ability to find leaded components is getting harder and harder. Some buyers are now attempting to acquire the remaining SnPb inventory, if it's not already obsolete. The introduction of components with lead-free terminations, termination finishes, or circuit boards presents a host of concerns to customers, suppliers, and maintainers of aerospace and military electronic systems such as:

1. Electrical shorting due to tin whiskers
2. Incompatibility of lead-free processes and parameters (including higher melting points of lead-free alloys) with other materials in the system
3. Unknown material properties and incompatibilities that could reduce solder joint reliability

As the transition to lead-free becomes a certain reality for military and aerospace applications, it will be critical to fully understand the implications of reworking lead-free assemblies.

Key words: lead-free, rework, reliability, harsh environments testing, aerospace

BACKGROUND
This project is a follow-on effort to the Joint Council on Aging Aircraft/Joint Group on Pollution Prevention (JCAA/JG-PP) Pb-free Solder Project which was the first group to test the reliability of Pb-free solder joints against the requirements of the aerospace and military community. The NASA-DoD Lead-Free Electronics Project builds on the results from the JCAA/JG-PP Lead-Free Solder Project while increasing scope to include the rework of SnPb and lead-free solder alloys and includes the mixing of SnPb and lead-free solder alloys. The majority of testing being conducted for this effort will mirror the testing completed for JCAA/JGPP LFS Project. Some changes were made in order to optimize the usefulness of the data.

OBJECTIVE
In response to concerns about risks from lead-free induced faults to high reliability products, the NASA-DoD Lead-Free Electronics Project Consortium outlined a multi-year project to provide manufacturers and users with data to clarify the risks of lead-free materials in their products. The project also provides useful data to component manufacturers supplying to high reliability markets. The project was launched in November 2006. The primary technical objective of the project is to undertake comprehensive testing to generate data on failure modes / criteria to better understand the reliability of packages (e.g., thin small outline package, ball grid array, plastic (dual inline package), chip scale package, quad flat pack (no leads) assembled and reworked with lead-free alloys and with mixed (lead/lead-free) alloys).

The intended goal of this project is to:

1. Determine the reliability of reworked solder joints in high-reliably military and aerospace electronics assemblies.

2. Assess the process parameters for reworking high-reliability lead-free military and aerospace electronics assemblies.

3. Develop baseline recommendations for process guidelines and a risk assessment for assembling high-reliability lead-free military and aerospace electronics assemblies.

PROCEDURES

Joint Test Report

The Joint Test Report (JTR) summarizes all activities associated with the NASA-DoD Lead-Free Electronics Project, focusing on the test results, data analysis and failure analysis activities. The JTR is constructed of excerpts from NASA-DoD Lead-Free Electronics Project documents that are available in their entirety on the NASA Technology Evaluation for Environmental Risk Mitigation (TEERM) website [1].

The following harsh environments tests are covered in the JTR:

1. Vibration Test
   a. NASA-DoD Test Vehicles (Boeing; Seattle, Washington)
   b. NSWC Crane Test Vehicles (Celestica; Toronto, Ontario, Canada)
2. Mechanical Shock Test (Boeing; Seattle, Washington)
3. Combined Environments Test (Raytheon; McKinney, Texas)
4. Thermal Cycle Test
   a. -55 to +125°C (Rockwell Collins; Cedar Rapids, Iowa)
   b. -20 to +80°C (Boeing; Seattle, Washington)
5. Drop Test (Celestica; Toronto, Ontario, Canada)

FUTURE WORK

Thermal cycle testing (-20 to +80°C) was on going at the time this paper was drafted. It is unknown when the -20 to +80°C testing will be complete.

ACKNOWLEDGEMENTS

The author would like to thank Lety Campuzano-Contreras of BAE Systems; Dr. Tom Woodrow of Boeing; Dave Hillman of Rockwell Collins; Cynthia Garcia and Jeff Bradford of Raytheon; Dr. Polina Snugovsky, Jason Bragg, and Jeff Kennedy of Celestica; Linda Woody and Ed Morris of Lockheed Martin; Paul Reid and Bill Birch of PWB Interconnect Solutions Inc; Jim Blanche of Jacobs Engineering; Vance Anderson of Defense Microelectronics Activity; Andy Ganster and Gary Latta of Crane Division, Naval Surface Warfare Center, and David Amidei and Chuck Griffin of NASA.

The author would also like to acknowledge the other members of the NASA-DoD Lead-Free Electronics Consortium not mentioned by name. This effort would not be possible without their contributions.

REFERENCES

[1] NASA Technology Evaluation for Environmental Risk Mitigation (TEERM) Principal Center website; http://teerm.nasa.gov

National Aeronautics and Space Administration

Technology Evaluation for Environmental Risk Mitigation Principal Center

NASA-DoD Lead-Free Electronics Project

DRAFT Joint Test Report

July 2011

NASA-DoD Lead-Free Electronics Project – Joint Test Report

This document is intended to summarize the test data generated from the NASA-DoD Lead-Free Electronics Project.

This document is disseminated under the sponsorship of the National Aeronautics and Space Administration (NASA) in the interest of information exchange. The United States Government assumes no liability for its contents or use thereof.

This report does not constitute a standard, specification, or regulation. The United States Government does not endorse products or manufacturers. Trade or manufacturers' names appear herein only because they are considered essential to the object of this document. The report may not be used for advertising or product endorsement purposes.

Table of Contents

1 Introduction 1
2 Test Vehicle 2
2.1 Test Vehicle Design 2
2.2 Board Material 2
2.3 Board Finish 2
2.4 Solder Alloys 3
2.4.1 SAC305 3
2.4.2 SN100C 3
2.5 Flux 4
2.6 Components 5
2.6.1 Component Characterization 5
3 Assembly 7
3.1 NSWC Crane Assembly and Rework Effort 7
4 Test Methods 8
5 Test Results 10
5.1 Vibration Test 10
5.1.1 Vibration Test Method 10
5.1.2 NASA-DoD Test Vehicle Vibration Testing Results Summary 13
5.1.3 NSWC Crane Test Vehicle Vibration Testing Results Summary 17
5.2 Mechanical Shock Test 28
5.2.1 Mechanical Shock Test Method 28
5.2.2 Mechanical Shock Testing Results Summary 30
5.3 Combined Environments Test 49
5.3.1 Combined Environments Test Method 49
5.3.2 Combined Environments Test Results Summary 50
5.3.3 Combined Environments Failure Analysis 57
5.3.4 Combined Environments Test Summary Tables 95
5.4 Thermal Cycle -55°C to +125°C Test 97
5.4.1 Thermal Cycle -55°C to +125°C Test Method 97
5.4.2 Thermal Cycle -55°C to +125°C Testing Results Summary (3600 cycles) 97
5.5 Thermal Cycle -20°C to +80°C Test 110
5.5.1 Thermal Cycle -20°C to +80°C Test Method 110
5.5.2 Thermal Cycle -20°C to +80°C Testing Results Summary 110
5.6 Drop Testing 111
5.6.1 Drop Test Method 111
5.6.2 NASA-DoD Test Vehicle Drop Testing Results Summary 112
5.6.3 NASA-DoD Test Vehicle Drop Test Failure Analysis 113
5.6.4 NSWC Crane Test Vehicle Drop Testing Results Summary 117
5.6.5 NSWC Crane Test Vehicle Drop Test Failure Analysis 118
6 Summary Tables 121
7 Conclusions 121
7.1 Assembly Conclusions 121
7.2 Reliability Conclusions 121

7.3 PDIP Discussion 121
8 Recommendations 121

Tables

Table 1 - Solder Alloys and Associated Flux 4
Table 2 - Components Table 5
Table 3 - Test Vehicle Performance Requirements 9
Table 4 - Vibration Profile 12
Table 5 - Percentage of Components Failed (Includes Mixed Solders) 13
Table 6 - Ranking of Solder Alloy/Component Finish Combinations 16
Table 7 - Component Percentage Failure by Force Level 17
Table 8 - Component Detachments 17
Table 9 - Mechanical Shock Test Methodology – Test Procedure 30
Table 10 - Mechanical Shock Testing; Relative Ranking (Solder/Component Finish) 32
Table 11 - Combined Environments Test Methodology 49
Table 12 - Number of Failed Components by Board Finish, Component, Component Finish and Solder Alloy on Manufactured Test Vehicles 52
Table 13 - Number of Failed Components by Board Finish, Component, Component Finish and Solder Alloy on Manufactured Test Vehicles 53
Table 14 - Number of Failed Components by Board Finish, Component, Component Finish, Solder Alloy, New Component Finish and Rework Solder on Rework Test Vehicles 55
Table 15 - Number of Failed Components by Board Finish, Component, Component Finish, Solder Alloy, New Component Finish and Rework Solder on Rework Test Vehicles 57
Table 16 - Components selected for failure analysis based on when a failure was recorded during Combined Environments Testing 58
Table 17 96
Table 18 - Thermal Cycling Test Methodology; -55°C to +125°C 97
Table 19 - Manufactured Test Vehicle Component Population Failure Rates after 3600 Thermal Cycles 98
Table 20 - Reworked Test Vehicle Component Population Failure Rates after 3600 Thermal Cycles 98
Table 21 - Thermal Cycling Test Methodology; -20°C to +80°C 110
Table 22 - NASA-DoD Lead-Free Electronics Test Vehicle Drop Test Methodology 112
Table 23 - NSWC Crane Test Vehicle Drop Test Methodology 112
Table 24 - Components that Celestica Performed Failure Analysis On 114

Figures

Figure 1 - NASA-DoD Lead-Free Electronics Project Test Vehicle 6
Figure 2 - Vibration Spectrum 11
Figure 3 - Test Minutes Required for Components to Fail (Test Vehicle 74 Data) 14
Figure 4 - Full Field Peak Strains at 65 Hz (1G Sine Dwell, Test Vehicle 74) 15
Figure 5 - SN63 U52, Left Side Pad 18
Figure 6 - SN67 U52, Left Side Pad 19
Figure 7 - SN63 U54, Left Side Pad 20
Figure 8 - SN68 U28, Right Side Pad 20
Figure 9 - SN63 U41. Left Lead 21
Figure 10 - SN61 U20 Right Lead 22
Figure 11 - SN67 U31 Left Lead 22
Figure 12 - SN68 U31, Right Lead 23
Figure 13 - SN79 U12, Left Lead 24
Figure 14 - SN66 U62, Right Lead 24
Figure 15 - SN65 U62, Left Lead 25
Figure 16 - SN63 U61, Right Lead 25
Figure 17 - SN63 U16, Left Lead 26
Figure 18 - SN68 U29, Right Lead 27
Figure 19 - Mechanical Shock SRS Test Levels 29
Figure 20 - Test Vehicle 34 - Four Corner Balls of BGA U6 (SnPb Solder/SnPb Balls) 33
Figure 21 - Test Vehicle 89 - Four Corner Balls of BGA U2 (SAC305 Solder/SAC405 Balls).. 34
Figure 22 - Test Vehicle 30 BGA U2 with Missing Pads (SnPb Solder/SnPb Balls) 35
Figure 23 - Test Vehicle 30 BGA U4 with Missing Pads (SnPb Solder/SnPb Balls) 35
Figure 24 - Test Vehicle 193 BGA U21 with Missing Pads (Flux Only/SAC405 Balls) 36
Figure 25 - Test Vehicle 193 BGA U21 with Missing Pads (Flux Only/SAC405 Balls) 37
Figure 26 - Combined Data from CLCC's U13 and U14 38
Figure 27 - Test Vehicle 191 CLCC U10 (Cracked SAC305/SnPb Solder Joint) 38
Figure 28 - X-Ray of a CSP-100 39
Figure 29 - Test Vehicle 34 – CSP U33 40
Figure 30 - Test Vehicle 89 – CSP U33 40
Figure 31 - Test Vehicle 34 – PDIPs U8 and U49 (a) Corner Lead, (b) Lead Adjacent to 41
Figure 32 - Test Vehicle 89 – PDIPs U8 and U49 (a) Corner Lead, (b) Lead Adjacent to 42
Figure 33 - Test Vehicle 89 PDIP U30 (Cracked Trace, SN100C) 43
Figure 34 - Test Vehicle 89 PDIP U38 (Cracked Trace, SN100C) 43
Figure 35 - Test Vehicle 89 PDIP U51 (SN100C) 44
Figure 36 - Test Vehicle 89 TQFP U3 (Cracked Leads, Missing Lead) 45
Figure 37 - Combined Data from TQFP's U20 and U58 46
Figure 38 - TSOP U25 Data 47
Figure 39 - TSOP U24 Data 47
Figure 40 - Test Vehicle 34 TSOP U61 (Cracked SnPb/SnPb Solder Joint) 48
Figure 41 - TV21 U34; Optical Micrograph, Insufficient Solder Observed 59
Figure 42 - TV21 U57; Optical Micrograph, Residue between Leads 59
Figure 43 - TV21 U57; Optical Micrograph, Residue between Leads 60
Figure 44 - TV21 U57; Optical Micrograph, Component Lead 1 60

Figure 45 - TV23 U30; Optical Micrograph, PDIP-20 61
Figure 46 - TV23 U30; Cross-Sectional Micrographs of PDIP-20 Leads 62
Figure 47 - TV23 U30; Micrographs, Lead 9 of PDIP-20 63
Figure 48 - TV23 U43; FA Results, BGA-225, Location U43 64
Figure 49 - TV23 U43; Cross-Sectional Micrographs 64
Figure 50 - TV23 U43; Cross-Sectional Micrographs 65
Figure 51 - TV23 U43; SEM Mapping 66
Figure 52 - TV23 U43; Cross-Sectional Micrographs Show Warping 67
Figure 53 - TV72 U29; Visual Inspection Showing Cracked Solder Joints 67
Figure 54 - TV72 U29; Cross-Section Micrographs Showing Open Solder Joints 68
Figure 55 - TV72 U29; SEM Mapping, Pb was Found Around Upper Part of the Both Leads ... 69
Figure 56 - TV117 U4; Orientation of the Corner Solder Balls 69
Figure 57 - TV117 U4; Cross-Sectional Micrographs of Corner Solder Balls 70
Figure 58 - TV117 U4; Diagram Showing Progression of Cracking in Component 70
Figure 59 - TV119 U36; X-Ray Image, CSP-100 71
Figure 60 - TV119 U36; X-Ray Image for Reference of the Cross-Section Analysis 71
Figure 61 - TV119 U36; Cross-Sectional Micrographs of Solder Balls A1, A2, A9 and A10 72
Figure 62 - TV119 U39; Optical Micrograph at 49X Magnification 73
Figure 63 - TV119 U39; SEM Image of Leads 19-25 at 22X Magnification 73
Figure 64 - TV119 U39; SEM Image, Lead 25 74
Figure 65 - TV119 U39; Cross-Sectional Micrograph, Lead 1 74
Figure 66 - TV119 U39; Cross-Sectional Micrograph, Lead 50 75
Figure 67 - TV140 U11; Optical Micrograph 75
Figure 68 - TV140 U11; Cross-Sectional Micrographs, Suspect PDIP-20 Lead 76
Figure 69 - TV142 U13; Optical Micrograph, CLCC Package Lead 76
Figure 70 - TV142 U13 Optical Micrographs of CLCC-20 Leads at 24X Magnification 77
Figure 71 - TV142 U13 X-Ray Inspection of CLCC-20 Component. 77
Figure 72 - TV142 U13 SEM Images of Component at 25X Magnification 77
Figure 73 - TV142 U13 SEM Images of Selected Leads at 55X Magnification. 78
Figure 74 - TV142 U13; CLCC-20 Component 78
Figure 75 - TV142 U13; Cross-Sectional Micrographs of Lead 1 and Lead 5 79
Figure 76 - TV142 U13; Cross-Sectional Micrograph 79
Figure 77 - TV142 U13; SEM Image 80
Figure 78 - TV158 U6; FA Results 80
Figure 79 - TV158 U6; Cross-Sectional Micrographs 81
Figure 80 - TV158 U6; Cross-Sectional Micrographs 82
Figure 81 - TV158 U6; Cross-Sectional Micrographs 83
Figure 82 - TV158 U6; SEM Mapping 84
Figure 83 - TV158 U6; SEM Mapping 85
Figure 84 - TV158 U6; Cross-Sectional Micrographs Show Warping on BGA-225 85
Figure 85 - TV180 U21; FA Results 86
Figure 86 - TV180 U21; Cross-Sectional Micrographs 87
Figure 87 - TV180 U21; Cross-Sectional Micrographs 88
Figure 88 - TV180 U21; SEM Mapping 89
Figure 89 - X-Ray Inspection of TV181 U56 BGA-225 89
Figure 90 - TV181 U56; X-Ray Image Showing the Grinding Levels 90
Figure 91 - TV181 U56; Cross-Sectional Micrographs of Via Hole Connected to Ball A1 90

Figure 92 - TV181 U56; Cross-Sectional Micrographs of Solder Balls 91
Figure 93 - TV181 U56; SEM Image of Solder Ball A9 Cross-Section 91
Figure 94 - TV181 U25; Optical Micrographs 92
Figure 95 - TV181 U25; X-Ray Images of Component Leads 92
Figure 96 - TV181 U25; SEM Images 93
Figure 97 - TV181 U25; Optical Micrographs 93
Figure 98 - TV181 U25; Cross-Sectional Micrographs 93
Figure 99 - TV181 U25; SEM Image 94
Figure 100 - TV183 U 41; Optical Micrographs of Suspect Lead 94
Figure 101 - TV183 U 41; Cross-Sectional Micrographs 95
Figure 102 - CLCC-20 Weibull Plot 99
Figure 103 - QFN-20 Weibull Plot 100
Figure 104 - TQFP-144 Weibull Plot 101
Figure 105 - PBGA-225 Weibull Plot 102
Figure 106 - Reworked PBGA-225 Weibull Plot 103
Figure 107 - CSP-100 Weibull Plot 104
Figure 108 - Reworked CSP-100 Weibull Plot 105
Figure 109 - TSOP-50 Weibull Plot 106
Figure 110 - Reworked TSOP-50 Weibull Plot 107
Figure 111 - PDIP-20 Weibull Plot 108
Figure 112 - Reworked PDIP-20 Weibull Plot 109
Figure 113 - Interconnect Fracture Modes (Solder Ball Array Device) IPC 9702 111
Figure 114 - Typical Pad Cratering seen on BGA225 after Dye-and-Pry 115
Figure 115 - Typical Pad Cratering seen on BGA225 after cross-section 115
Figure 116 - SEM of Brittle Intermetallic Failure on BGA225 116
Figure 117 – Mechanical Failure Mapping 117
Figure 118 - Pad Cratering seen on CLCC-20 119
Figure 119 - Dye and Pry of a QFN-20 showing dye penetration through the bulk solder 119
Figure 120 – Fatigue Failure of TQFP-144 with 1x Rework as seen through cross sectioning . 120

1 Introduction

The use of conventional tin-lead (SnPb) in circuit board manufacturing is under ever-increasing political scrutiny due to increasing regulations concerning lead. The "Restriction of Hazardous Substances" (RoHS) directive enacted by the European Union (EU) and a pact between the United States National Electronics Manufacturing Initiative (NEMI), Europe's Soldertec at Tin Technology Ltd. and the Japan Electronics and Information Technology Industries Association (JEITA) are just two examples where worldwide legislative actions and partnerships/agreements are affecting the electronics industry. As a result, many global commercial-grade electronic component suppliers are initiating efforts to transition to lead-free (Pb-free) in order to retain their worldwide market. Pb-free components are likely to find their way into the inventory of aerospace or military assembly processes under current government acquisition reform initiatives. Inventories "contaminated" by Pb-free will result in increased risks associated with the manufacturing, product reliability, and subsequent repair of aerospace and military electronic systems.

Although electronics for military and aerospace applications are not included in the RoHS legislation, engineers are beginning to find that the commercial industry's move towards RoHS compliance has affected their supply chain and changed their parts. Most parts suppliers plan to phase out their non-compliant, leaded production and many have already done so. As a result, the ability to find leaded components is getting harder and harder. Some buyers are now attempting to acquire the remaining SnPb inventory, if it's not already obsolete.

Original Equipment Manufacturers (OEMs), depots, and support contractors have to be prepared to deal with an electronics supply chain that increasingly provides more and more parts with Pb-free finishes—some labeled no differently than their Pb counterparts—while at the same time providing the traditional Pb parts. The longer the transition period, the greater the likelihood of Pb-free parts inadvertently being mixed with Pb parts and ending up on what are supposed to be Pb systems. As a result, OEMs, depots, and support contractors need to take action now to either abate the influx of Pb-free parts, or accept it and deal with the likely interim consequences of reduced reliability due to a wide variety of matters, such as Pb contamination, high temperature incompatibility, and tin whiskering.

Allowance of Pb-free components produces one of the greatest risks to the reliability of a weapon system. This is due to new and poorly understood failure mechanisms, as well as unknown long-term reliability. If the decision is made to consciously allow Pb-free solder and component finishes into SnPb electronics, additional effort (and cost) will be required to make the significant number of changes to drawings and task order procedures.

This project is a follow-on effort to the Joint Council on Aging Aircraft/Joint Group on Pollution Prevention (JCAA/JG-PP) Pb-free Solder Project which was the first group to test the reliability of Pb-free solder joints against the requirements of the aerospace and military community.

2 Test Vehicle

2.1 Test Vehicle Design

The test vehicle for this project is a printed wiring assembly (PWA), designed to evaluate solder joint reliability.

Test vehicle size is 14.5 X 9 X 0.09 inches with six 0.5-ounce copper layers. The design incorporates components representative of the parts used for military and aerospace systems and was designed to reveal relative differences in solder alloy performance.

The test vehicle includes a variety of plated-through hole (PTH) and surface mount technology (SMT) components. All components are "dummy" devices with pins internally daisy-chained and contain simulated die. The circuit board was designed with daisy-chained pads that are complementary to the components. Therefore, the solder joints on each component are part of a continuous electrical pathway that was monitored during testing by an event detector (Anatech or equivalent). Failure of a solder joint on a component breaks the continuous pathway and is recorded as an event. Each component has its own distinct pathway (channel).

2.2 Board Material

Project stakeholders selected FR4 per IPC-4101/26 (Specification for Base Materials for Rigid and Multilayer Printed Boards) with a minimum glass transition ($T_{g)}$ of 170ºC for the test vehicles. Test vehicle raw boards comply with IPC-6012 (Qualification and Performance Specification for Rigid Printed Boards), Class 3, Type 3. Pho-Tronics supplied the circuit cards and used Isola 370HR laminate.

2.3 Board Finish

Project stakeholders and participants selected immersion silver (.2 - .4 microns; MacDermid Sterling) as the surface finish for the majority of the test vehicles. The consensus of the project team was that immersion silver has the best balance of desirable properties: good wetting by solders, good solder joint reliability, good long-term solderability upon storage, and retention of solderability after multiple reflow cycles. In addition, several major electronic manufacturing companies are currently using immersion silver in production.

A limited number of test vehicles were assembled using an Electroless Nickel Immersion Gold (ENIG) surface finish (Uyemura Kat 450 ENIG). The project stakeholders felt that ENIG would be a good secondary surface finish since it provides good planarity and solderability which can withstand multiple reflows. ENIG has also been shown to perform well with regards to: substrate shelf-life, corrosion resistance, assembly process window, thermal resistance over several temperature excursions, and good reworkability.

2.4 Solder Alloys

Selection criteria of prime importance included commercial availability, industry trends, and past reliability testing performance. Eutectic 63Sn37Pb (SnPb) alloy was used as the control for all testing.

2.4.1 SAC305[1]

SnAgCu solder alloys are believed to be the leading choice of the commercial electronics industry for Pb-free solder. The Sn3.0Ag0.5Cu is recommended by industry and research consortia as a prime candidate for replacing SnPb solder. Sn3.0Ag0.5Cu is commercially available and currently used in electronic applications. It has been determined that alloys with compositions within the range of Sn3.0-4.0Ag0.5-1.0Cu all have a liquidus temperature around 217°C and have similar microstructures and mechanical properties.

This alloy was chosen for reflow soldering because this particular solder alloy has shown the most promise as a primary replacement for SnPb solder. The team decided that they wanted to select at least one "general purpose" alloy to be evaluated and it was determined that the SnAgCu solder alloy would best serve this purpose. Conclusions drawn from literature suggest that this alloy has good mechanical properties and may be as reliable as SnPb in some applications. BAE Systems reviewed several SAC305 solder alloys for printing, reflow, and cleaning characteristics before choosing EnviroMark™ 907 from Kester.

2.4.2 SN100C[2]

This alloy is commercially available and the general trend in industry has been to switch to the nickel stabilized tin-copper alloy over standard tin-copper due to its superior performance. In addition, this nickel-stabilized alloy does not require special solder pots and has shown no joint failures in specimens with over four (4) years of service. The cost of this alloy in the form of bar solder is relatively low when compared to other Pb-free solder alloys in bar form.

The superior performance of the tin-copper-nickel alloy has been confirmed by university research which has found that the nickel addition works by facilitating solidification of the alloy as a fine uniform eutectic structure and suppressing the growth of primary tin dendrites that are the cause of shrinkage defects in the unmodified alloy. This mode of solidification enhances the fluidity of the alloy close to the melting point, a property that is important in a solder so that it is comparable with that of tin-lead solder at the same superheat. The tin-copper-nickel alloy is representative of a new class of modified tin-copper solders that are increasing in popularity as the limitations of the tin-silver-copper alloys in some applications become apparent. Nihon Superior SN100C will be used for this project.

---

[1] Sn3.0Ag0.5Cu = Tin (Sn); Silver (Ag); Copper (Cu)
[2] Sn-0.7Cu-0.05Ni + Ge = Tin (Sn); Copper (Cu); Nickel (Ni); Germanium (Ge)

2.5 Flux

The flux systems used during soldering were "low residue" or no-clean fluxes and the group chose to clean the test vehicles after processing even though no-clean fluxes were used with some solders. Additionally, reflow was accomplished without nitrogen inerting, which might have created a smaller soldering process window (a credit to the BAE Systems crew for creating a quality test vehicle under such tough process conditions).

Table 1 - Solder Alloys and Associated Flux

Solder Alloy	Flux		
	Reflow Soldering	**Wave Soldering**	**Manual Soldering**
SAC305	ROL1	N/A	ROL0 Tacky Flux
SN100C	ROL0	ORL0	ROL0 Tacky Flux
SnPb baseline	ROL0	ORM0	ROL0 Tacky Flux

- Table provided by BAE Systems Irving, Texas
- During rework, flux was only used for BGA rework
- N/A = Due to limitations on board numbers and components, these solder alloys were not used during the noted assembly processes
- R = Rosin base
- {IPC J-STD-004B; Table 1-1, Flux Identification System}
  - ROL0 = Rosin, Low flux/flux residue activity, < 0.05% halide
  - ROL1 = Rosin, Low flux/flux residue activity, < 0.5% halide
  - ORL0 = Organic, Low flux/flux residue activity, < 0.05% halide
  - ORM0 = Organic, Moderate flux/flux residue activity, < 0.05% halide

2.6 Components

The project stakeholder's agreed to populate the test vehicles with the following components:

Table 2 - Components Table

20LCC-1.27mm-8.90mm-DC-L-Au = **Tinning-SAC305**
20LCC-1.27mm-8.90mm-DC-L-Au = **Tinning-SnPb**
A-MLF20-5mm-.65mm-DC(30467)
A-MLF20-5mm-.65mm-DC-Sn(30801)
A-TQFP144-20mm-.5mm-2.0-DC-Sn(30643)
A-TQFP144-20mm-.5mm-2.0-DC-NiPdAu
A-TQFP144-20mm-.5mm-2.0-DC-Sn(30643) = **Tinning-SAC305**
A-TQFP144-20mm-.5mm-2.0-DC-Sn(30643) =**Tinning-SnPb**
PBGA225-1.5mm-27mm-DC(10565)
PBGA225-1.5mm-27mm-DC-LF(16074)
A-PDIP20T-7.6mm-DC-Sn (30737)
PDIP20T-DC (12006)
PDIP-20 – NiPdAu
A-CABGA100-.8mm-10mm-DC(30102)
A-CABGA100-.8mm-10mm-DC-LF(30695)
A-CABGA100-.8mm-10mm-DC-105
A-TII-TSOP50-10.16x20.95mm-.8mm-DC-TR
A-TII-TSOP50-10.16x20.95mm-.8mm-DC-SnBi-TR
A-TII-TSOP50-10.16x20.95mm-.8mm-DC-Sn-TR

Note – The TSOP-50 components do not have a dummy die. For more information on the decision not to include dummy die, please see "NASA-DoD Lead-Free Electronics Project; Project Plan – December 2009".

2.6.1 Component Characterization

Destructive physical analysis (DPA) was performed on samples from each of the component types that were placed onto the test vehicles. The DPA process was used to ensure that the components used for testing meet the consortia required standards and to evaluate the quality of construction. Results from destructive physical analysis are available on the NASA TEERM website; http://teerm.nasa.gov/NASA_DODLeadFreeElectronics_Proj2.html.

Figure 1 - NASA-DoD Lead-Free Electronics Project Test Vehicle

3 Assembly

One hundred and ninety three (193) test vehicles were assembled by BAE Systems in Irving, Texas. One hundred and twenty (120) of these test vehicles were "Manufactured" PWA's and seventy three (73) were "Rework" PWA's.

Test vehicles were initially assembled per IPC J-STD-001D "Requirements for Soldered Electrical and Electronic Assemblies", end-product Class 3 "High Performance Electronics Products". Class 3 is defined in IPC J-STD-001D as "Includes products where continued high performance or performance-on-demand is critical, equipment downtime cannot be tolerated, end-use environment may be uncommonly harsh, and the equipment must function when required, such as life support or other critical systems."

Please note that IPC J-STD-001DS "Space Applications Electronic Hardware Addendum to IPC J-STD-001D" and NASA-STD-8739.2 "Workmanship Standard for Surface Mount Technology" were not referenced during the assembly of the test vehicles.

"Manufactured" (Mfg.) test vehicles represent printed wiring assemblies newly manufactured for use in new product. Test vehicles being subjected to thermal cycle and combined environments testing will include forward and backward compatibility. Test vehicles assembled for vibration, mechanical shock and drop testing will not include forward and backward compatibility. The "Manufactured" test vehicles were assembled using immersion silver (Ag) and a limited number of electroless nickel / immersion gold (ENIG) finished glass fiber (GF) laminate (IPC-4101/26) printed circuit boards with a glass transition temperature, T_g, of 170°C minimum.

The "Rework" (Rwk.) test vehicles represent printed wiring assemblies manufactured and reworked prior to being tested. Solder mixing (SnPb/Pb-free & Pb-free/SnPb) will be evaluated on all "Rework" test vehicles. The "Rework" test vehicles were assembled using immersion silver (Ag) and a limited number of electroless nickel / immersion gold (ENIG) finished glass fiber (GF) laminate (IPC-4101/26) printed circuit boards with a glass transition temperature, T_g, of 170°C minimum.

For this project, forward and backward compatibility have been defined as:

- Forward Compatibility is a SnPb component attached to a printed wiring assembly using Pb-free solder with a Pb-free profile.
- Backward compatibility is a Pb-free component attached to a printed wiring assembly using SnPb solder with a SnPb solder profile.

For all details relating to the assembly of the test vehicles, please see "NASA-DoD Pb-free Electronics Project; Project Plan – December 2009".

3.1 NSWC Crane Assembly and Rework Effort

Thirty (30) of the one hundred and ninety three (193) test vehicles assembled by BAE Systems in Irving, Texas were built for Naval Surface Warfare Center, Crane Division, a NASA-DoD Consortium member, in support of their Naval Supply Command (NAVSUP) sponsored "Logistics Impact of Pb-free Circuits/Components" project.

The 30 test vehicles were built as "Manufactured" (Mfg.) test vehicles using Pb-free solder alloys and Pb-free component finishes. Following assembly, NSWC Crane performed SnPb rework on random Pb-free DIP, TQFP-144, TSOP-50, and LCC components. BEST Inc. performed the QFN rework for NSWC Crane. Some of the components were reworked 2 times.

The goal of the NSWC Crane effort is to generate data supporting the qualification of existing SnPb rework procedures for all military hardware built with Pb-free processes through analysis of thermal cycling, vibration, and drop test data including microsection analysis.

Testing of the NSWC Crane test vehicles included -55°C to +125°C thermal cycling testing conducted by Rockwell Collins, Cedar Rapids, Iowa. The NSWC Crane test vehicles were tested with the NASA-DoD Lead-free Electronics test vehicles during -55°C to +125°C thermal cycle testing.

Drop testing, performed by Celestica, Toronto, Ontario, was conducted on the NSWC Crane test vehicles prior to testing the NASA-DoD Lead-free Electronics test vehicles. Initially, the testing procedures for both the NSWC Crane and NASA-DoD Lead-free Electronics test vehicles were to be identical. However, lessons learned during the testing of the NSWC Crane test vehicles lead the consortium to change the testing procedure for the NASA-DoD Lead-free Electronics test vehicles. Details on the Drop Testing procedures can be found in section 0.

Vibration testing, performed by Celestica, Toronto, Ontario, was conducted on the NSWC Crane test vehicles since the facility that tested the NASA-DoD test vehicles could not accommodate the Crane vibration test vehicles. The testing followed the document specifications contained in the NASA-DoD Lead-Free Electronics Project Joint Test Protocol. Nine assemblies in all were tested. Each board was monitored for vibration response and net resistance for all 63 components. The assemblies were attached to the table with the supplied test fixture.

For all details relating to the assembly of the test vehicles, please see "NASA-DoD Lead-Free Electronics Project; Project Plan – March 2010".

4 Test Methods

Project technical representatives identified the engineering, performance, and operational impact (supportability) requirements for printed wiring assemblies, reaching consensus on the tests, procedures and acceptance criteria to be applied. This information was documented in "NASA-DoD Lead-Free Electronics Project, Joint Test Protocol (JTP); September 2009".

The performance requirements and related tests for the NASA-DoD Lead-Free Electronics test vehicles are listed in Table 3. These tests were required by all military and aerospace systems that participated in the development of the NASA-DoD Lead-Free Electronics Project. Both "Manufactured" and "Rework" test vehicles were tested.

Table 3 - Test Vehicle Performance Requirements

Test	Location	Reference	Electrical Test	Acceptance Criteria [(a)]
Vibration	Boeing Seattle, WA	MIL-STD-810F, Method 514.5, Procedure I	Electrical continuity failure	Better than or equal to SnPb controls
Mechanical Shock	Boeing Seattle, WA	MIL-STD-810F, Method 516.5	Electrical continuity failure	Better than or equal to SnPb controls
Thermal Cycling	Boeing Seattle, WA Rockwell Collins Cedar Rapids, IA	IPC-SM-785	Electrical continuity failure	Better than or equal to SnPb controls at 10%[b] Weibull cumulative failures
Combined Environments Test	Raytheon McKinney, TX	MIL-STD-810F Method 520.2 Procedure I	Electrical continuity failure	Better than or equal to SnPb controls at 10%[b] Weibull cumulative failures
Drop Testing	Celestica Toronto, Ontario	JEDEC Standard JESD22-B110A	Electrical continuity failure	Better than or equal to SnPb controls
Interconnect Stress Test (IST)	PWB Interconnect Solutions Inc. Toronto, Ontario	IPC-TM-650-2.6.26	Electrical continuity testing	3 thermal cycles simulate assembly and 6 thermal cycles simulate assembly and rework
Copper Dissolution	Celestica Toronto, Ontario Rockwell Collins Cedar Rapids, IA	IPC-TM-650-2.1.1 ASTM-E-3	Cross section/ metallographic analysis	N/A

[a] Failure of a test board in a specific test does not necessarily disqualify a Pb-free solder alloy for use in an application for which that test does not apply. Electrical performance requirements for a particular circuit apply only to parts containing that circuit.

[b] 10% noncompliance of minimal Weibull distribution data for Thermal Cycling and Combined Environments Testing was selected because it was a compromise between the 63.2% failures which is taken as normal life, and 1% failures (or first failure) which is most important in high reliability systems.

5 Test Results

5.1 Vibration Test

5.1.1 Vibration Test Method

This test quantifies solder joint failures on the test vehicles during exposure to vibration. The limits identified in the vibration testing were used to compare performance differences in the Pb-free test alloys and mixed solder joints vs. the baseline standard SnPb (63/37) alloy.

The testing satisfies the general requirements of MIL-STD-810F (Test Method Standard for Environmental Engineering Considerations and Laboratory Tests) Method 514.5 (Vibration) and was performed using the following procedure:

- Confirm the electrical continuity of each test channel prior to testing. One channel will be used per component.
- Place the PWAs into a test fixture in random order and mount the test fixture onto an electrodynamic shaker.
- Conduct a step stress test in the Z-axis only (i.e., perpendicular to the plane of the circuit board). Most failures will occur with displacements applied in the Z-axis as that will result in maximum board bending for each of the major modes.
- Run the test using the stress steps shown in Figure 2 and Table 4. Subject the test vehicles to 8.0 g_{rms} for one hour. Then increase the Z-axis vibration level in 2.0 g_{rms} increments, shaking for one hour per step until the 20.0 g_{rms} level is completed. Then subject the test vehicles to a final one hour of vibration at 28.0 g_{rms}.
- Continuously monitor the electrical continuity of the solder joints during the test using event detectors with shielded cables. All wires used for monitoring will be soldered directly to the test vehicles and then glued to the test vehicles (with stress relief) to minimize wire fatigue during the test.
- If feasible, a complete modal analysis should be conducted on one test vehicle using a laser vibrometer system in order to determine the resonant frequencies and the actual deflection shapes for each mode

The stakeholders agreed that a stress step test representing increasingly severe vibration environments was appropriate for this test. A step stress test is required since a test conducted at a constant 8.0 g_{rms} level (Step 1) would take thousands of hours to fail the same number of components as a step stress test. This is because some locations on a circuit assembly experience very low stresses and severe vibration is required in order to fail components at these locations. The shape of the PSD (Power Spectral Density) curve for each step stress level was designed so that all of the major resonances of the test vehicles would be excited by the random vibration input. The PSD curves presented in MIL-STD-810F were used as guides for the creation of this step stress test but were not directly duplicated.

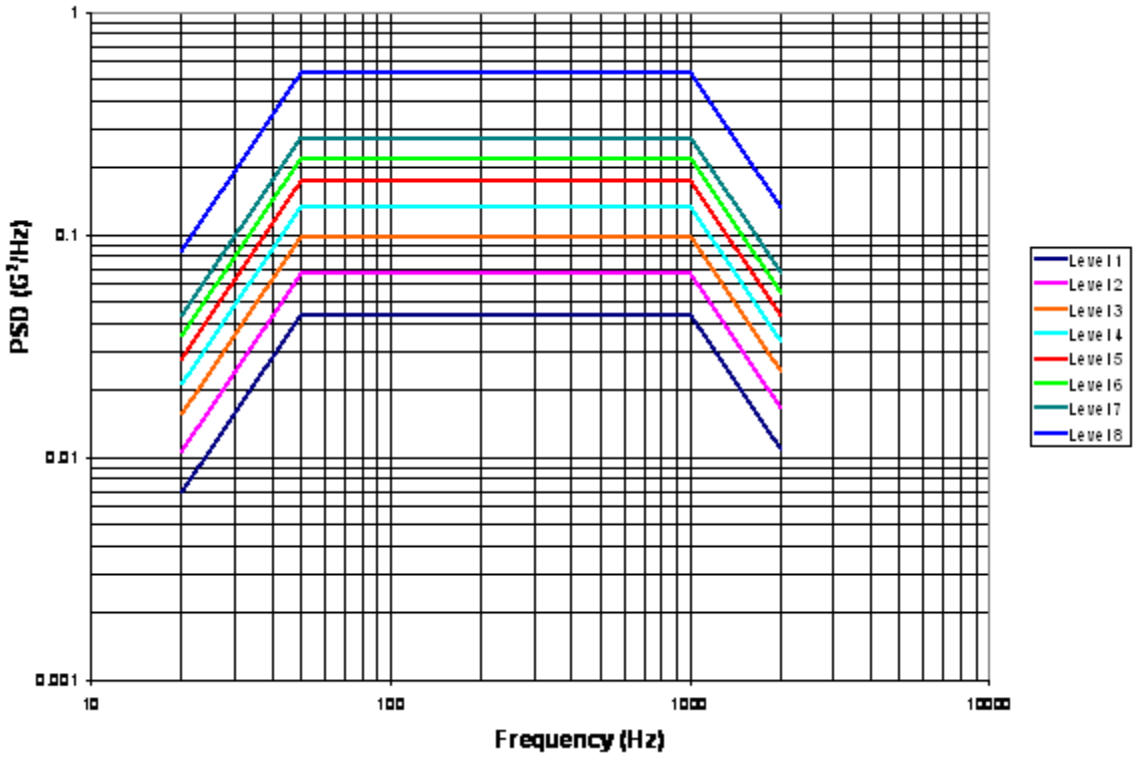

Figure 2 - Vibration Spectrum

Table 4 - Vibration Profile

Level 1	Level 2	Level 3
20 Hz @0.00698 G^2/Hz	20 Hz @0.0107 G^2/Hz	20 Hz @0.0157 G^2/Hz
20 - 50 Hz @ +6.0 dB/octave	20 - 50 Hz @ +6.0 dB/octave	20 - 50 Hz @ +6.0 dB/octave
50 - 1000 Hz @0.0438 G^2/Hz	50 - 1000 Hz @0.067 G^2/Hz	50 - 1000 Hz @0.0984 G^2/Hz
1000 -2000 Hz @ -6.0 dB/octave	1000 - 2000 Hz @ -6.0 dB/octave	1000 - 2000 Hz @ -6.0 dB/octave
2000 Hz @ 0.0 109 G^2/Hz	2000 Hz @ 0.0 167 G^2/Hz	2000 Hz @ 0.0245 G^2/Hz
Composite = 8.0 G_{rms}	**Composite = 9.9 G_{rms}**	**Composite = 12.0 G_{rms}**

Level 4	Level 5	Level 6
20 Hz @ 0.02 14 G^2/Hz	20 Hz @ 0.0279 G^2/Hz	20 Hz @ 0.0354 G^2/Hz
20 - 50 Hz @ +6.0 dB/octave	20 - 50 Hz @ +6.0 dB/octave	20 - 50 Hz @ +6.0 dB/octave
50 - 1000 Hz @ 0.134 G^2/Hz	50 - 1000 Hz @ 0.175 G^2/Hz	50 - 1000 Hz @ 0.22 15 G^2/Hz
1000 -2000 Hz @ -6.0 dB/octave	1000 - 2000 Hz @ -6.0 dB/octave	1000 - 2000 Hz @ -6.0 dB/octave
2000 Hz @ 0.0334 G^2/Hz	2000 Hz @ 0.0436 G^2/Hz	2000 Hz @ 0.0552 G^2/Hz
Composite = 14.0 G_{rms}	**Composite = 16.0 G_{rms}**	**Composite = 18.0 G_{rms}**

Level 7	Level 8
20 Hz @ 0.0437 G^2/Hz	20 Hz @ 0.0855 G^2/Hz
20 - 50 Hz @ +6.0 dB/octave	20 - 50 Hz @ +6.0 dB/octave
50 - 1000 Hz @ 0.2734 G^2/Hz	50 - 1000 Hz @ 0.5360 G^2/Hz
1000 -2000 Hz @ -6.0 dB/octave	1000 - 2000 Hz @ -6.0 dB/octave
2000 Hz @0.0682 G^2/Hz	2000 Hz @0.1330 G^2/Hz
Composite = 20.0 G_{rms}	**Composite = 28.0 G_{rms}**

5.1.2 NASA-DoD Test Vehicle Vibration Testing Results Summary

The complete test report, "NASA-DoD Lead-Free Electronics Project: Vibration Test", can be found on the NASA TEERM website (http://teerm.nasa.gov/NASA_DODLeadFreeElectronics_Proj2.html).

The objective of this study was to determine the effects of random vibration on the relative reliability of Pb-free and tin/lead solder joints (i.e., which solder survived the longest). Modal data and strain data were also collected during this study in an effort to provide data that would be useful to those that may want to try to model the behavior of the NASA-DoD test vehicle.

Twenty seven test vehicles were delivered to Boeing for vibration testing. These consisted of 5 SnPb "Manufactured" test vehicles; 6 Pb-free "Manufactured" test vehicles assembled with SAC305 paste; 5 Pb-free "Manufactured" test vehicles assembled with SN100C paste; 6 SnPb "Rework" test vehicles; and 5 Pb-free "Rework" test vehicles. Most of the test vehicles had an immersion silver PWB finish except for one SAC305 "Manufactured" test vehicle (Test Vehicle 96) with ENIG PWB finish and one SnPb "Rework" test vehicle (Test Vehicle 157) with ENIG PWB finish.

Table 5 shows the percent of each component type that failed on both the "Manufactured" and the "Rework" test vehicles at the end of the test. Notice that the QFN-20's were resistant to failure due to vibration.

Table 5 - Percentage of Components Failed (Includes Mixed Solders)

	% of Components Failed During Vibration Testing				
	"Manufactured" Test Vehicles			"Rework" Test Vehicles	
	SnPb Paste	SAC305 Paste	SN100C Paste	SnPb Paste	Pb-Free Paste
Component					
BGA-225	84	98	100	100	100
CLCC-20	32	43	90	35	68
CSP-100	62	73	70	62	80
PDIP-20	98	92	100	88	96
QFN-20	0	21	20	8	10
TQFP-144	60	63	64	70	70
TSOP-50	62	73	86	77	80

Figure 3 shows when the components failed on Test Vehicle 74. The failures are colored coded according to how many test minutes were required to cause the failure (red = 1 to 60 test

minutes; orange = 61 to 120 minutes; yellow = 121 to 180 minutes; green = 181 to 240 minutes; blue = 241 to 300 minutes; purple = 301 to 360 minutes; pink = 361-420 minutes; and white = 421 to 480+ minutes). In general, the components tended to fail first down the centerline and along the edges of the test vehicle (near the wedgelocks). Therefore, the first component failures coincide with the regions of highest strain as shown in Figure 4.

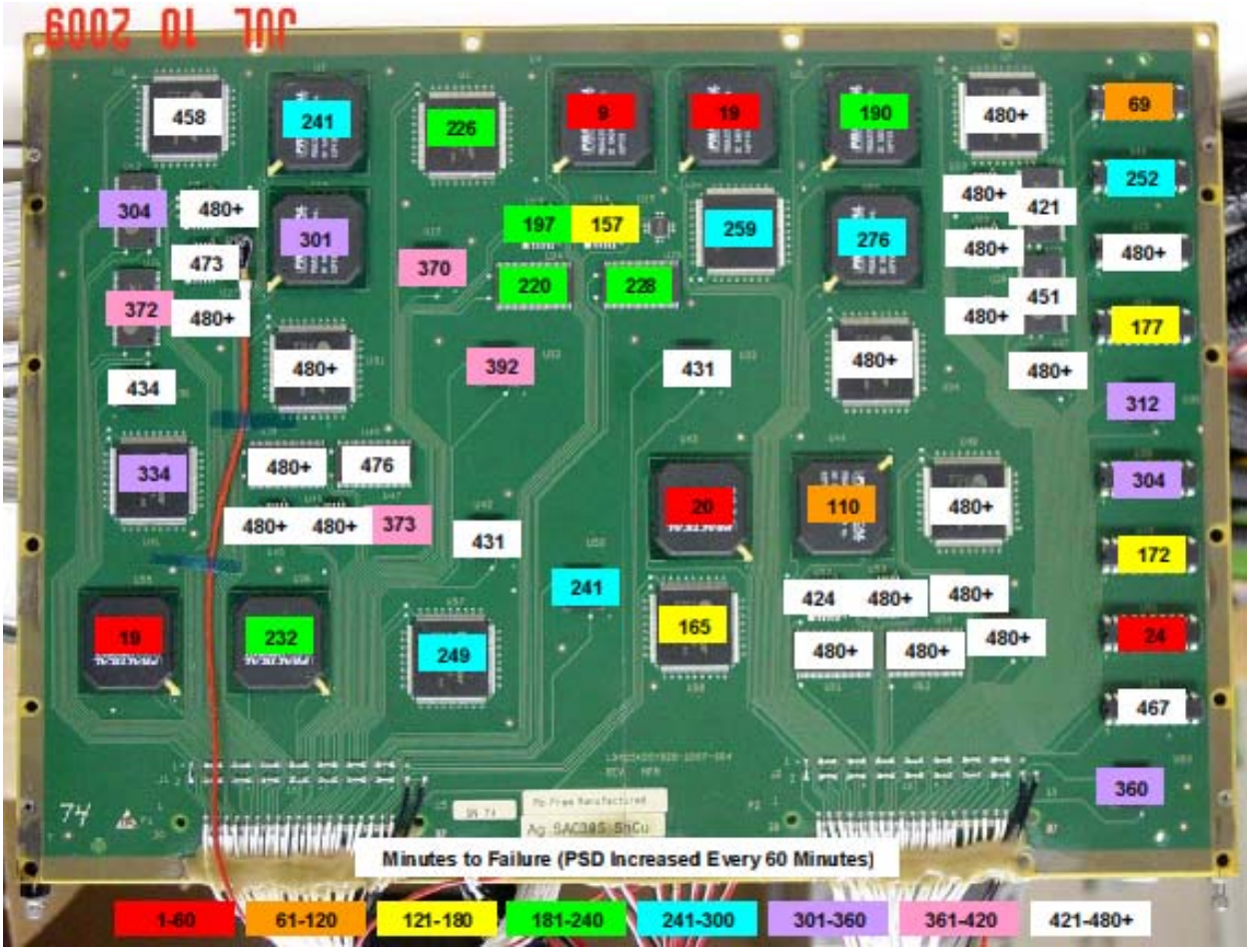

Figure 3 - Test Minutes Required for Components to Fail (Test Vehicle 74 Data)

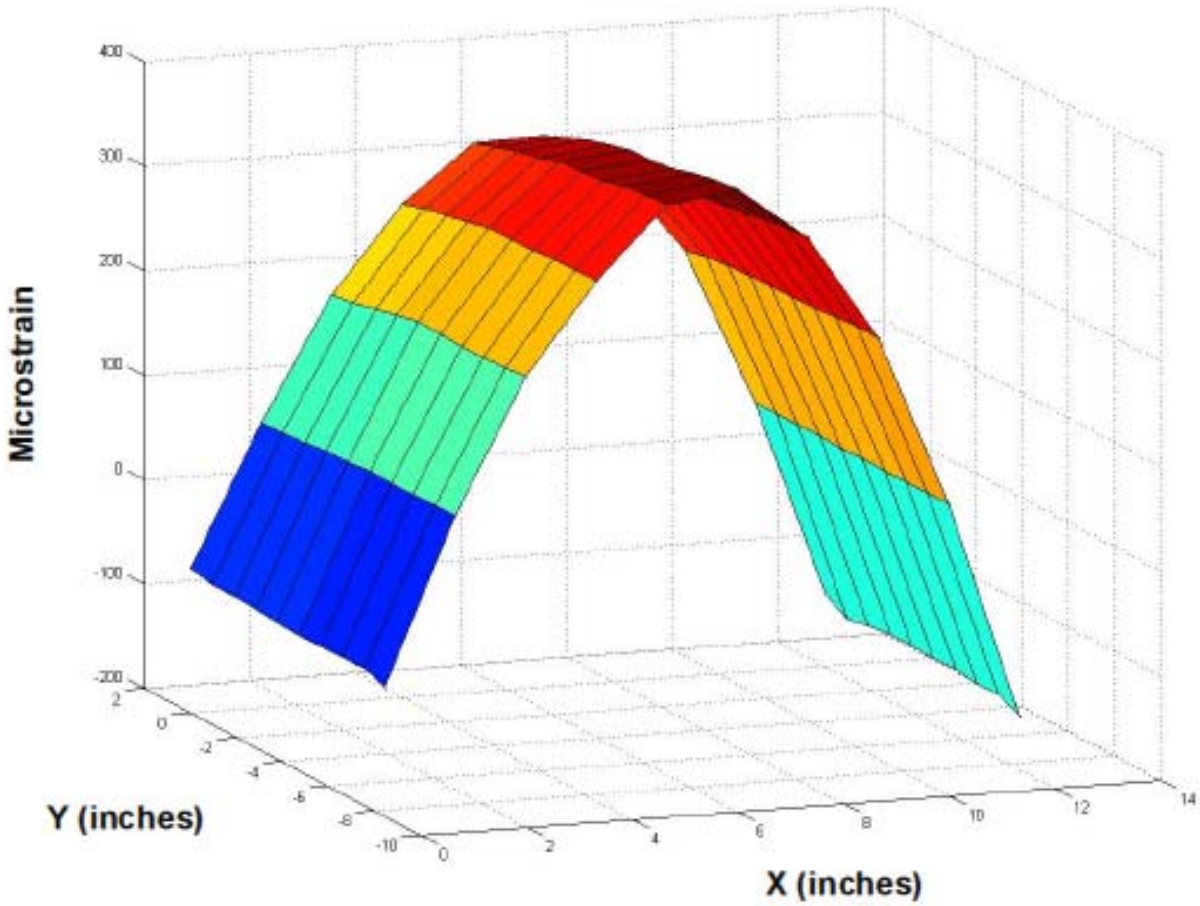

Figure 4 - Full Field Peak Strains at 65 Hz (1G Sine Dwell, Test Vehicle 74)

The overall results of the vibration testing are summarized in Table 6. If a solder alloy/component finish combination performed as well or better than the SnPb control, it was assigned the number "1" and the color "green". Solders that performed worse than the SnPb control were assigned a "2" and the color "yellow". Solders that performed much worse than the SnPb control were assigned a "3" and the color "red".

The rankings in Table 6 are somewhat subjective due to the scatter in the data for some component types. The TSOP data was difficult to interpret since the orientation of the TSOP on the test vehicle appeared to influence how the solder/component finish combinations performed relative to the Sn37Pb/SnPb controls. Weibull plots were not used since the test conditions were changed during the test (i.e., the PSD was increased every 60 minutes) which renders the Weibull parameters meaningless.

Table 6 - Ranking of Solder Alloy/Component Finish Combinations

	Relative Ranking (Solder Alloy / Component Finish)											
BGA-225	Sn37Pb/ Sn37Pb	SAC305/ SAC405	Sn37Pb/ SAC405	SAC305/ Sn37Pb	Rwk Flux Only/ Sn37Pb	Rwk Flux Only/ SAC405	Rwk Sn37Pb/SAC405 (SnPb Profile)	Rwk Sn37Pb/SAC405 (Pb-Free Profile)	SN100C/ SAC405			
	1	3	3	3	3	3	3	3	3			
CLCC-20	Sn37Pb/ Sn37Pb	SAC305/ SAC305	Sn37Pb/ SAC305	SAC305/ Sn37Pb	SN100C/ SAC305							
	1	3	2	3	3							
CSP-100	Sn37Pb/ Sn37Pb	SAC305/ SAC105	Sn37Pb/ SAC105	SAC305/ Sn37Pb	Rwk Flux Only/ Sn37Pb	Rwk Flux Only/ SAC105	Rwk Sn37Pb/SAC105 (SnPb Profile)	Rwk Sn37Pb/SAC105 (Pb-Free Profile)	SN100C/ SAC105			
	1	1	1	2	1	2	1	3	1			
PDIP-20	Sn37Pb/ SnPb	SN100C/ Sn	Sn37Pb/ NiPdAu	Rwk Sn37Pb/ Sn	Rwk Sn100C/ Sn	SN100C/ NiPdAu						
	1	3	2	3	3	3						
QFN-20	Sn37Pb/ Sn37Pb	SAC305/ Sn	Sn37Pb/ Sn	SAC305/ Sn37Pb	SN100C/ Sn							
	1	2	1	1	2							
TQFP-144	Sn37Pb/ Sn	SAC305/ Sn	Sn37Pb/ NiPdAu	SAC305/ NiPdAu	Sn37Pb/ Sn37Pb Dip	SAC305/ SAC305 Dip	SN100C/ Sn					
	1	1	1	2	1	2	1					
TSOP-50	Sn37Pb/ SnPb	Sn37Pb/ Sn	Sn37Pb/ SnBi	SAC305/ Sn	SAC305/ SnBi	SAC305/ SnPb	Rwk Sn37Pb/ SnPb	Rwk Sn37Pb/Sn (SnPb Profile)	Rwk Sn37Pb/Sn (Pb-free Profile)	Rwk SAC305/ SnBi	SN100C/ Sn	SN100C/ SnBi
	1	2*	2*	2*	2*	2	2	2*	2*	2	2	2

*Performance relative to Sn37Pb control may depend on orientation of the TSOP

1 = as good as or better than Sn37Pb control

2 = worse than Sn37Pb control

3 = much worse than Sn37Pb control

5.1.3 NSWC Crane Test Vehicle Vibration Testing Results Summary

The complete test report, "Vibration Testing Report for Crane; TOL0901051", can be found on the NASA TEERM website (http://teerm.nasa.gov/NASA_DODLeadFreeElectronics_Proj2.html).

For this effort, 9 NSWC Crane test vehicles were subjected to vibration testing per the test method outlined in section 5.1. The vibration testing resulted in electrical failures in over 80% of all components; see Table 7 and Table 8 for details. In total, 63 components on each board were in-situ resistance monitored during the vibration testing. An average of 51 components failed electrically on each board.

Table 7 - Component Percentage Failure by Force Level

Vibration Level	Components Failed	%	Total %
8	51	9.0	9
10	45	7.9	16.9
12	43	7.6	24.5
14	39	6.9	31.4
16	39	6.9	38.3
18	59	10.4	48.7
20	73	12.9	61.6
28	111	19.6	81.1

Table 8 - Component Detachments

Vibration Level	Card	Components
20	79	U16
28	61	U16, U29
	62	U12, U16
	64	U16
	65	U7,U12, U16, U29
	66	U12, U16, U29
	67	U7,U12, U16, U29, U34
	79	U29

Out of the 9 test vehicles tested, 33 parts representing electrical failures were selected for cross-section analysis. Test vehicles were submitted to Celestica's Performance Innovation Laboratories for physical failure analysis. The cross-sections revealed a high degree of damage throughout the solder joints. This damage occurred across all cross-sectioned parts and did not seem to correlate to the part type, location on the board or type of solder, i.e. no significant difference between the Pb-free (non-reworked) parts and the reworked SnPb parts.

5.1.3.1 CLCC Components

All of the tested CLCC-20s had SAC305 component finish. None of these solder joints were reworked. Solder cracks we observed around every solder joint. The cross sections of all CCLC-20 packages were performed on corner pads. Each cross section revealed cracking across the length of the solder, see Figure 5. SN67 also showed voiding, in this case the crack traveled along the void, see Figure 6.

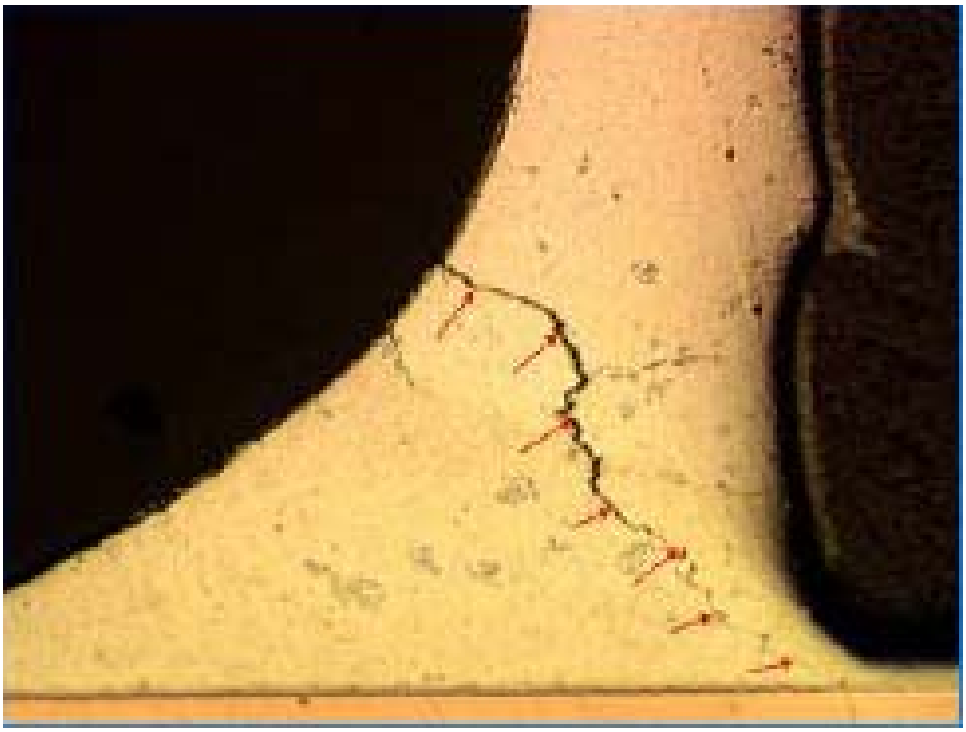

Figure 5 - SN63 U52, Left Side Pad

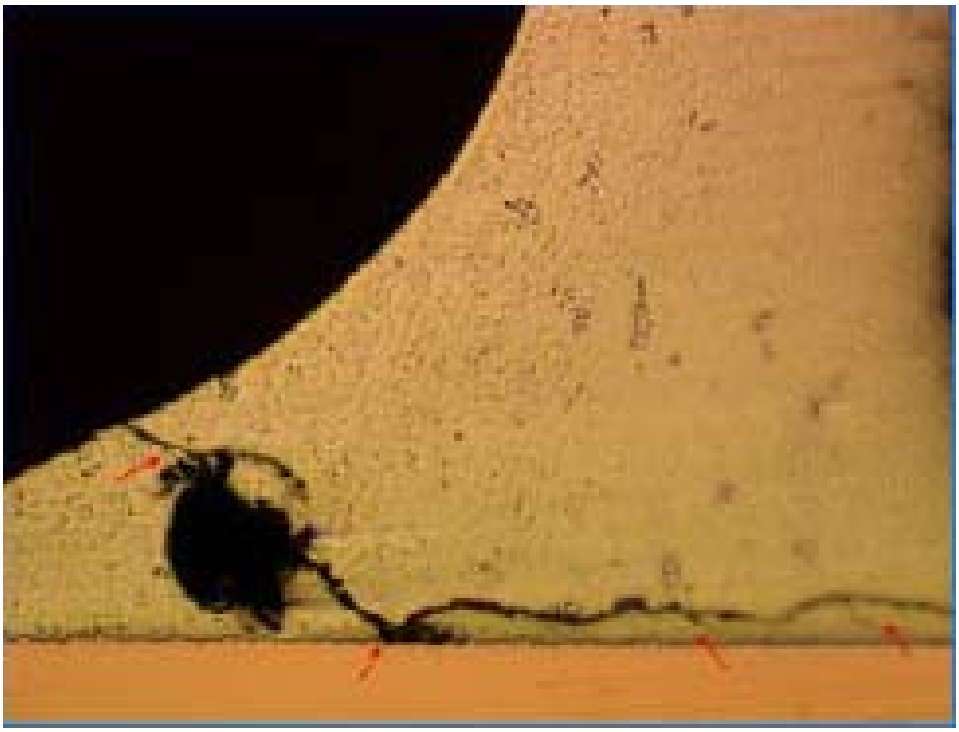

Figure 6 - SN67 U52, Left Side Pad

All of the QFN-20 packages were fabricated using Sn finish and were exposed to one or two reworks with SnPb solder. Approximately half of the solder joints exhibited cracks which ran along the component pad. There does not appear to be a correlation between the cracked solder and the number of re-work cycles to which the part was exposed. Cross sections of the QFN-20 packages reveal that the cracks propagated along the component pad, see Figure 7 and Figure 8.

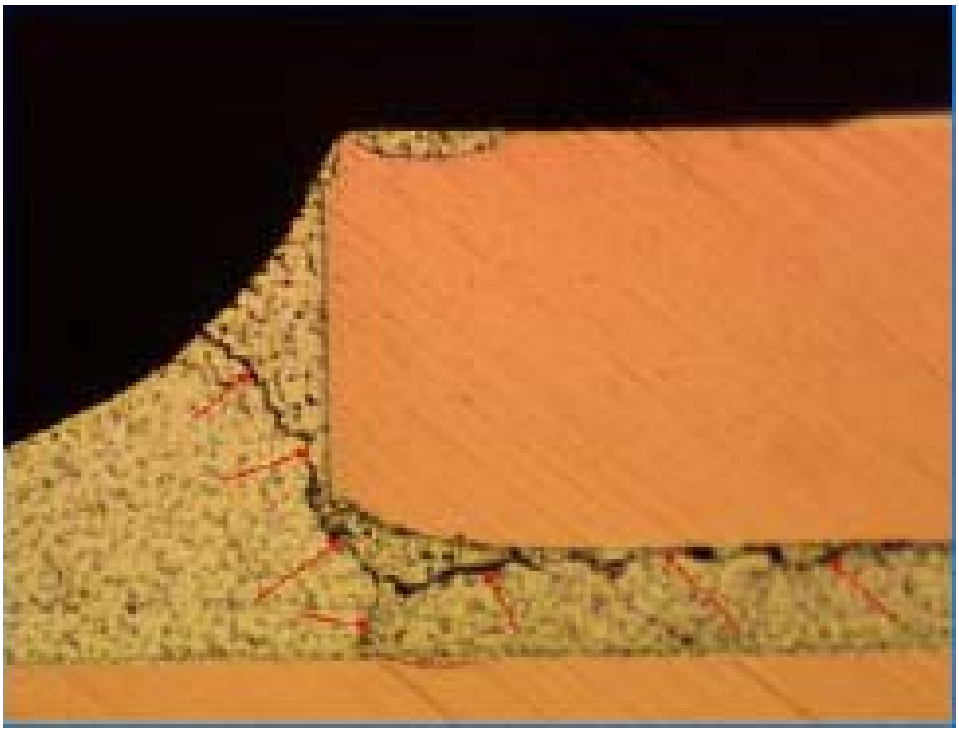

Figure 7 - SN63 U54, Left Side Pad

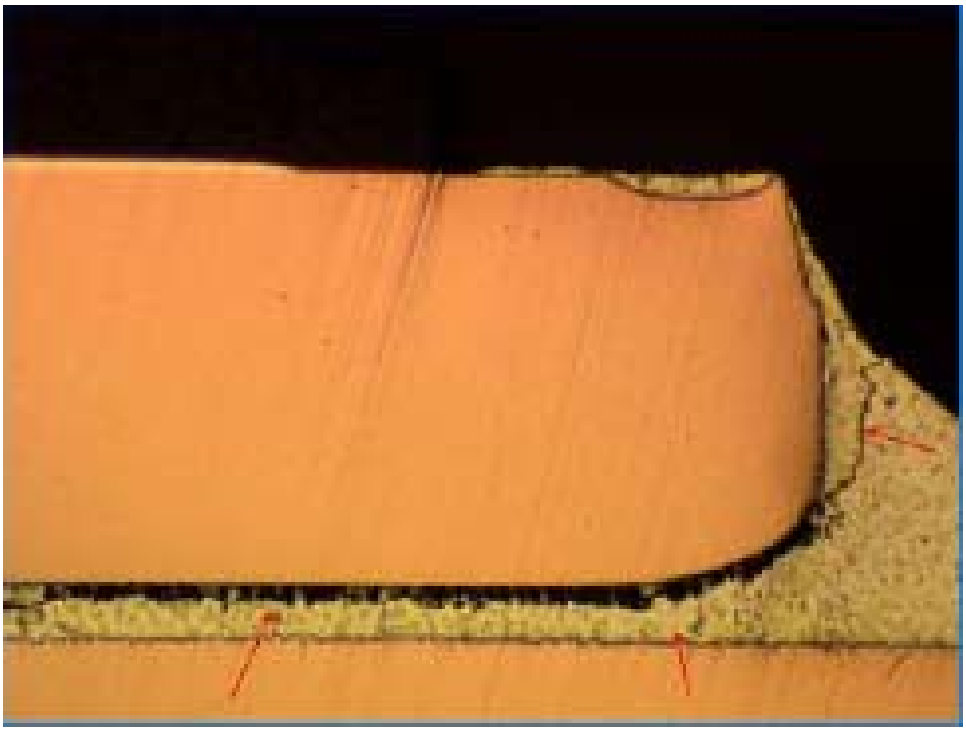

Figure 8 - SN68 U28, Right Side Pad

5.1.3.2 TQFP Components

All of the TQFP-144 packages were fabricated using Sn finish on the leads, and four of the nine were exposed to one or two re-work cycles with SnPb solder. All of the solder joints experienced significant cracking. Additionally, eight leads broke, all corresponding to components that did not undergo any re-work and therefore contained only Pb-free solder.

Cross-sectioning revealed cracks in the actual copper leads of the TQFP-144 packages. This damage was observed only on parts which were not reworked and therefore the solder joint was Pb-free. This is to be expected as the Pb-free solder is stiffer than the SnPb solder and transfers the stress to the weaker copper leads. Figure 9 and Figure 10 illustrate TQFP-144 packages which were not reworked and therefore contain only Pb-free solders.

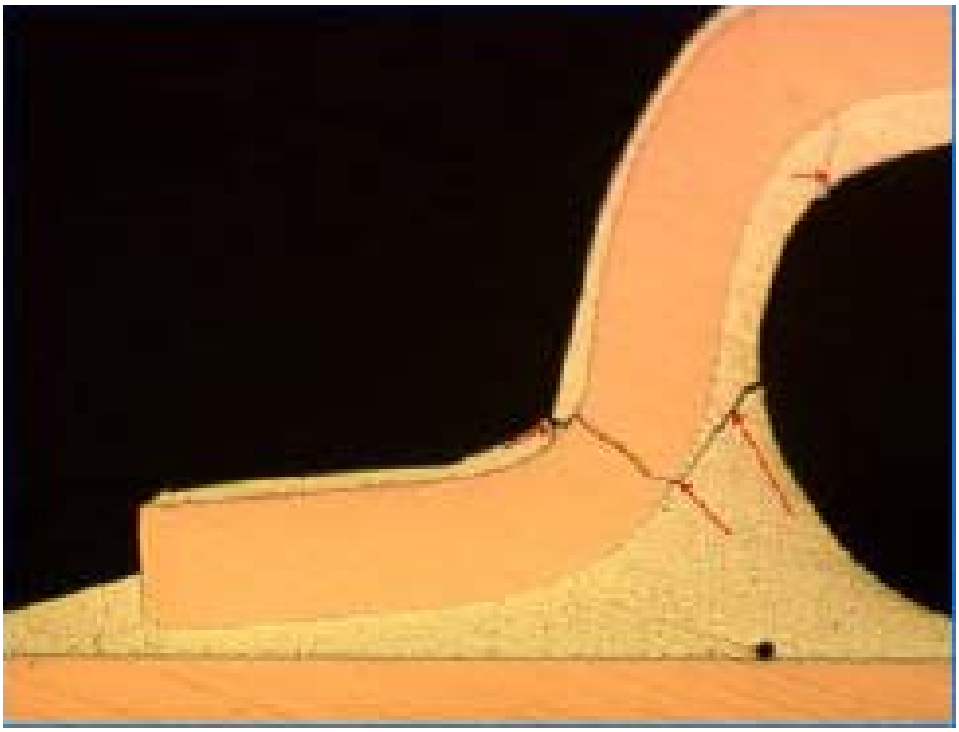

Figure 9 - SN63 U41. Left Lead

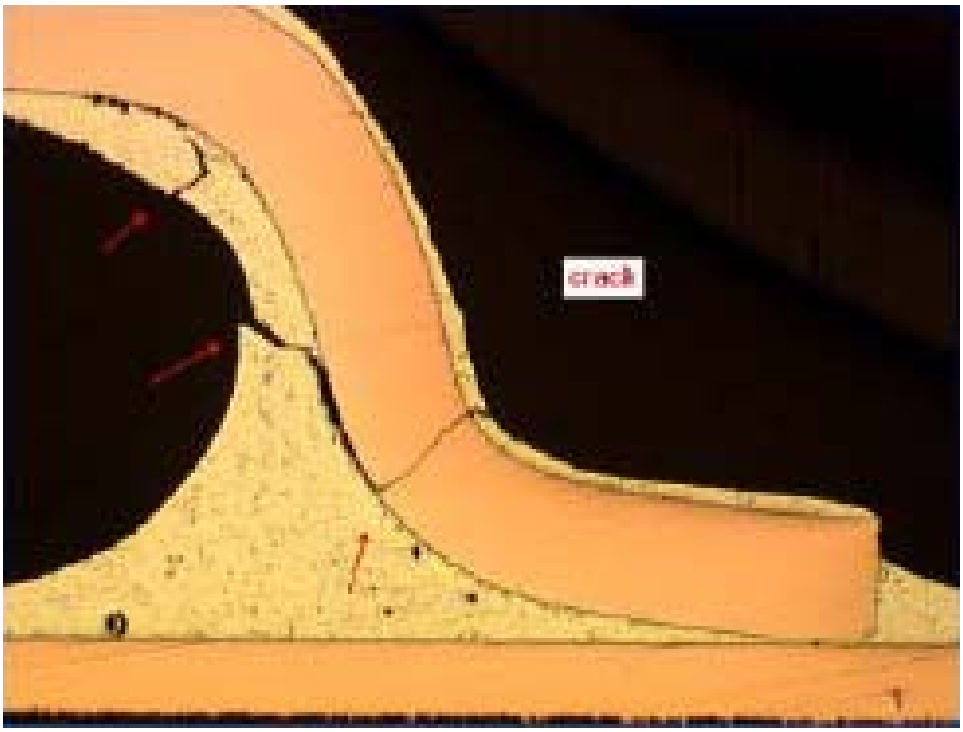

Figure 10 - SN61 U20 Right Lead

Cross-sections of TQFP-144 packages which were re-worked, either once or twice, revealed cracked solder joints in all cases. However, all of the leads on these samples survived, see Figure 11 and Figure 12.

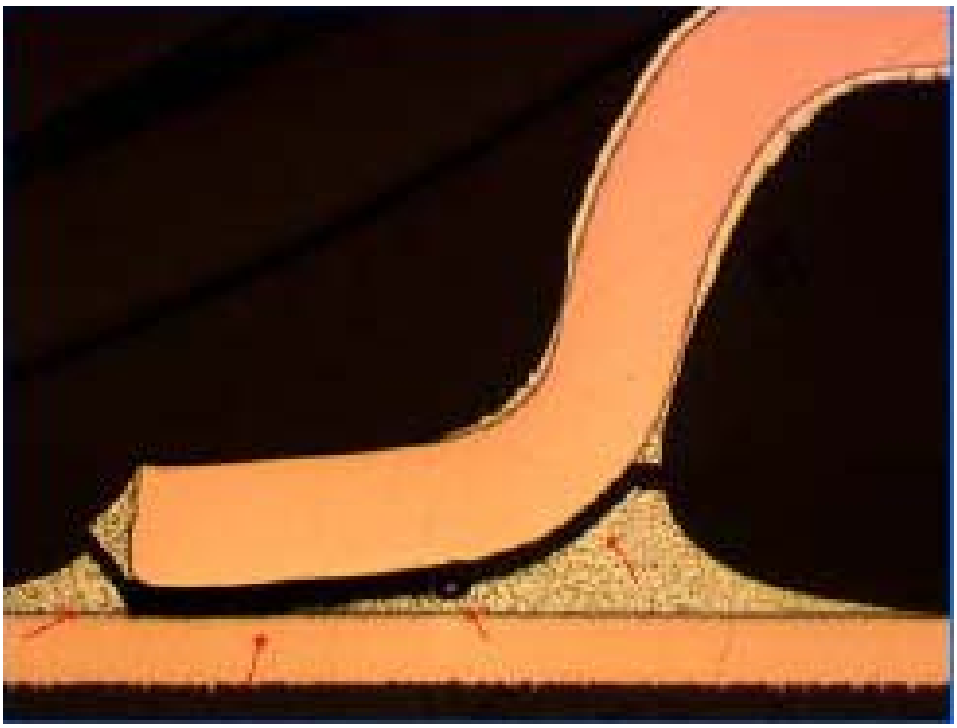

Figure 11 - SN67 U31 Left Lead

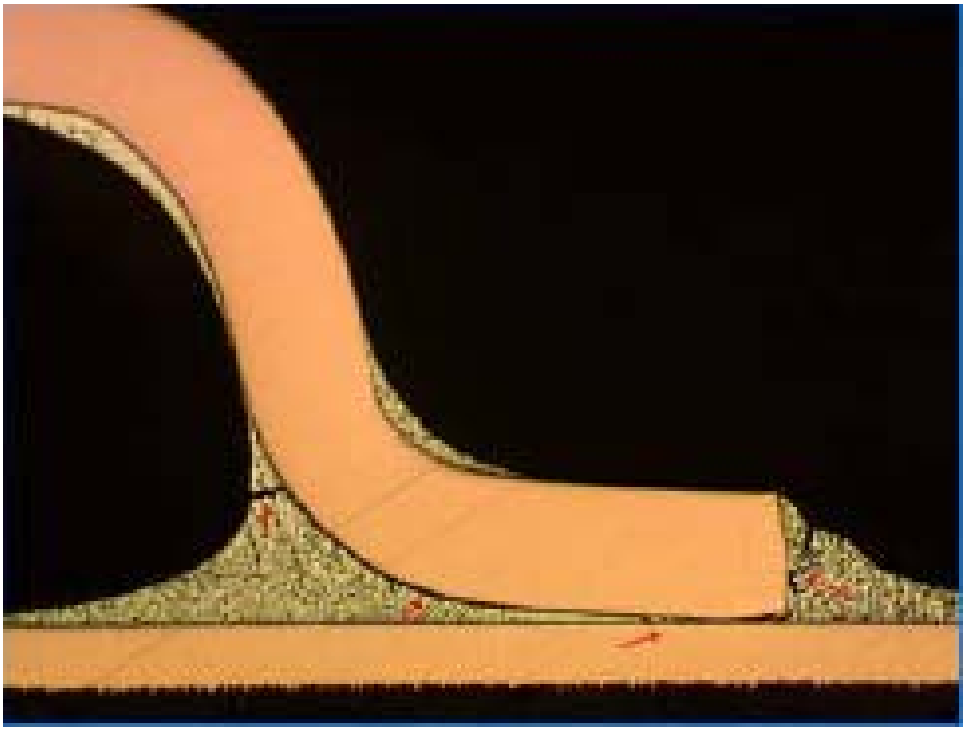

Figure 12 - SN68 U31, Right Lead

5.1.3.3 TSOP Components

Of the twenty one TSOPs tested, seven fell off of the board during the vibration test and where therefore not cross sectioned. All of these parts were in an area closest to the edge of the board. Among the cross sectioned parts, all of the leads remained intact however almost all of the solder joints experienced significant cracking. The TSOPs had finishes of either Sn or SnBi, and two thirds were re-worked either one or two times using SnPb solder. There does not appear to be any correlation between the lead finish or the number of re-works with the incident of cracking in the solder joint.

SN79 U12 (Figure 13) and SN66 U62 (Figure 14) are examples of TSOPs which did not undergo any re-work. They have Sn and SnBi finishes respectively. Both experienced sever solder cracking in leads on both sides of the component.

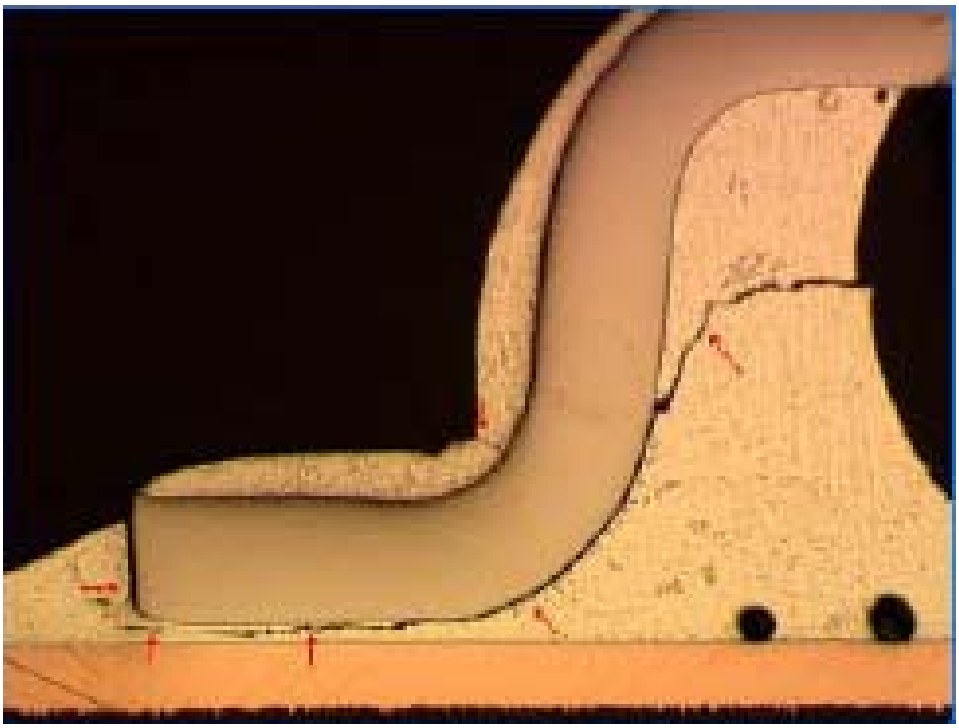

Figure 13 - SN79 U12, Left Lead

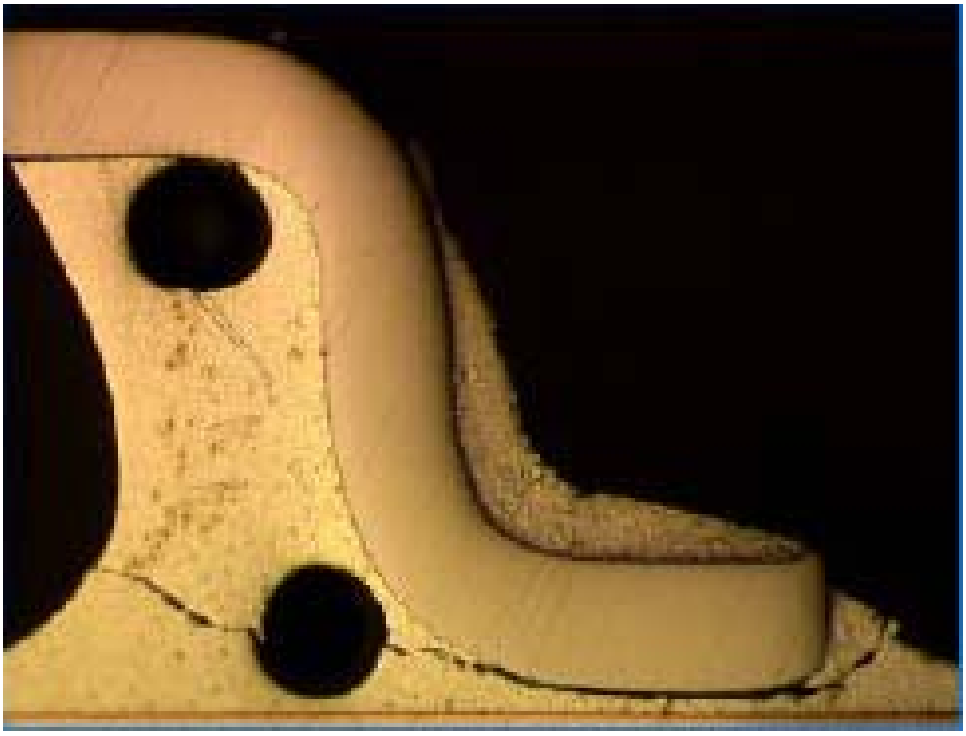

Figure 14 - SN66 U62, Right Lead

SN65 U62 (Figure 15) and SN63 U61 (Figure 16) are examples of parts which underwent one re-work cycle with SnPb solder. They have Sn and SnBi finishes respectively and both components

showed significant cracking within the solder at both sides of the component. This is consistent with all parts which have undergone one re-work cycle.

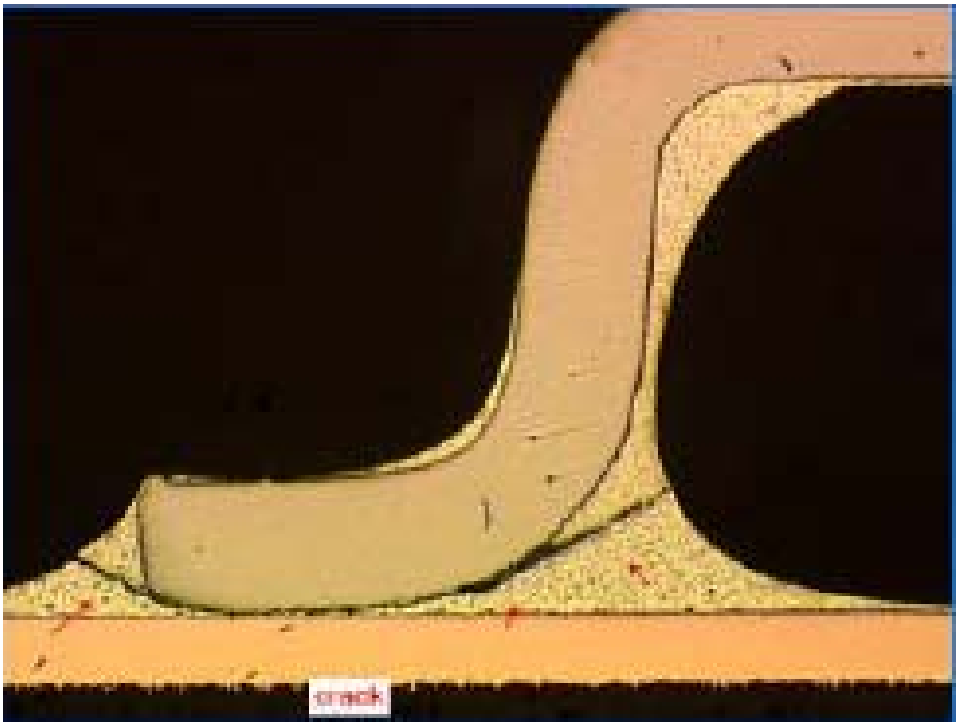

Figure 15 - SN65 U62, Left Lead

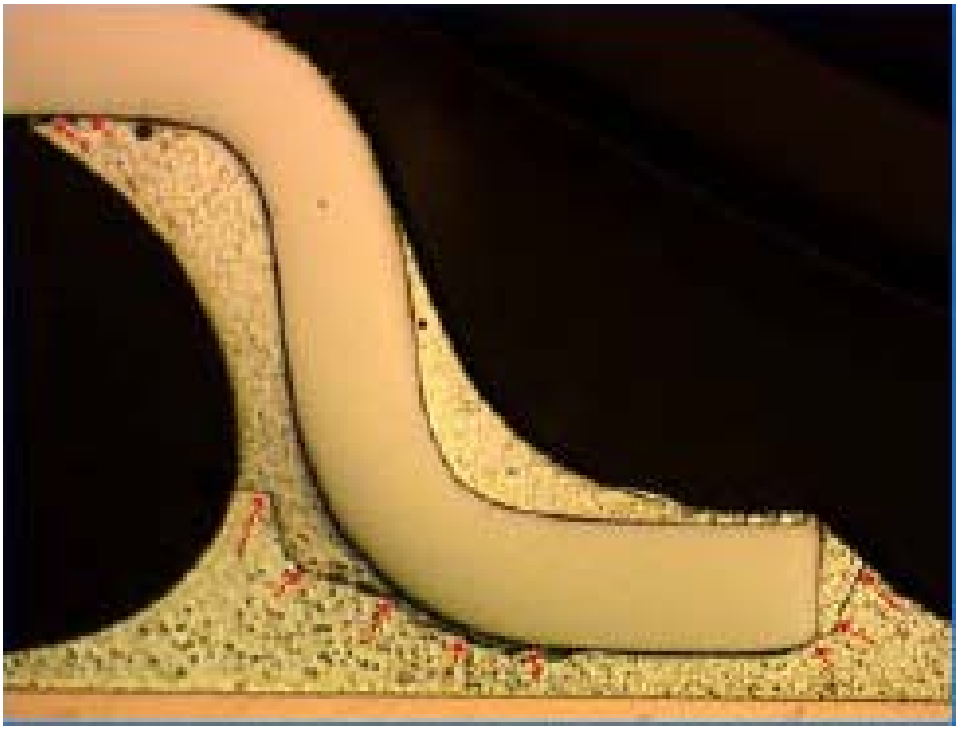

Figure 16 - SN63 U61, Right Lead

SN63 U16 (Figure 17) and SN68 U29 (Figure 18) were both re-worked twice with SnPb solder. SN63 U16 is finished with SnBi and SN68 U29 is finished with Sn. The SnBi part experienced extensive solder cracking through-out. The Sn finished part experienced solder cracking at one side of the component.

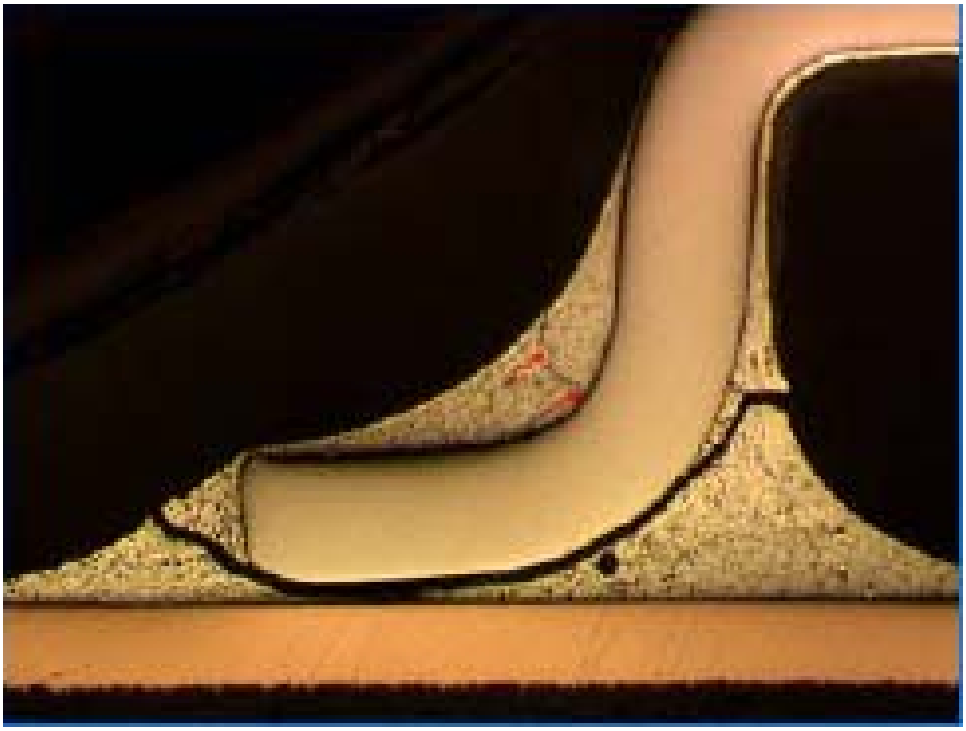

Figure 17 - SN63 U16, Left Lead

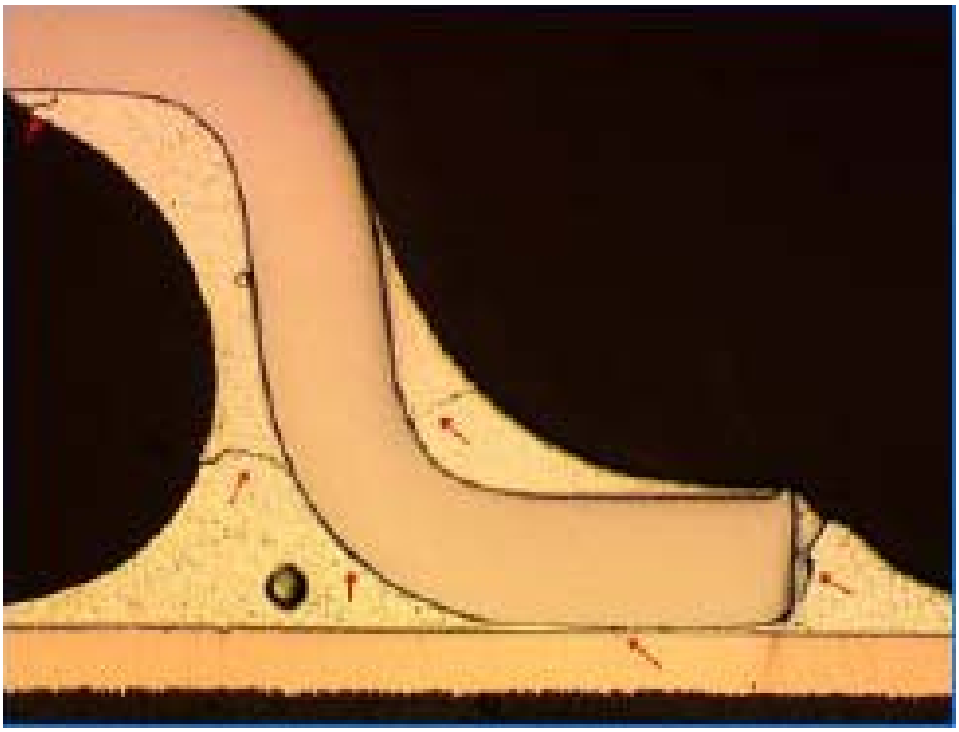

Figure 18 - SN68 U29, Right Lead

Based on the limited number of cross-section completed, there does not appear to be a correlation between component lead finish and the damage to the leads or bulk solder. The TQFPs show some correlation to number of re-work cycles and damaged leads, as only those leads which did not undergo any re-work broke. As the re-work solder was SnPb, this would indicate that the leads with Pb-free solder joints broke, while those with some Pb in the solder survived.

5.2 Mechanical Shock Test

5.2.1 Mechanical Shock Test Method

The purpose of this test was to determine the resistance of solders to the stresses associated with high-intensity shocks. Testing was performed in accordance with the requirements specified in MIL-STD-810F (with modifications). A step stress shock test was performed to maximize the number of failures generated which allowed comparisons of solder reliability.

The test vehicles were mounted in a fixture on an electro-dynamic shaker. The required shock response spectrum (SRS) was programmed into the digital shock controller which in turn generated the required transient shock time history.

Testing followed MIL-STD-810F, Method 516.5 with the following modifications: (1)100 shocks applied per test level (rather than 3) and all of the shocks applied in the Z-axis, and (2) the shock transients applied at the levels specified in MIL-STD-810F, Method 516.5 for the Functional Test for Flight Equipment, the Functional Test for Ground Equipment, and the Crash Hazard Test for Ground Equipment followed the modified parameters given in Table 9. Additional step stress test was then conducted (per Table 9 and Figure 19) with the shocks being applied in the Z-axis only. For Level 6 (300 G's), 400 shocks were applied instead of 100. Testing continued until a majority (approximately 63 percent) of components failed. Shock levels, pulse durations and/or frequencies may be modified during testing based on the actual capabilities of the electrodynamic shaker used.

The test SRS shall be within +3dB and -1.5dB of the nominal requirement over a minimum of 90% of the frequency band when using a 1/12-octave analysis bandwidth. The remaining 10% of the frequency band shall be within +6dB and -3dB of the nominal requirement.

The electrical continuity of the solder joints was continuously monitored during the test. All test results were recorded.

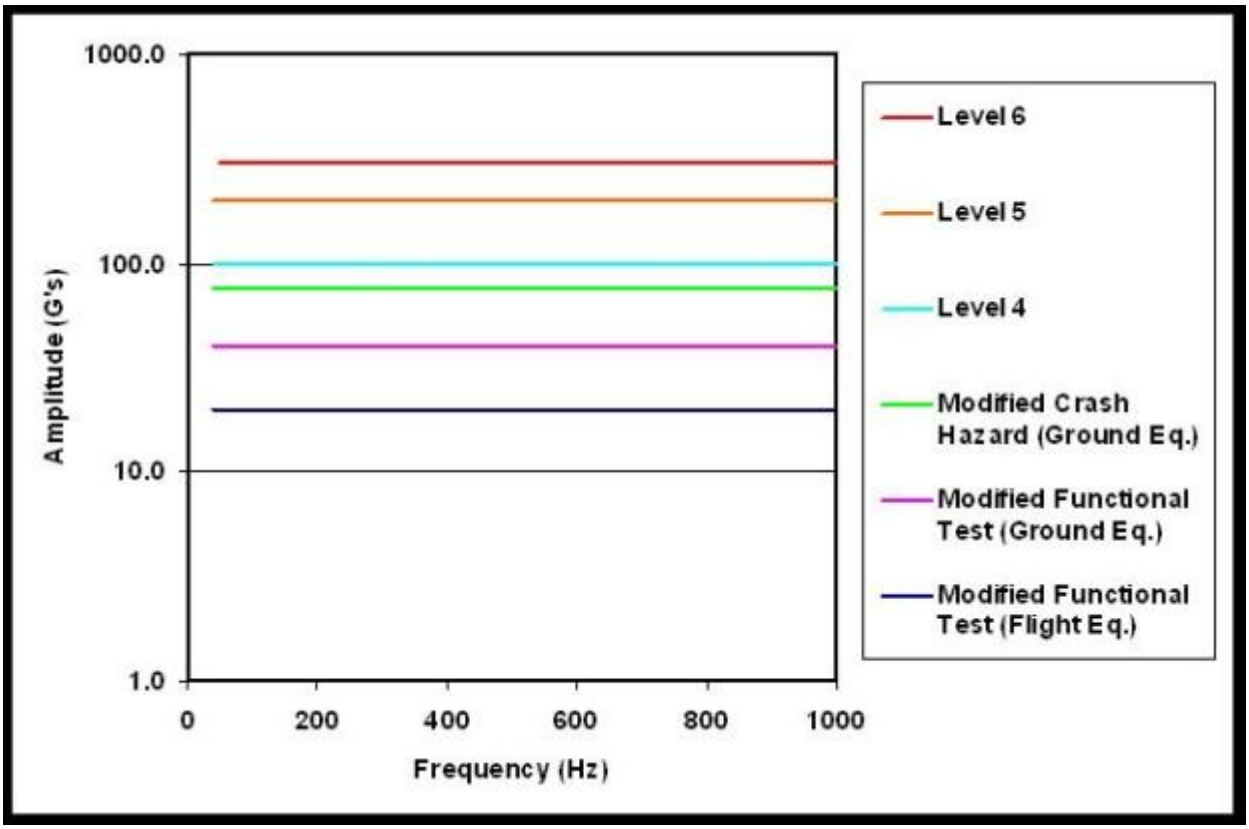

Figure 19 - Mechanical Shock SRS Test Levels

Table 9 - Mechanical Shock Test Methodology – Test Procedure

Parameters	The shock transients will be applied perpendicular to the plane of the board and will be increased after every 100 shocks (i.e., a step stress test). For Level 6 (300 G's), 400 shocks will be applied. Frequency range is 40 to 1000 Hz. SRS damping: 5%			
	Test Shock Response Spectra	Amplitude (G's)	Te (msec)	Shocks per Level
	Modified Functional Test for Flight Equipment (Level 1)	20	<30	100
	Modified Functional Test for Ground Equipment (Level 2)	40	<30	100
	Modified Crash Hazard Test for Ground Equipment (Level 3)	75	<30	100
	Level 4	100	<30	100
	Level 5	200	<30	100
	Level 6	300	<30	400
Number of Test Vehicles Required				
Mfg. SnPb = 5		Mfg. LF = 5		
Rwk. SnPb = 5	Rwk. SnPb {ENIG} = 1		Rwk. LF = 5	
Trials per Specimen		1		

5.2.2 Mechanical Shock Testing Results Summary

The complete test report, "NASA-DoD Lead-Free Electronics Project: Mechanical Shock Test", can be found on the NASA TEERM website (http://teerm.nasa.gov/NASA_DODLeadFreeElectronics_Proj2.html).

The overall results of the mechanical shock testing are summarized in Table 10. If a solder alloy/component finish combination performed as well or better than the SnPb control, it was assigned the number "1" and the color "green". Solders that performed worse than the SnPb control were assigned a "2" and the color "yellow". For those cases where both the SnPb controls and a Pb-free solder had few or no failures after 900 shock pulses, they were not ranked.

The rankings in Table 10 are somewhat subjective since the data for some component types contained a lot of scatter and other component types had few failures which complicated the ranking process. In addition, if some of the component/solder combinations had only a few early failures, these failures did not count in the ranking process.

In general, the pure Pb-free systems (SAC305/SAC405 balls, SAC305/SAC105 balls, SAC305/Sn, and SN100C/Sn) performed as well or better than the SnPb controls (SnPb/SnPb or SnPb/Sn).

For mixed technologies, SnPb solder balls combined with SAC305 paste (and reflowed with a Pb-free profile) performed as well as the SnPb controls on both the BGA's and the CSP's. In

contrast, SnPb solder paste combined with either SAC405 or SAC105 balls (and reflowed with a SnPb thermal profile) underperformed the SnPb/SnPb controls.

Rework operations on the PDIP's and TSOP's reduced the reliability of both the SnPb and the Pb-free solders when compared to the unreworked SnPb/SnPb controls. In contrast, rework of SnPb and SAC405 BGA's and SAC105 CSP's using flux only gave equivalent performance to the unreworked SnPb/SnPb controls. Pb-free BGA's reworked with SnPb paste and SAC405 balls (and a Pb-free thermal profile) were also equivalent to the SnPb controls.

Table 10 - Mechanical Shock Testing; Relative Ranking (Solder/Component Finish)

Component	Sn37Pb/Sn37Pb	SAC305/SAC405	Sn37Pb/SAC405	SAC305/Sn37Pb	Rwk Flux Only /Sn37Pb	Rwk Flux Only /SAC405	Rwk Sn37Pb/SAC405 (SnPb Profile)	Rwk Sn37Pb/SAC405 (Pb-Free Profile)
BGA-225	1	1	2	1	1	1	2	1

Component	Sn37Pb/Sn37Pb	SAC305/SAC305	Sn37Pb/SAC305	SAC305/Sn37Pb
CLCC-20	1	2	2	2

Component	Sn37Pb/Sn37Pb	SAC305/SAC105	Sn37Pb/SAC105	SAC305/Sn37Pb	Rwk Flux Only /Sn37Pb	Rwk Flux Only /SAC105	Rwk Sn37Pb/SAC105 (SnPb Profile)	Rwk Sn37Pb/SAC105 (Pb-Free Profile)
CSP-100	1	1	2	1	2	1	2	2

Component	Sn37Pb/SnPb	SN100C/Sn	Sn37Pb/NiPdAu	Rwk Sn37Pb/Sn	Rwk SN100C/Sn
PDIP-20	1	1	1	2	2

Component	Sn37Pb/Sn37Pb	SAC305/Sn	Sn37Pb/Sn	SAC305/Sn37Pb
QFN-20	Not enough failures to rank	Not enough failures to rank	Not enough failures to rank	Not enough failures to rank

Component	Sn37Pb/Sn	SAC305/Sn	Sn37Pb/NiPdAu	SAC305/NiPdAu	Sn37Pb /Sn37Pb Dip	SAC305 /SAC305 Dip
TQFP-144	1	1	1	1	1	2

Component	Sn37Pb/SnPb	Sn37Pb/Sn	Sn37Pb/SnBi	SAC305/Sn	SAC305/SnBi	SAC305/SnPb	Rwk Sn37Pb/SnPb	Rwk Sn37Pb/Sn (SnPb Profile)	Rwk Sn37Pb/Sn (Pb-Free Profile)	Rwk SAC305/SnBi
TSOP-50	Not enough failures to rank	Not enough failures to rank	Not enough failures to rank	Not enough failures to rank	Not enough failures to rank	Not enough failures to rank	2	2	2	2

5.2.2.1 BGA Components

Many of the BGA failures (SnPb/SnPb balls, SAC305/SAC405 balls, and mixed technologies) were due to pad cratering. This suggests that Pb-free laminates may be the weakest link for large area array components.

Microsections made at the end of Mechanical Shock Testing showed that the corner solder joints failed first. The SnPb/SnPb sections showed pad cratering, PWB trace cracking, and solder joint cracking on the component side (Figure 20).

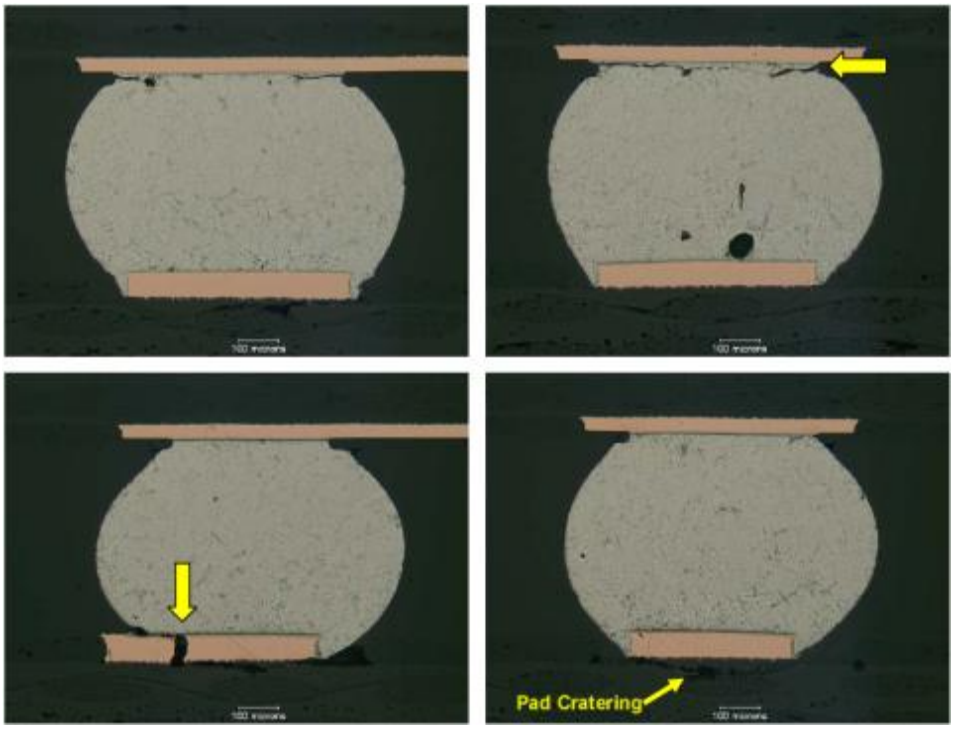

Figure 20 - Test Vehicle 34 - Four Corner Balls of BGA U6 (SnPb Solder/SnPb Balls)

The SAC305/SAC405 sections showed PWB trace cracking and solder joint cracking at the component side intermetallic layer (Figure 21). Which failure mechanism occurred first could not be determined from the microsections.

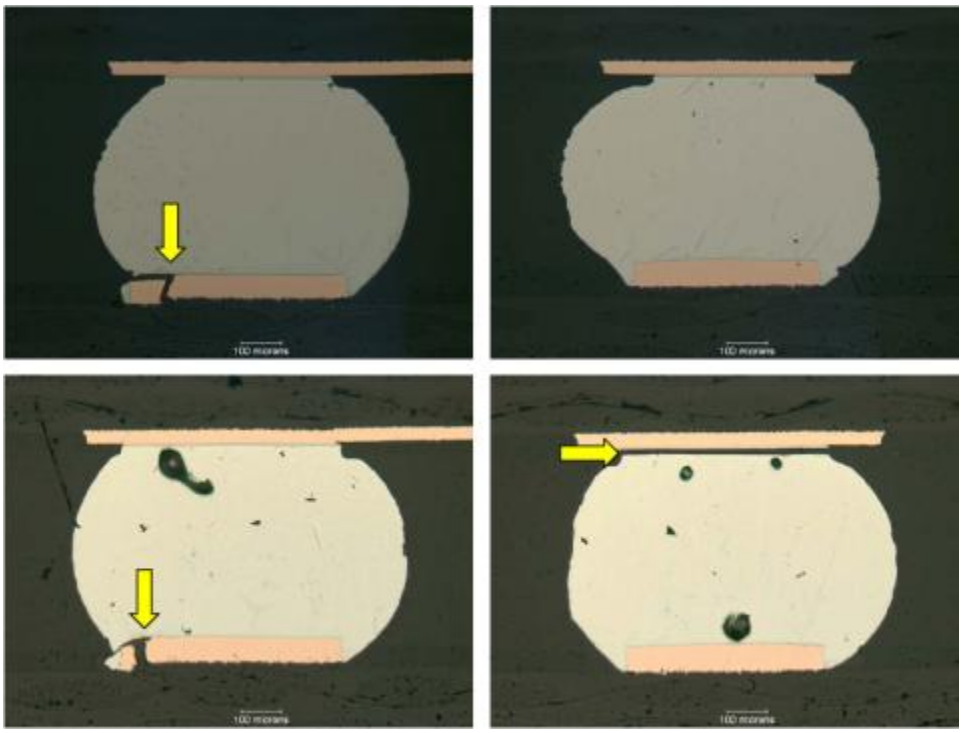

Figure 21 - Test Vehicle 89 - Four Corner Balls of BGA U2 (SAC305 Solder/SAC405 Balls)

A number of BGA's fell off of the test vehicles during the shock test which allowed the failure mechanisms to be examined more closely.

Surprisingly, on the SnPb/SnPb BGA's that fell off, almost 100% of the solder joints failed by pad cratering. The BGA balls and associated PWB copper pads were missing from the test vehicles (Figure 22 and Figure 23).

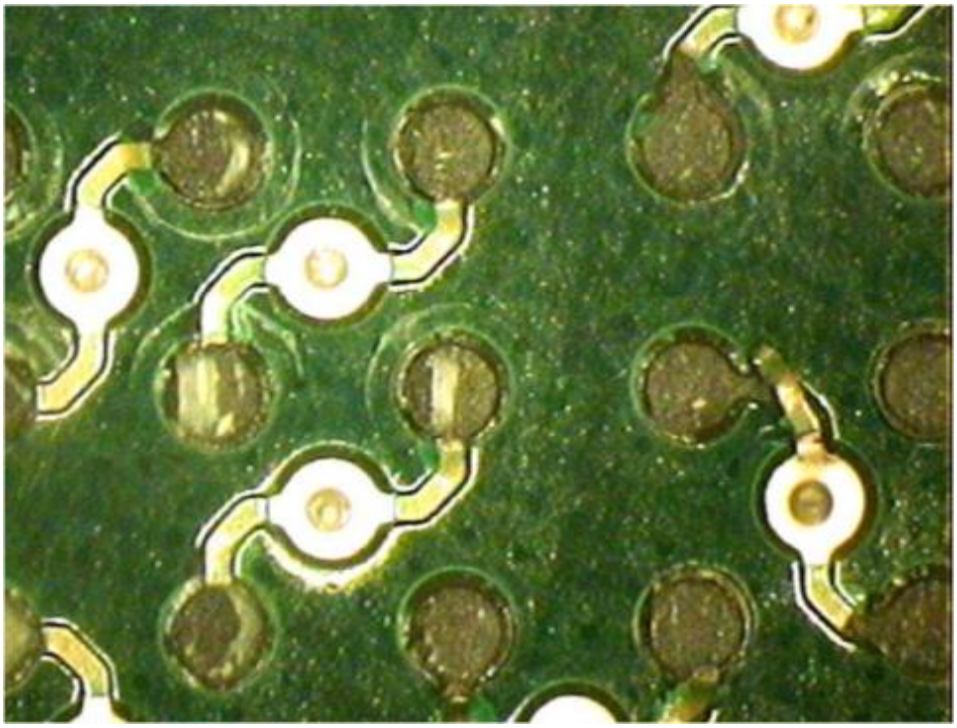

Figure 22 - Test Vehicle 30 BGA U2 with Missing Pads (SnPb Solder/SnPb Balls)

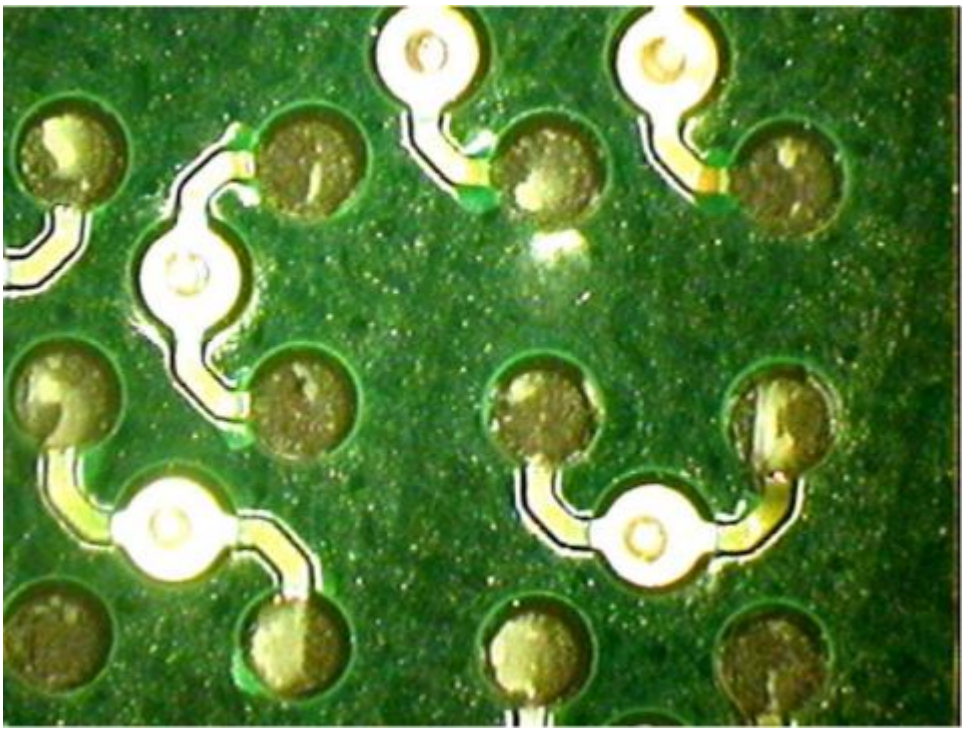

Figure 23 - Test Vehicle 30 BGA U4 with Missing Pads (SnPb Solder/SnPb Balls)

No SAC305/SAC405 BGA's fell off during the test. The only purely Pb-free BGA that fell off was one reworked using flux only and a BGA with SAC405 balls. For this BGA, 16% of the balls remained with the PWB with the solder joints failing on the component side (although most

of the remaining balls also showed signs of PWB pad cratering). The balance of the BGA balls and associated PWB copper pads were missing from the test vehicle (Figure 24 and Figure 25).

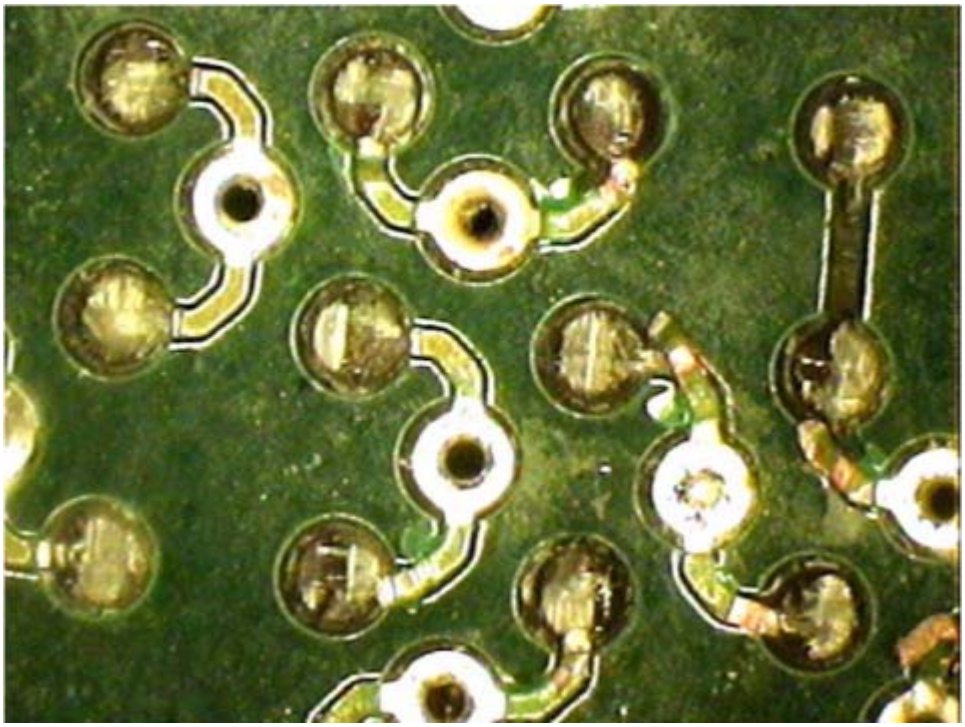

Figure 24 - Test Vehicle 193 BGA U21 with Missing Pads (Flux Only/SAC405 Balls)

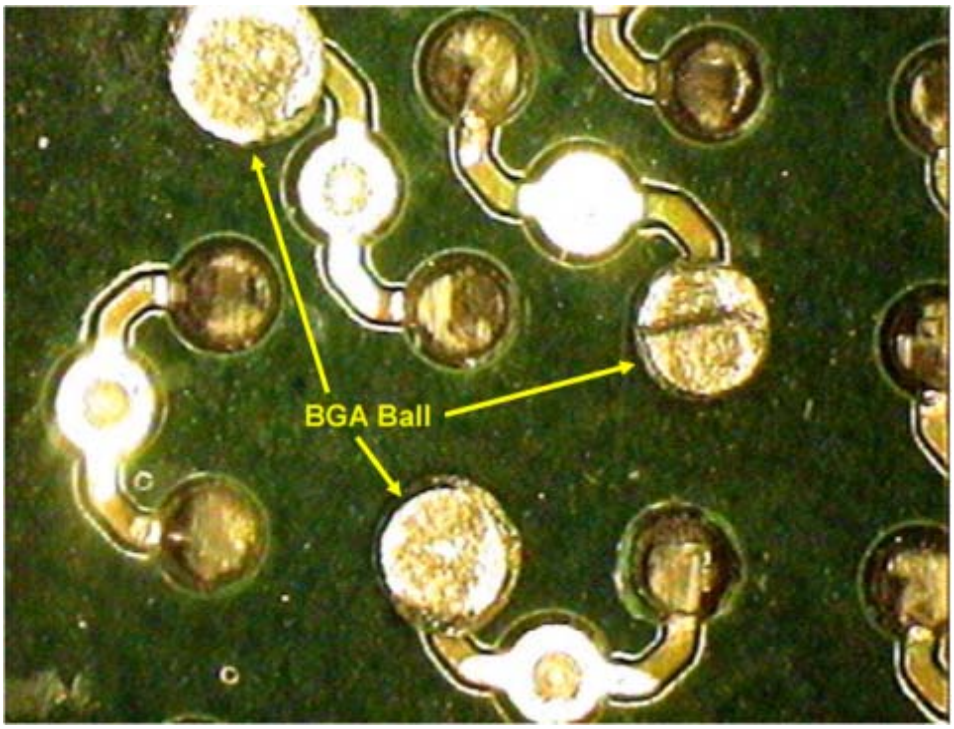

Figure 25 - Test Vehicle 193 BGA U21 with Missing Pads (Flux Only/SAC405 Balls)

5.2.2.2 CLCC Components

For the CLCC-20 components, the SnPb/SnPb controls outperformed the combinations of SAC305/SAC305, SnPb/SAC305, and SAC305/SnPb (Figure 26).

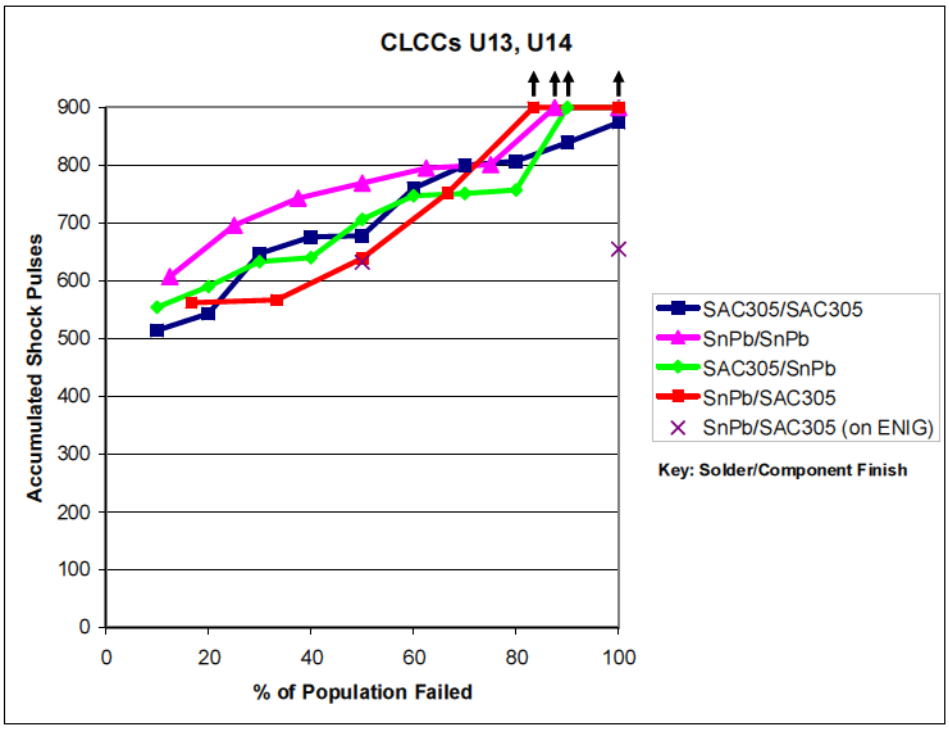

Figure 26 - Combined Data from CLCC's U13 and U14

Test vehicle inspections made at the end of Mechanical Shock Testing showed cracks in a CLCC solder joint (Figure 27).

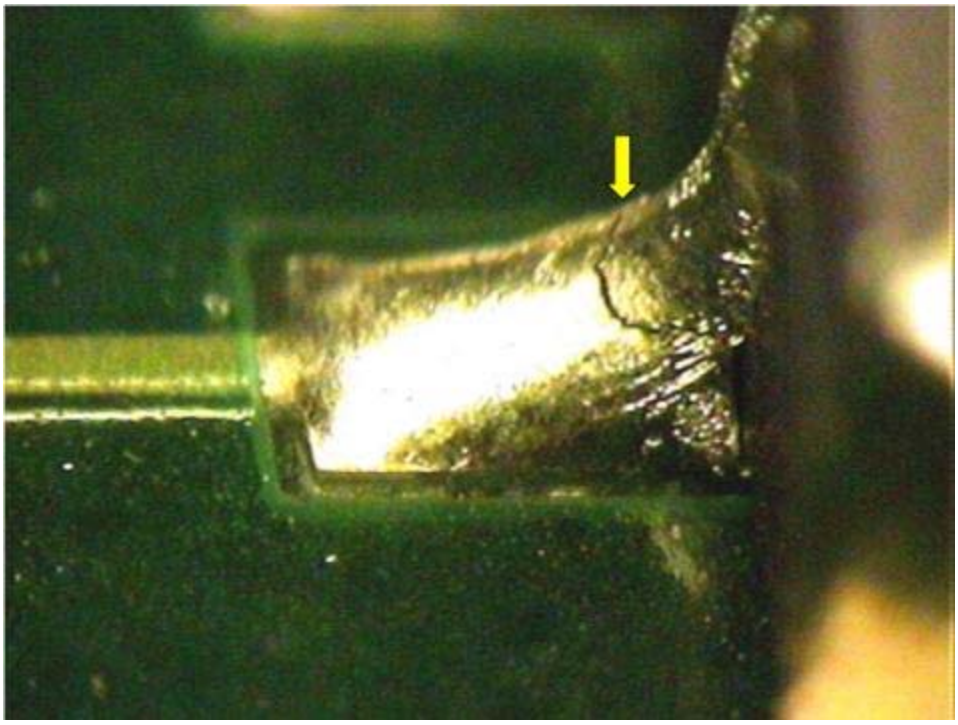

Figure 27 - Test Vehicle 191 CLCC U10 (Cracked SAC305/SnPb Solder Joint)

5.2.2.3 CSP Components

The CSP daisy chain pattern on the test vehicles was incorrect with the result that only the outer perimeter balls of each CSP formed an electrically continuous path (Figure 28). In order for a CSP to be detected as failed, both legs of the outer perimeter needed to fail.

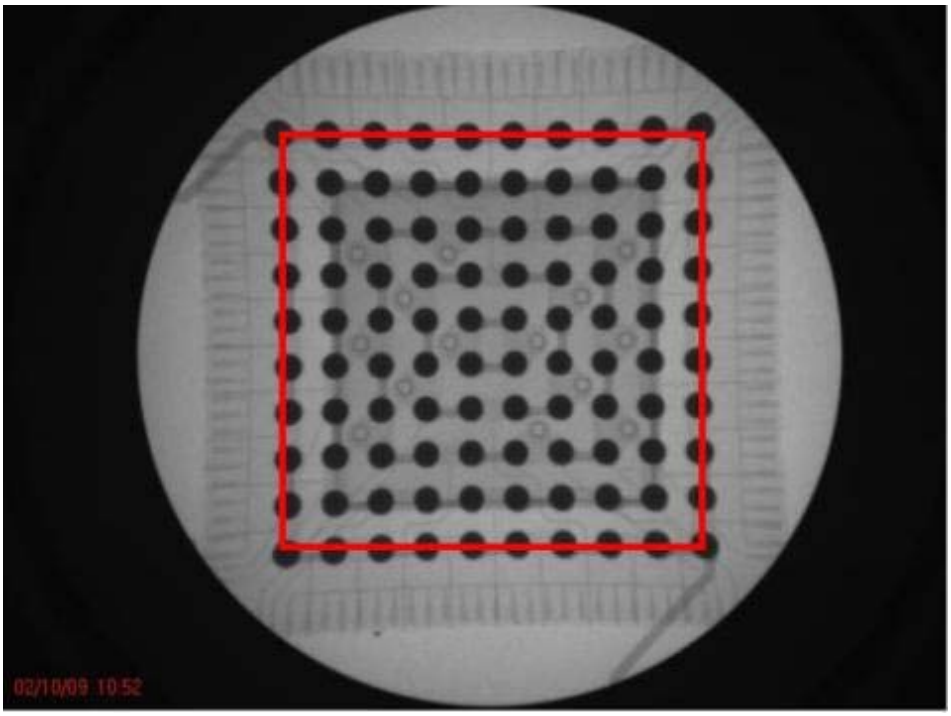

Figure 28 - X-Ray of a CSP-100
Showing that only the outer balls form a daisy-chain (Red Lines).

The combination of SAC305 solder/SAC105 balls generally performed as well as the SnPb/SnPb controls in mechanical shock. Microsections made at the end of the test showed that the corner solder joints failed first. The SnPb/SnPb solder joints formed cracks primarily on the component side (Figure 29). The SAC305/SAC105 solder joints formed cracks primarily on the component side and also showed evidence of pad cratering (Figure 30).

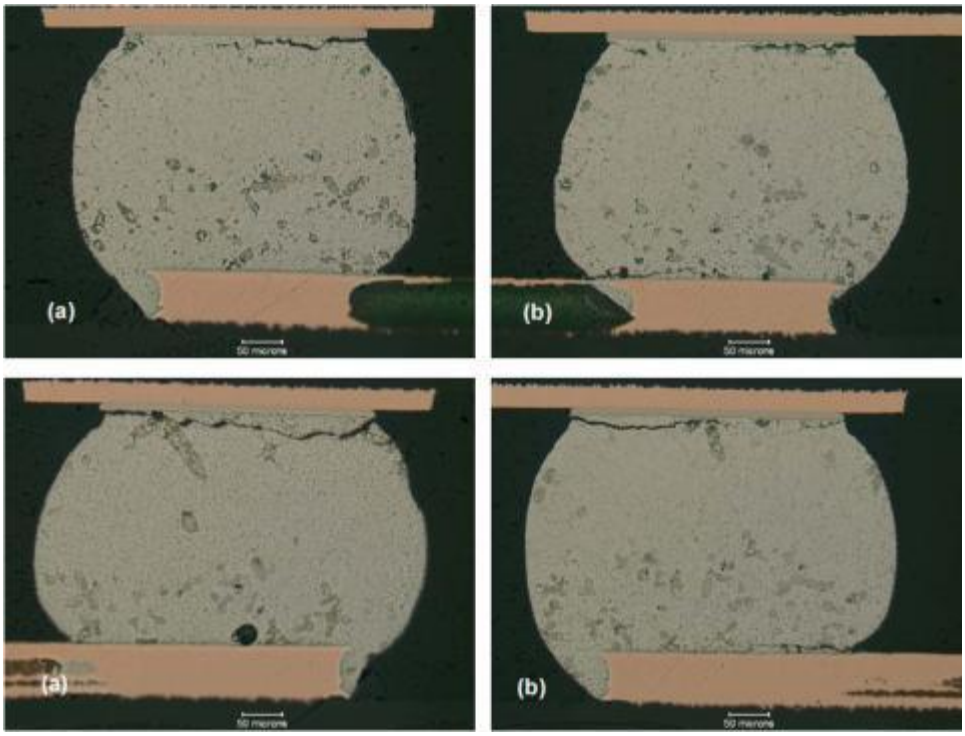

Figure 29 - Test Vehicle 34 – CSP U33
(a) Corner Ball, (b) Ball Adjacent to Corner Ball (SnPb Solder/SnPb Balls)

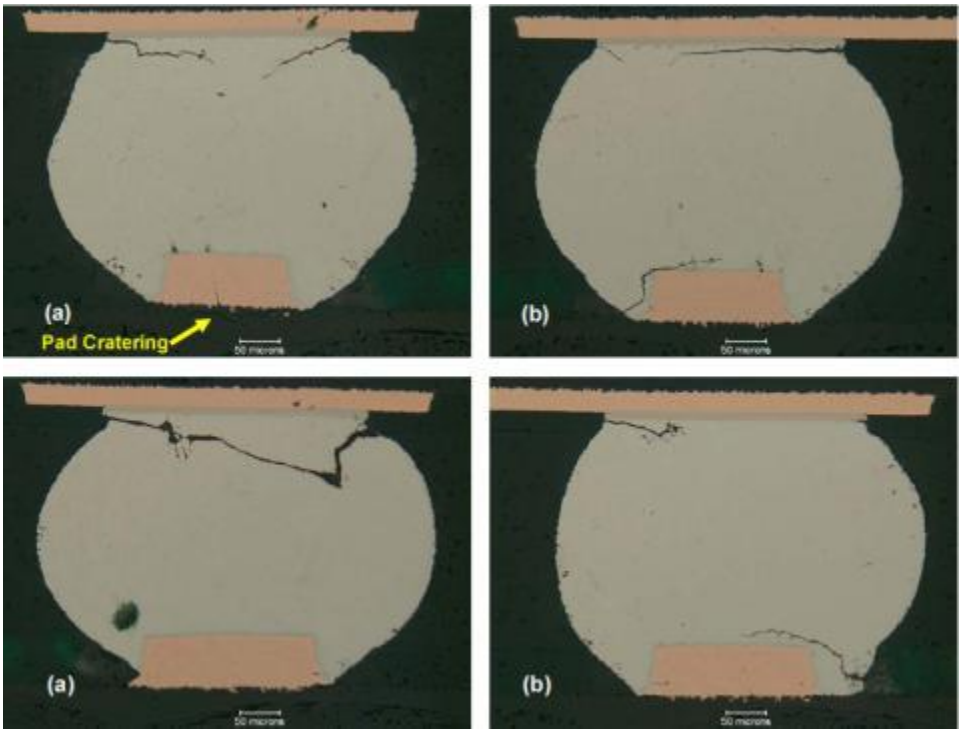

Figure 30 - Test Vehicle 89 – CSP U33
(a) Corner Ball, (b) Ball Adjacent to Corner Ball (SAC305 Solder/SAC105 Balls)

5.2.2.4 PDIP Components

The combination of SN100C solder/Sn component finish generally performed as well as the SnPb/SnPb controls in mechanical shock although some of the SN100C/Sn solder joints failed early. Microsections made at the end of the test showed that the corner solder joints failed before the other solder joints. The topside solder fillet would crack first followed by cracking of the lead where it necks down at the top of the PTH (Figure 31 and Figure 32).

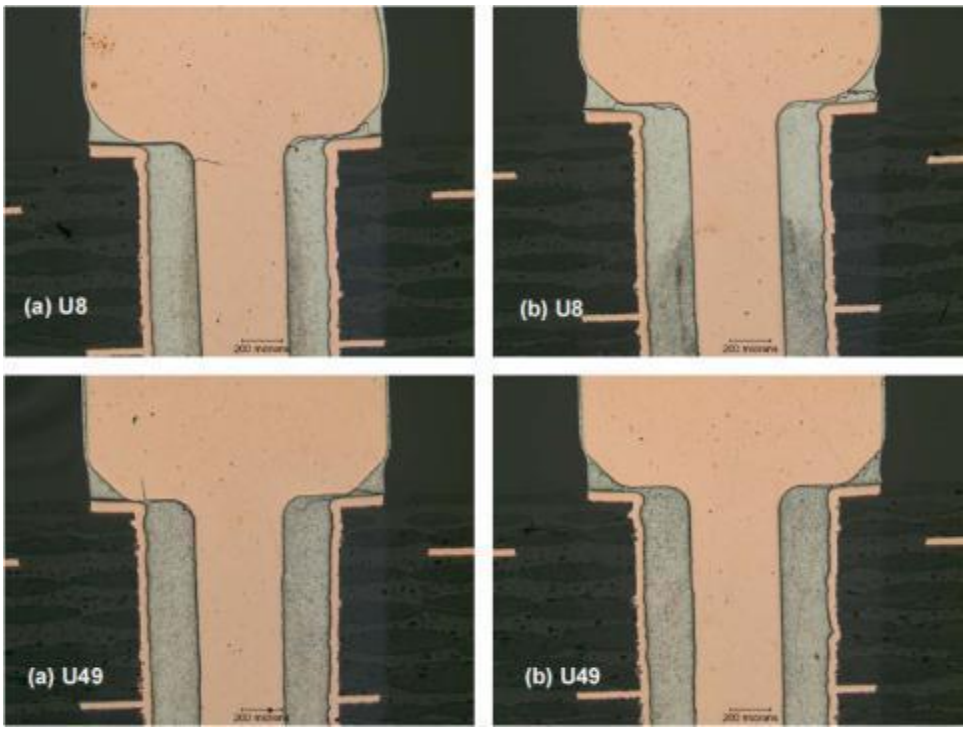

Figure 31 - Test Vehicle 34 – PDIPs U8 and U49 (a) Corner Lead, (b) Lead Adjacent to Corner Lead (SnPb Solder/SnPb Finish)

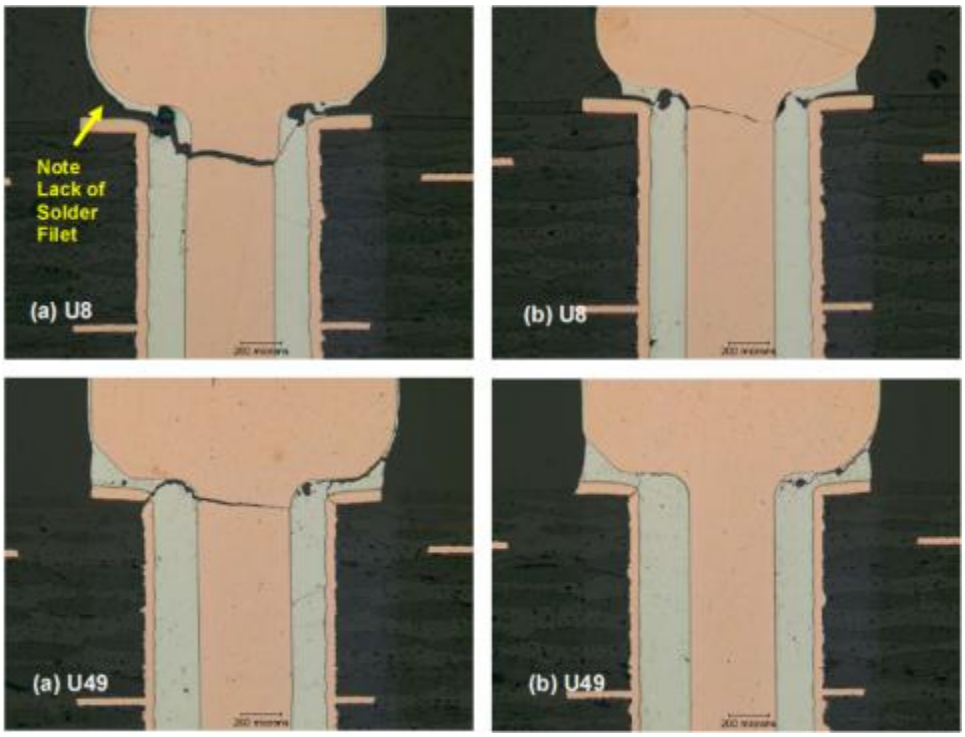

Figure 32 - Test Vehicle 89 – PDIPs U8 and U49 (a) Corner Lead, (b) Lead Adjacent to Corner Lead (SN100C Solder/Sn Finish)

Another observation is that many of the PDIP's soldered with SN100C exhibited trace cracking at the corner solder joints (Figure 33 and Figure 34). This failure mode was not observed as often with the PDIP's assembled with SnPb solder.

Figure 33 - Test Vehicle 89 PDIP U30 (Cracked Trace, SN100C)

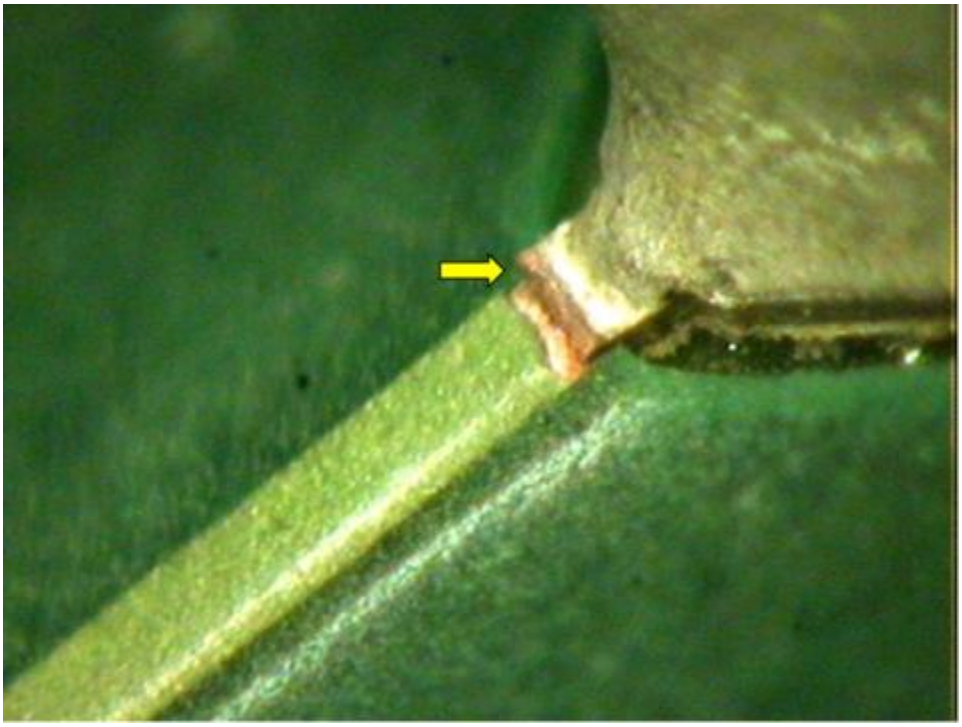

Figure 34 - Test Vehicle 89 PDIP U38 (Cracked Trace, SN100C)

Several of the earliest failures on the "Manufactured" test vehicles were SN100C/Sn solder joints. One possible cause is that some of the SN100C joints did not have a substantial topside solder filet (Figure 35). This could have resulted in a point of high stress concentration where the PDIP lead necked down resulting in premature failure of the lead. The trace cracking mentioned above is another possible cause for the early failures. Many of the PDIP's that failed early exhibited both failure modes so it could not be definitely determined which occurred first.

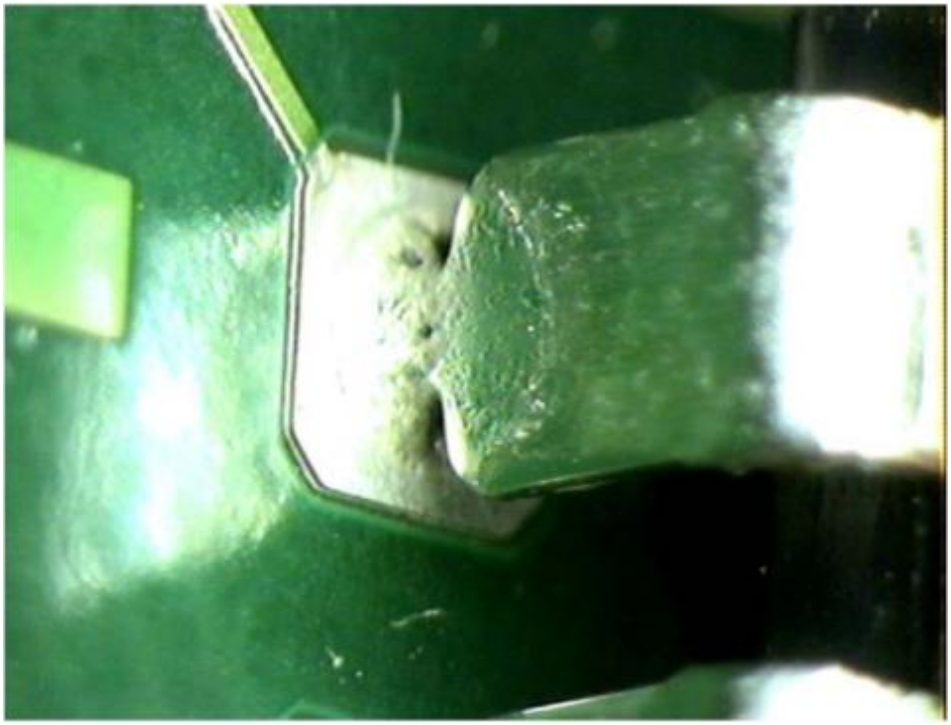

Figure 35 - Test Vehicle 89 PDIP U51 (SN100C)

5.2.2.5 QFN Components

The QFN components were resistant to failure under the conditions of this test. Only two QFN's failed (on Shocks 827 and 873) and they were both SAC305/Sn. Not enough failures occurred to rank the solders. A PWB trace required for electrically monitoring QFN U15 was missing on every test vehicle due to a design error. Therefore, no data was generated for this component.

5.2.2.6 TQFP Components

Most of the TQFP-144's had broken and/or missing leads at the end of the test (Figure 36). Since most of the failures appeared to be due to broken leads, the scatter in the test data for all of the TQFP solder/finish combinations was small. SAC305/Sn was equivalent in performance to SnPb/Sn, SnPb/NiPdAu (on immersion Ag), and SnPb/NiPdAu (on ENIG). SAC305/NiPdAu was superior to the SnPb/Sn controls in performance.

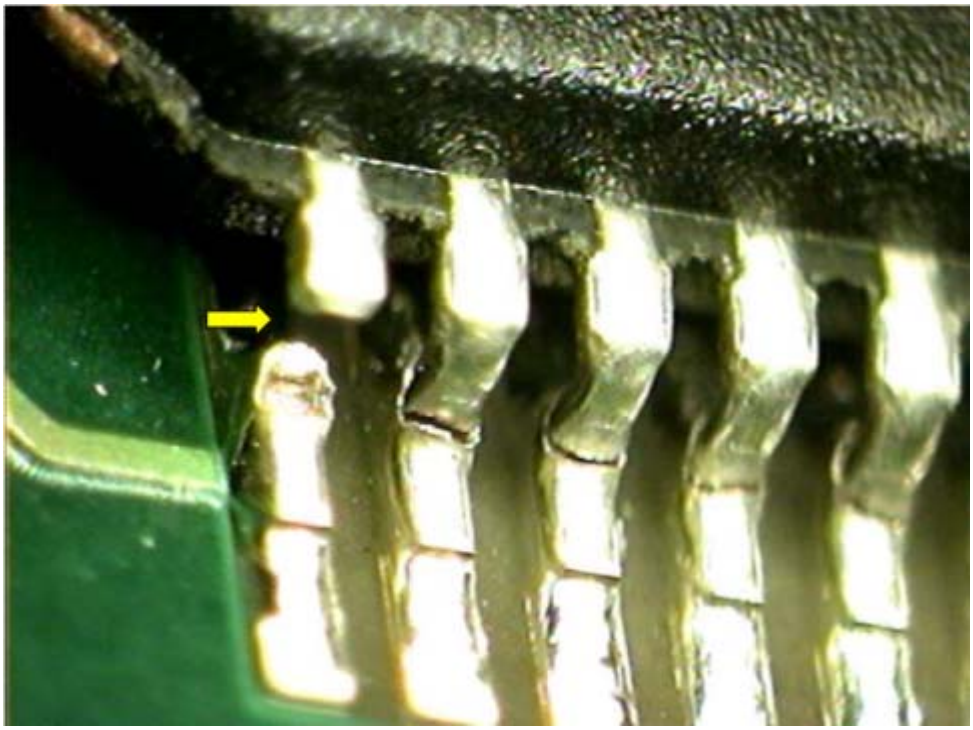

Figure 36 - Test Vehicle 89 TQFP U3 (Cracked Leads, Missing Lead)

For this test, some Sn-plated TQFP-144 leads were dipped into either molten SnPb or SAC305 to evaluate the effectiveness of the hot solder dipping on tin whisker formation. The combination of SnPb/SnPb Dip was equivalent to the SnPb/Sn control in performance but the SAC305/SAC305 Dip performance was inferior to that of the SnPb/Sn control due to some early failures (Figure 37).

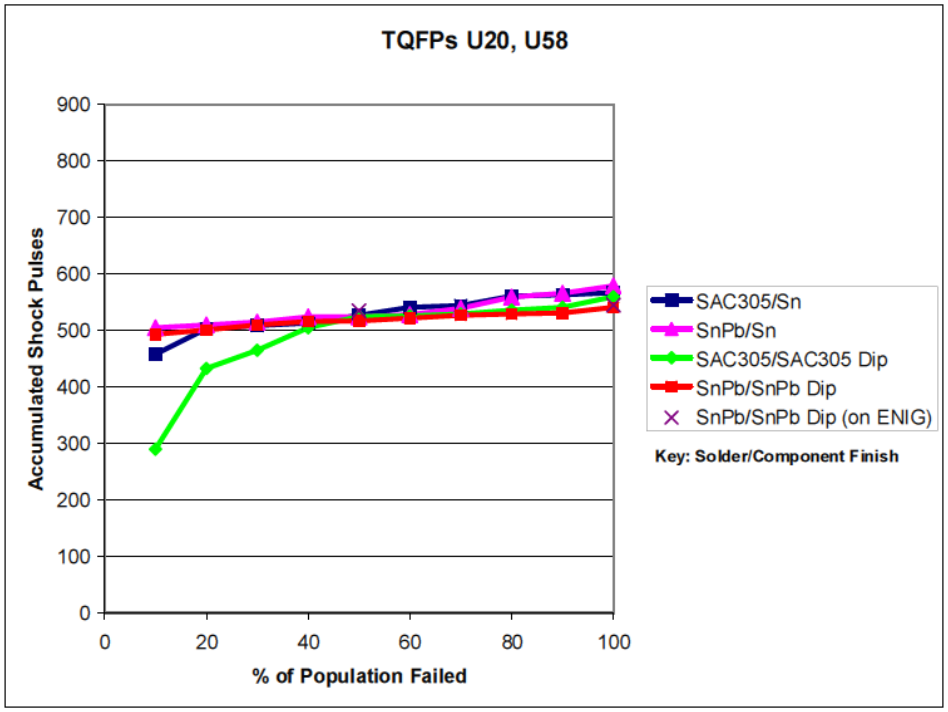

Figure 37 - Combined Data from TQFP's U20 and U58

5.2.2.7 TSOP Components

TSOP components that were not reworked were resistant to failure under the mechanical shock conditions of this test and the lack of failures made it impossible to rank the solder/finish combinations. Un-reworked SnPb/Sn on ENIG did have a few failures but they occurred late in the test. Mixed solder/finish combinations also had few failures.

Rework had a definite negative effect on performance. SnPb/SnPb reworked with SnPb/SnPb and SAC305/Sn reworked with SnPb/Sn underperformed the un-reworked SnPb/SnPb controls which had no failures (Figure 38).

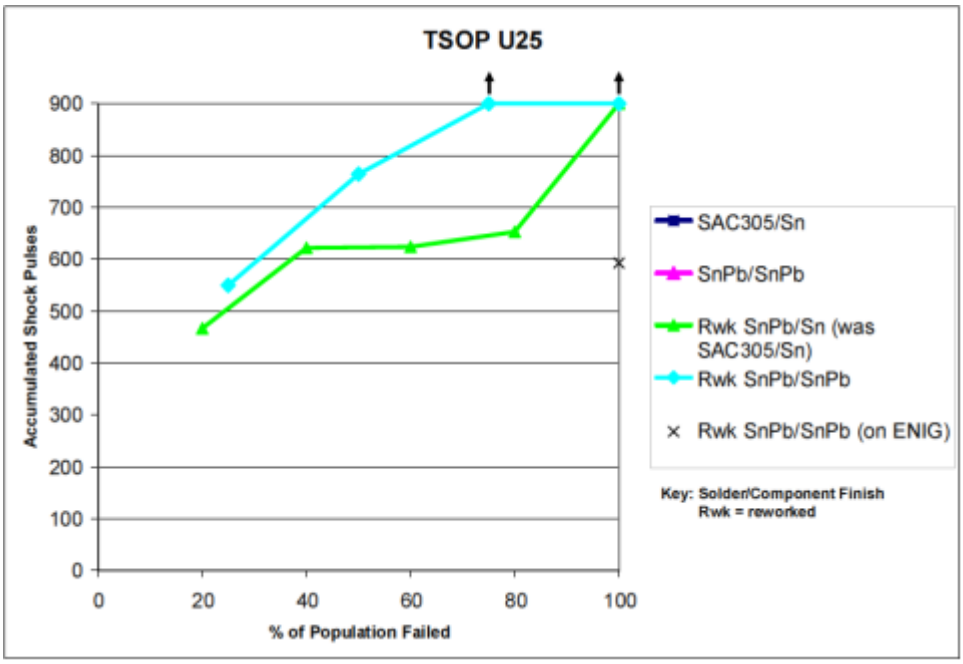

Figure 38 - TSOP U25 Data

SnPb/SnPb reworked with SnPb/Sn and SAC305/SnBi reworked with SAC305/SnBi underperformed the un-reworked SnPb/SnPb and SAC305/SnBi controls which had no failures (Figure 39).

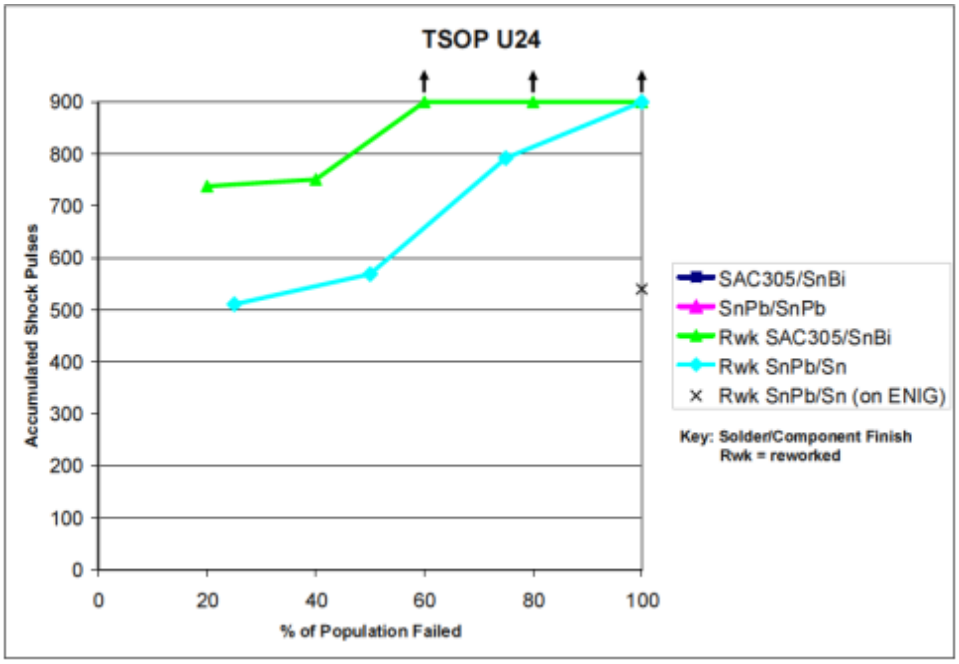

Figure 39 - TSOP U24 Data

Test vehicle inspection made at the end of Mechanical Shock Testing showed cracks in a TSOP solder joint (Figure 40).

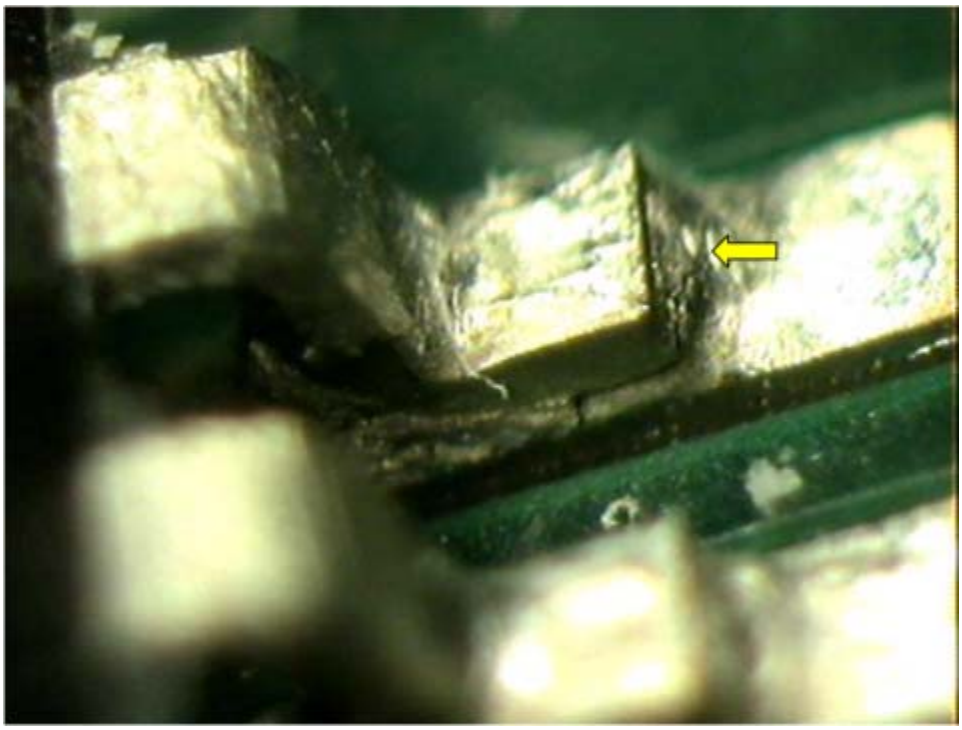

Figure 40 - Test Vehicle 34 TSOP U61 (Cracked SnPb/SnPb Solder Joint)

5.3 Combined Environments Test

5.3.1 Combined Environments Test Method

The Combined Environments Test (CET) for the NASA-DoD Lead-Free Electronics Project was based on a modified Highly Accelerated Life Test (HALT), a process in which products are subjected to accelerated environments to find weak links in the design and/or manufacturing process.

The CET process can identify design and process related problems in a much shorter time frame than other development tests. In this project, CET was used determine the operation and endurance limits of the solder alloys by subjecting the test vehicles to accelerated environments. The limits identified in CET were used to compare performance differences in the Pb-free test alloys and mixed solder joints vs. the baseline standard SnPb (63/37) alloy. The primary accelerated environments are temperature extremes (both limits and rate of change) and vibration (pseudo-random six degrees of freedom [DOF]) used in combination.

This test was performed utilizing a temperature range of –55 to 125°C with 20°C/minute ramps. The dwell times at each temperature extreme are the times required to stabilize the test sample plus a 15-minute soak. 10 g_{rms} pseudo-random vibration was applied for the duration of the thermal cycle. Testing was continued until sufficient data was generated to obtain statistically significant Weibull plots indicating relative solder joint endurance (cycles to failure) rates. If significant failure rates were not evidenced after 50 cycles, the vibration levels were increased in increments of $5g_{rms}$ and continued cycling for an additional 50 cycles. The process was repeated until all parts failed or 55 g_{rms} was reached.

Table 11 - Combined Environments Test Methodology

Parameters	▪ -55°C to +125°C ▪ Number of cycles ≥ 500 ▪ 20°C/minute ramp ▪ 15 minute soak ▪ Vibration for duration of thermal cycle ▪ 10 G_{rms}, initial ▪ Increase 5 G_{rms} after every 50 cycles ▪ 55 G_{rms}, maximum		
Number of Test Vehicles Required			
Mfg. SnPb = 5	Mfg. LF = 5	Mfg. LF {SN100C} = 5	Mfg. LF {ENIG} = 1
Rwk. SnPb = 5	Rwk. SnPb {ENIG} = 1	Rwk. LF = 5	
Trials per Specimens	1		

5.3.2 **Combined Environments Test Results Summary**

The complete test report, "NASA/DOD Lead-Free Electronics Project: Combined Environments Test", can be found on the NASA TEERM website (http://teerm.nasa.gov/NASA_DODLeadFreeElectronics_Proj2.html).

Overall, the component type had the greatest effect on solder joint reliability performance. The plated-through-hole components {PDIP-20} proved to be more reliable than the surface mount technology components. Of the surface mount technology, the TQFP-144 and QFN-20 components performed the best while the BGA-225 components performed the worst.

The solder alloy had a secondary effect on solder joint reliability. In general, tin-lead finished components soldered with tin-lead solder paste were the most reliable. In general, tin-silver copper soldered components were less reliable than the tin-lead soldered controls. The lower reliability of the tin-silver-copper 305 solder joints does not necessarily rule out the use of tin silver copper solder alloy on military electronics. In several cases, tin-silver-copper 305 solder performed statistically as good as or equal to the baseline, tin-lead solder.

The effect of tin-lead contamination on BGA-225 components degrades early life performance of tin-copper solder paste. It can also degrade early life performance of tin-silver-copper 305 solder paste. The effect of tin-lead contamination on BGA-225 components soldered with tin-silver-copper 305 solder paste was less than the effect on tin-lead contamination on tin-copper solder.

CSP-100 components are the exception, where tin-lead CSP-100 components soldered with tin-silver-copper 305 solder paste performed better than or equal to tin-lead CSP-100 components soldered with tin-lead solder paste. The chip scale package components were not drafted correctly during the design stage, therefore CSP-100 components results can only be used to compare within chip scale packages.

The probability plots of soldering tin-lead and tin-silver-copper 305 solder components onto electroless nickel immersion gold (ENIG) finished test vehicles were compared using BGA-225 and CLCC-20 components. In general, tin-lead components soldered with tin-silver-copper 305 solder paste onto immersion gold performed better than tin-silver-copper 305 components soldered onto ENIG finished test vehicles. One exception is the performance of tin-lead CLCC-20 components soldered with tin-silver-copper 305 solder paste onto ENIG test vehicle performing better than the immersion gold test vehicle. Keep in mind, the ENIG sample size consisted of only two test vehicles.

In general, reworked components were less reliable than the unreworked components. This is especially true with reworked Pb-free CSP-100, reworked Pb-free BGA-225 and unreworked Pb-free TQFP-144 components; these components did not survive beyond 200 cycles. The exceptions were the immersion gold plated-through hole components, nickel-palladium-gold TQFP-144, matte tin and tin-lead QFN-20, and tin PDIP-20 components where a majority of these components were soldered with tin-lead solder and did not fail. Approximately, 37% of rework test vehicle components soldered with tin-lead solder paste failed, whereas, 53% of

rework test vehicle components soldered with tin-silver-copper 305 solder paste failed. This suggests that reworking surface mount technology components with Pb-free solder continues to pose processing challenges.

When comparing the performance of components soldered onto the two different test vehicle board finishes of immersion silver and electroless nickel immersion gold (ENIG), the immersion silver finish of the manufactured test vehicles had better reliability of solder joints than components soldered onto and ENIG surface finish. This is supported in several of the 2-parameter Weibull plots generated with the data.

Data from the Combined Environments Test was segregated by component type, component finish and solder alloy, see Table 12 and Table 13. Test vehicles soldered with tin-lead solder had the fewest solder joint failures overall. Test vehicles soldered with tin-silver-copper solder were second best. Lastly, the test vehicles soldered with tin-copper solder paste had the worst performance.

Table 12 - Number of Failed Components by Board Finish, Component, Component Finish and Solder Alloy on Manufactured Test Vehicles

Board Finish	Component	Finish	Solder	Number of Failed Components
Im. Ag	BGA-225	SAC405	SAC305	76% (19 of 25)
			SN100C	76% (19 of 25)
			SnPb	92% (23 of 25)
		SnPb	SAC305	84% (21 of 25)
			SN100C	88% (22 of 25)
			SnPb	60% (15 of 25)
Im. Ag	CLCC-20	SAC305	SAC305	96% (24 of 25)
			SN100C	96% (24 of 25)
			SnPb	92% (23 of 25)
		SnPb	SAC305	100% (25 of 25)
			SN100C	88% (22 of 25)
			SnPb	84% (21 of 25)
Im. Ag	CSP-100	SAC105	SAC305	32% (8 of 25)
			SN100C	44% (11 of 25)
			SnPb	68% (17 of 25)
		SnPb	SAC305	20% (5 of 25)
			SN100C	48% (12 of 25)
			SnPb	16% (4 of 25)
Im. Ag	PDIP-20	NiPdAu	SN100C	0% (0 of 28)
			SnPb	0% (0 of 20)
		Sn	SN100C	10% (5 of 52)
			SnPb	0% (0 of 20)
Im. Ag	PTH	Im. Ag	SN100C	0% (0 of 10)
			SnPb	0% (0 of 5)
Im. Ag	QFN-20	Matte Sn	SAC305	20% (5 of 25)
			SN100C	40% (10 of 25)
			SnPb	20% (5 of 25)
Im. Ag	TQFP-144	Matte Sn	SAC305	24% (6 of 25)
			SN100C	52% (13 of 25)
			SnPb	32% (8 of 25)
		SnPb Dip	SAC305	0% (0 of 25)
			SN100C	60% (15 of 25)
			SnPb	8% (2 of 25)
Im. Ag	TSOP-50	SnBi	SAC305	92% (23 of 25)
			SN100C	92% (23 of 25)
			SnPb	64% (16 of 25)
		SnPb	SAC305	60% (15 of 25)
			SN100C	84% (21 of 25)
			SnPb	64% (16 of 25)

Table 13 - Number of Failed Components by Board Finish, Component, Component Finish and Solder Alloy on Manufactured Test Vehicles

Board Finish	Component	Finish	Solder	Number of Failed Components
ENIG	BGA-225	SAC405	SAC305	0% (0 of 5)
		SnPb	SAC305	100% (5 of 5)
ENIG	CLCC-20	SAC305	SAC305	60% (3 of 5)
		SnPb	SAC305	60% (3 of 5)
ENIG	CSP-100	SAC105	SAC305	0% (0 of 5)
		SnPb	SAC305	0% (0 of 5)
ENIG	PDIP-20	Sn	SN100C	0% (0 of 8)
ENIG	PTH	ENIG	SN100C	0% (0 of 1)
ENIG	QFN-20	Matte Sn	SAC305	20% (1 of 5)
ENIG	TQFP-144	Matte Sn	SAC305	0% (0 of 5)
		SnPb Dip	SAC305	0% (0 of 5)
ENIG	TSOP-50	SnBi	SAC305	20% (1 of 5)
		SnPb	SAC305	20% (1 of 5)

Data from the Combined Environments Test, rework test vehicles, was segregated by component type, component finish and solder alloy, see Table 14 and Table 15. Test vehicles soldered with or reworked with tin-lead solder had the fewest solder joint failures. Test vehicles soldered with tin-silver-copper solder were second best. Lastly, the test vehicles soldered with tin-copper solder had the worst performance.

Table 14 - Number of Failed Components by Board Finish, Component, Component Finish, Solder Alloy, New Component Finish and Rework Solder on Rework Test Vehicles

Board Finish	Component	Finish	Solder	New Component Finish	Rework Solder	Number of Failed Components
Im. Ag	BGA-225	SAC405	SAC305	SAC405	Flux Only	60% (9 of 15)
					SnPb	33% (5 of 15)
			SnPb			50% (10 of 20)
		SnPb	SAC305			65% (13 of 20)
			SnPb	SAC405	SnPb	80% (12 of 15)
				SnPb	Flux Only	20% (3 of 15)
Im. Ag	CLCC-20	SAC305	SnPb			98% (49 0f 50)
		SnPb	SAC305			100% (50 of 50)
Im. Ag	CSP-100	SAC105	SAC305	SAC105	Flux Only	20% (3 of 15)
					SnPb	93% (14 of 15)
						60% (3 of 5)
			SnPb			55% (11 of 20)
		SnPb	SAC305			0% (0 of 15)
			SnPb	SAC105	SnPb	7% (1 of 15)
				SnPb	Flux Only	0% (0 of 15)
Im. Ag	PDIP-20	NiPdAu	SnPb			7% (1 of 15)
		Sn	SN100C	Sn	SN100C	20% (2 of 10)
						7% (2 of 30)
			SnPb			13% (2 of 15)
		SnPb	SnPb	Sn	SnPb	40% (4 of 10)
Im. Ag	PTH	ImAg	SN100C			0% (0 of 5)
			SnPb			0% (0 of 5)
Im. Ag	QFN-20	Matte Sn	SnPb			20% (5 of 25)
		SnPb	SAC305			24% (6 of 25)
Im. Ag	TQFP-144	NiPdAu	SAC305			0% (0 of 25)
			SnPb			0% (0 of 25)
		SAC305	SAC305			44% (11 of 25)
		SnPb Dip	SnPb			12% (3 of 25)
Im. Ag	TSOP-50	Sn	SAC305	Sn	SnPb	60% (6 of 10)
			SnPb			20% (3 of 15)
		SnBi	SAC305	SnBi	SAC305	90% (9 of 10)
						67% (10 of 15)
			SnPb			33% (5 of 15)
		SnPb	SAC305			33% (5 of 15)
			SnPb	Sn	SnPb	50% (5 of 10)
				SnPb	SnPb	60% (6 of 10)

Table 15 - Number of Failed Components by Board Finish, Component, Component Finish, Solder Alloy, New Component Finish and Rework Solder on Rework Test Vehicles

Board Finish	Component	Finish	Solder	New Component Finish	Rework Solder	Number of Failed Components
ENIG	BGA-225	SAC405	SnPb			75% (3 of 4)
		SnPb	SnPb	SAC405	SnPb	100% (3 of 3)
		SnPb	SnPb	SnPb	Flux Only	33% (1 of 3)
ENIG	CLCC-20	SAC305	SnPb			100% (10 of 10)
ENIG	CSP-100	SAC105	SnPb			25% (1 of 4)
		SnPb	SnPb	SAC105	SnPb	33% (1 of 3)
		SnPb	SnPb	SnPb	Flux Only	0% (0 of 3)
ENIG	PDIP-20	NiPdAu	SnPb			0% (0 of 3)
		Sn	SnPb			33% (1 of 3)
		SnPb	SnPb	Sn	SnPb	0% (0 of 2)
ENIG	PTH	ENIG	SnPb			0% (0 of 1)
ENIG	QFN-20	Matte Sn	SnPb			20% (1 of 5)
ENIG	TQFP-144	NiPdAu	SnPb			20% (1 of 5)
		SnPb Dip	SnPb			60% (3 of 5)
ENIG	TSOP-50	Sn	SnPb			33% (1 of 3)
		SnBi	SnPb			33% (1 of 3)
		SnPb	SnPb	Sn	SnPb	100% (2 of 2)
		SnPb	SnPb	SnPb	SnPb	100% (2 of 2)

5.3.3 Combined Environments Failure Analysis

After completing Combined Environments Testing, the test vehicles were removed from the test chamber and inspected per J-STD-001, Class 3 requirements. The components selected for failure analysis are listed in Table 16.

Table 16 - Components selected for failure analysis based on when a failure was recorded during Combined Environments Testing

Test Vehicle	Component Location	Reason for Failure Analysis	FA Performed by
21	U34	Mfg group - No signal, failed at 0 cycles	COM DEV
21	U57	Mfg group - Failed at cycle 1	COM DEV
23	U30	Mfg group - Survived 650 cycles, surrounded by components that fell off	Nihon Superior
23	U43	Mfg group - Failed at 120 cycles, located near center of TV	Nihon Superior
72	U29	Mfg group - Location in chamber (low fails); failed at 161 cycles	Nihon Superior
117	U4	Mfg group - Failed at 20 cycles; SN100C solder paste used	Lockheed Martin
119	U36	Mfg group - Surrounded by components that fell off; failed at 233 cycles	COM DEV
119	U39	Mfg group - Surrounded by components that fell off; failed at 318 cycles	COM DEV
140	U11	Rwk group - Damaged pad from rework - Failed at 398 cycles	Lockheed Martin
142	U13	Rwk group - Adjacent to Reworked components, survived all 650 cycles	COM DEV
158	U6	Rwk group - Reworked component failed at cycle 1	Nihon Superior
180	U21	Rwk group - Reworked component failed at cycle 1	Nihon Superior
181	U56	Rwk group - Reworked component failed at cycle 1	COM DEV
181	U25	Rwk group - Reworked component failed at cycle 1	COM DEV
183	U41	Rwk group - Failed at cycle 1, was not reworked	Lockheed Martin

5.3.3.1 Test Vehicle 21

Component location U34 is a TQFP-144 component from SnPb manufactured (Batch C), soldered with SnPb on SnPb dip component finish. This component did not have a signal and failed before one complete cycle. Figure 41 is the optical micrograph showing insufficient solder observed on lead 72 at 49X magnification.

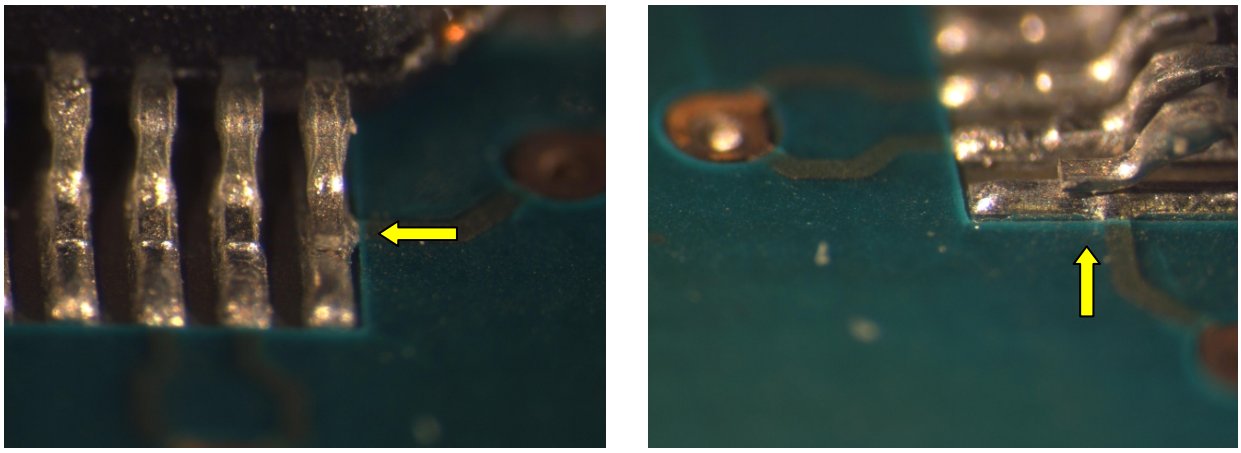

Figure 41 - TV21 U34; Optical Micrograph, Insufficient Solder Observed

Component location U57 is a TQFP-144 component from SnPb manufactured (Batch C), soldered with SnPb on SnPb dip component finish. This component failed at cycle one. Figure 42 is the optical micrograph of residue that was found between leads in two locations. The image on the left shows residue between leads 35 and 36, magnified at 38X. The image on the right shows residue between leads 38 and 39, magnified at 38X.

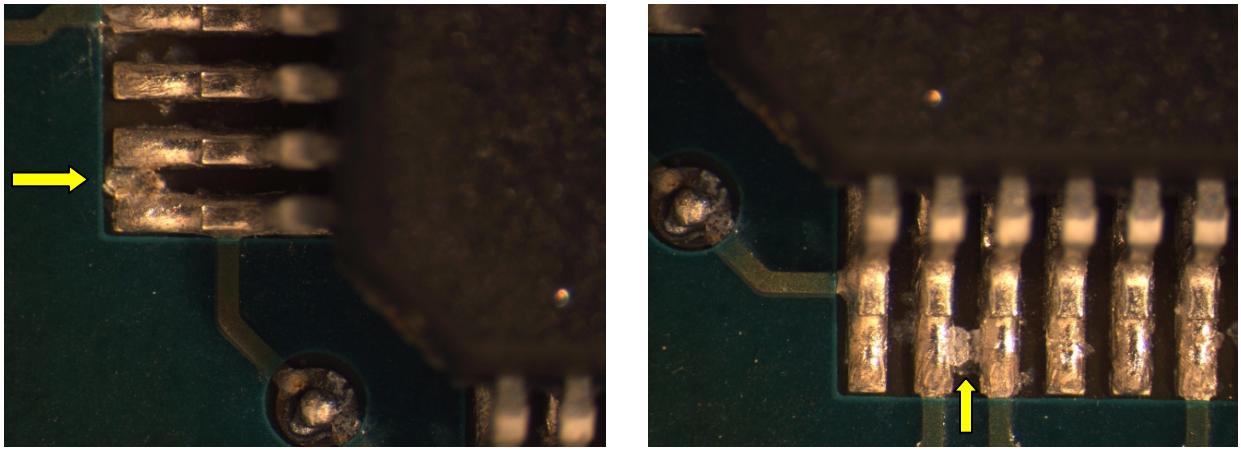

Figure 42 - TV21 U57; Optical Micrograph, Residue between Leads

Figure 43 shows Scanning Electron Microscope (SEM) images taken of the residue found from the images in Figure 42. The image on the left shows the residue that was found between leads 35 and 36, magnified at 90X. The image on the right shows the residue found between leads 38 and 39, magnified at 55X.

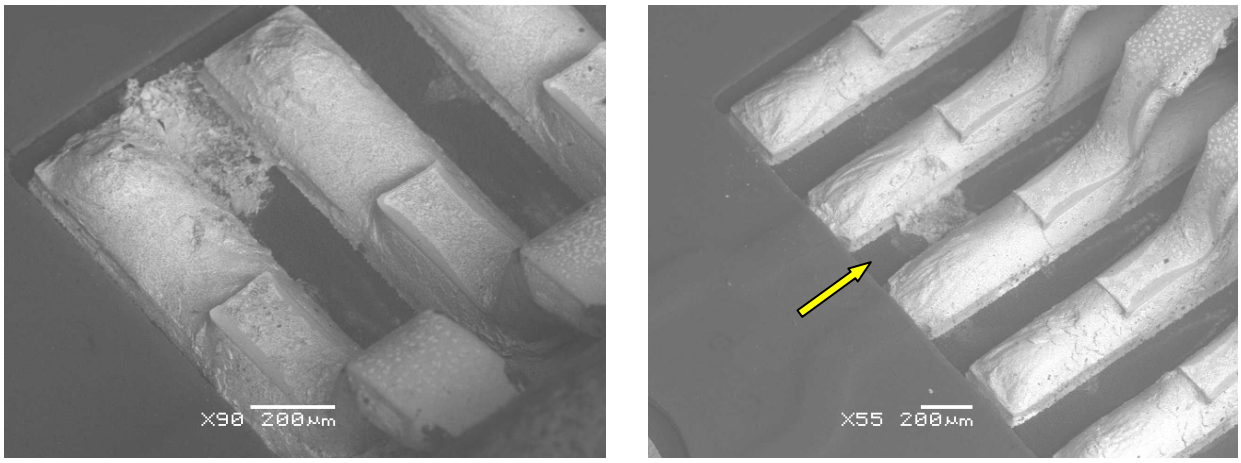

Figure 43 - TV21 U57; Optical Micrograph, Residue between Leads

The possible cause for the immediate failure at cycle one can be found in the Figure 44. The Optical micrograph shows component lead 1 does not contact solder on PWB pad at 49X magnification.

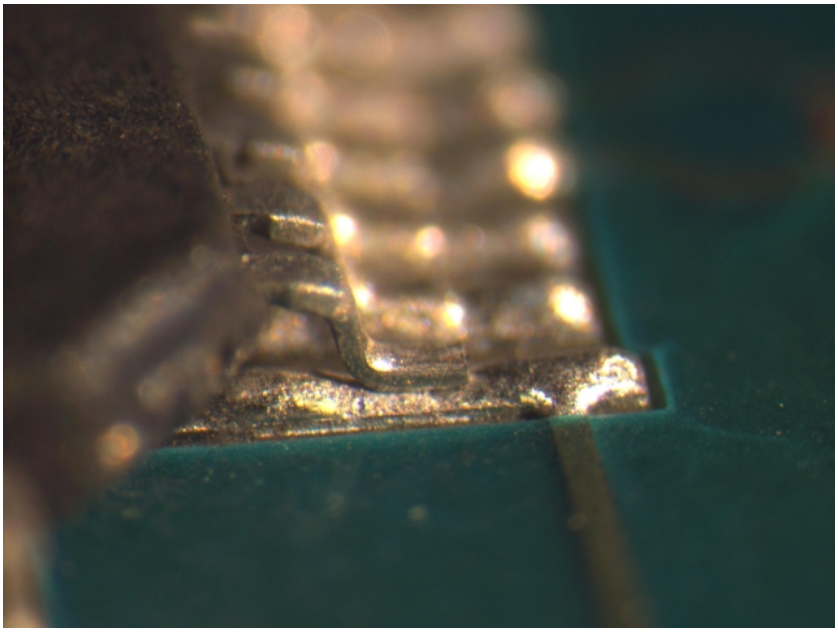

Figure 44 - TV21 U57; Optical Micrograph, Component Lead 1

5.3.3.2 Test Vehicle 23

Component location U30 is a PDIP-20 from the SnPb manufactured (Batch C), soldered with SnPb on tin plated component finish. This component survived all 650 cycles of combined environments testing and it was surrounded by components that fell off during testing.

Figure 45 is an optical micrograph of a PDIP-20 component. The red boxes highlight the two leads that were magnified to indicate observed cracking in the solder joints. The image in the upper right is of lead 11, which indicates two areas with cracking. The image in the bottom left is the top portion of lead 11 and the bottom right image is of lead 10 showing a small crack near the pad. Crack has not caused an electrical failure, yet.

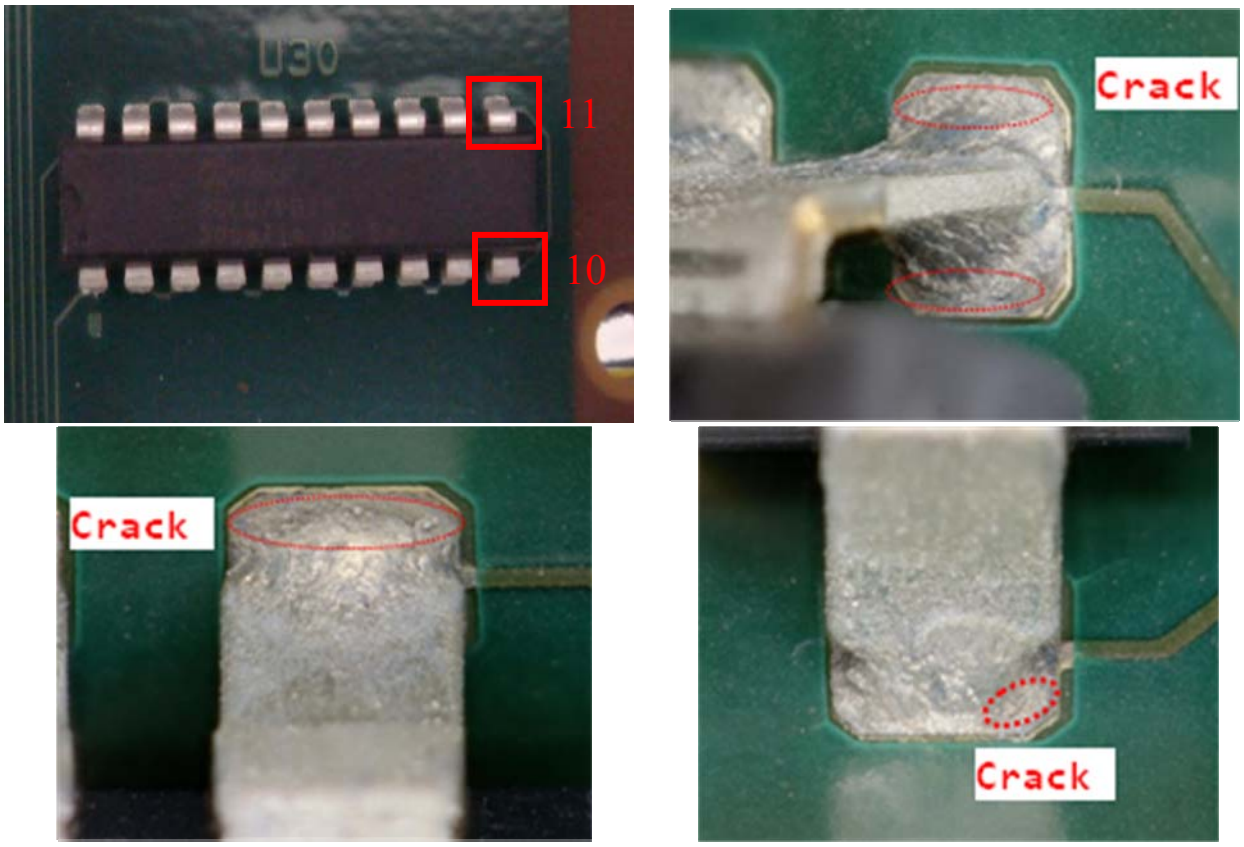

Figure 45 - TV23 U30; Optical Micrograph, PDIP-20

Figure 46 shows cross-sectional micrographs of PDIP-20 leads where the two images on the top are indicating the lead numbering. The cross-sections of leads 1, 5, 19 and 20 were selected as an example of the leads that had large quantities of voids, relative to the other component leads. The dotted lines indicate solder cracks that were found; no break off solder was found during failure analysis.

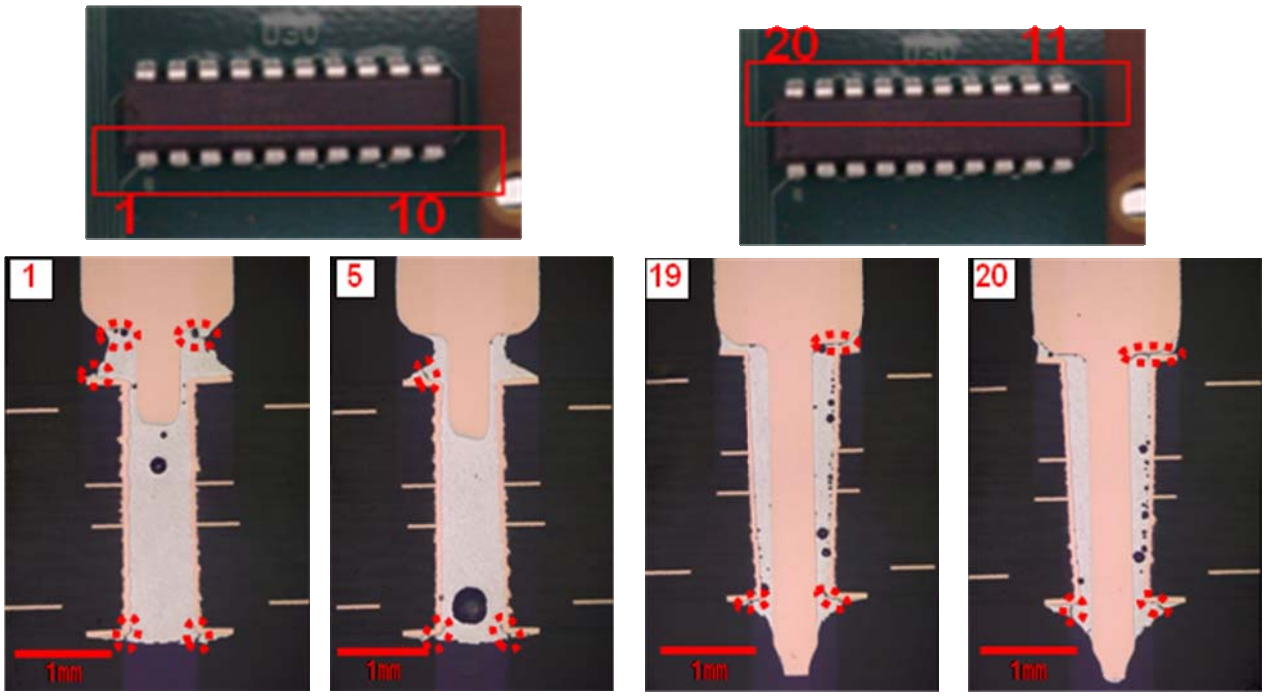

Figure 46 - TV23 U30; Cross-Sectional Micrographs of PDIP-20 Leads

The micrographs in Figure 47 show progression of analysis for lead 9 of PDIP-20 component beginning with upper left and following the arrows to the image on the bottom right. This analysis found silver (bottom right) within the solder joint. The source of the silver may have been the immersion silver board finish.

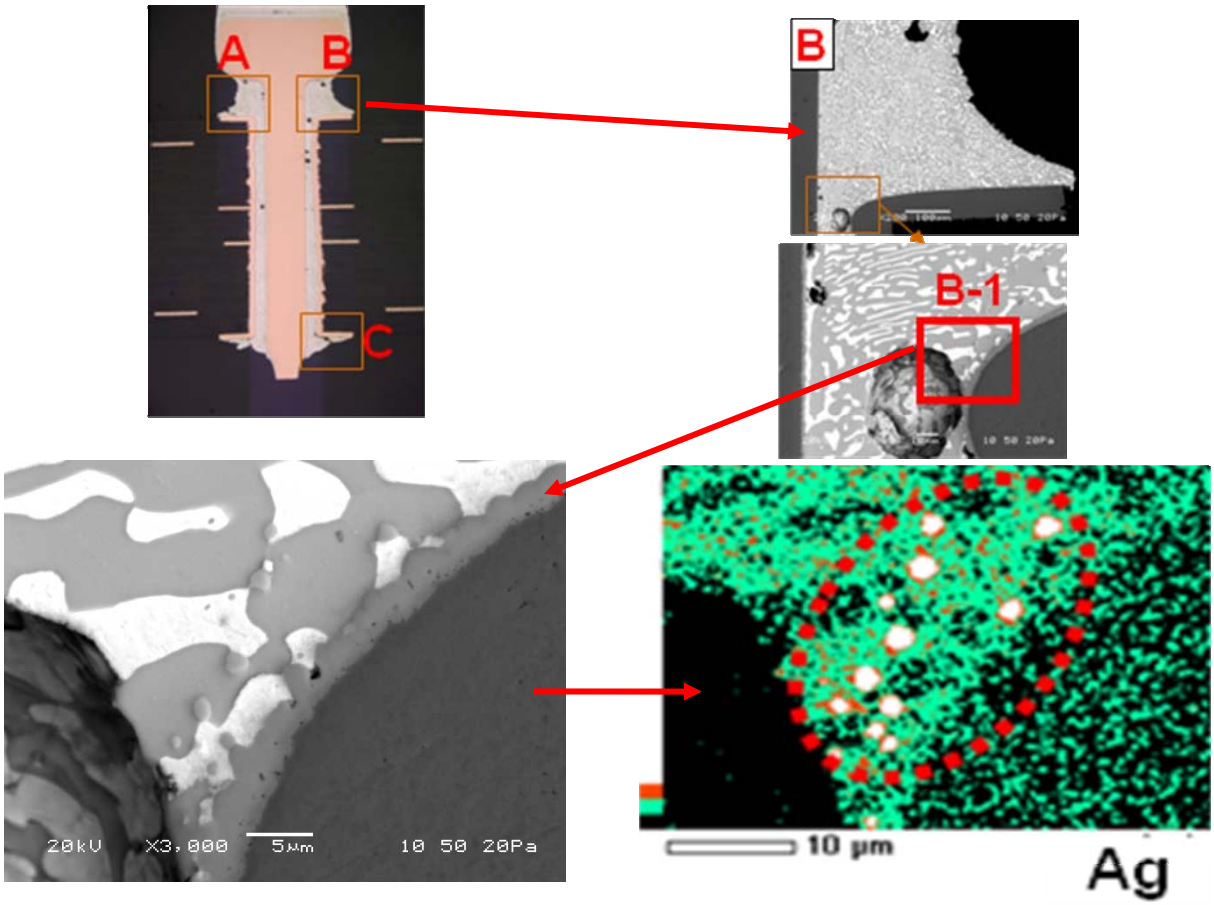

Figure 47 - TV23 U30; Micrographs, Lead 9 of PDIP-20

5.3.3.2.1 Component location U43

Component location U43 is a BGA-225 from the SnPb manufactured (Batch C), soldered with SnPb with SAC405 component finish located near the center of the test vehicle. This component failed at 120 cycles of combined environments. In Figure 48, yellow circles indicate solder joints with high resistance and red circles indicating failed solder joints that are open.

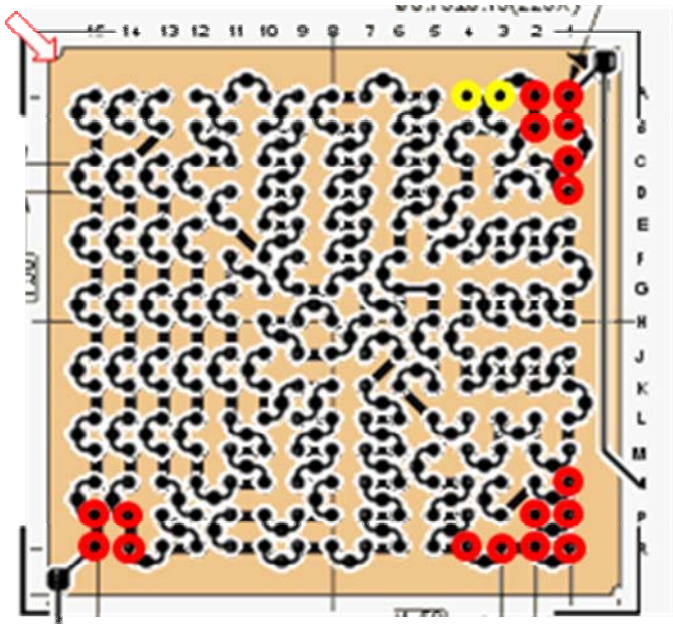

Figure 48 - TV23 U43; FA Results, BGA-225, Location U43

Cross-sectional micrographs in Figure 49 show different solder structure in lands on board (3, 4, 7, 8) and lands on component (1, 2, 5, 6). Cracking to open along land on board observed at 3-A.

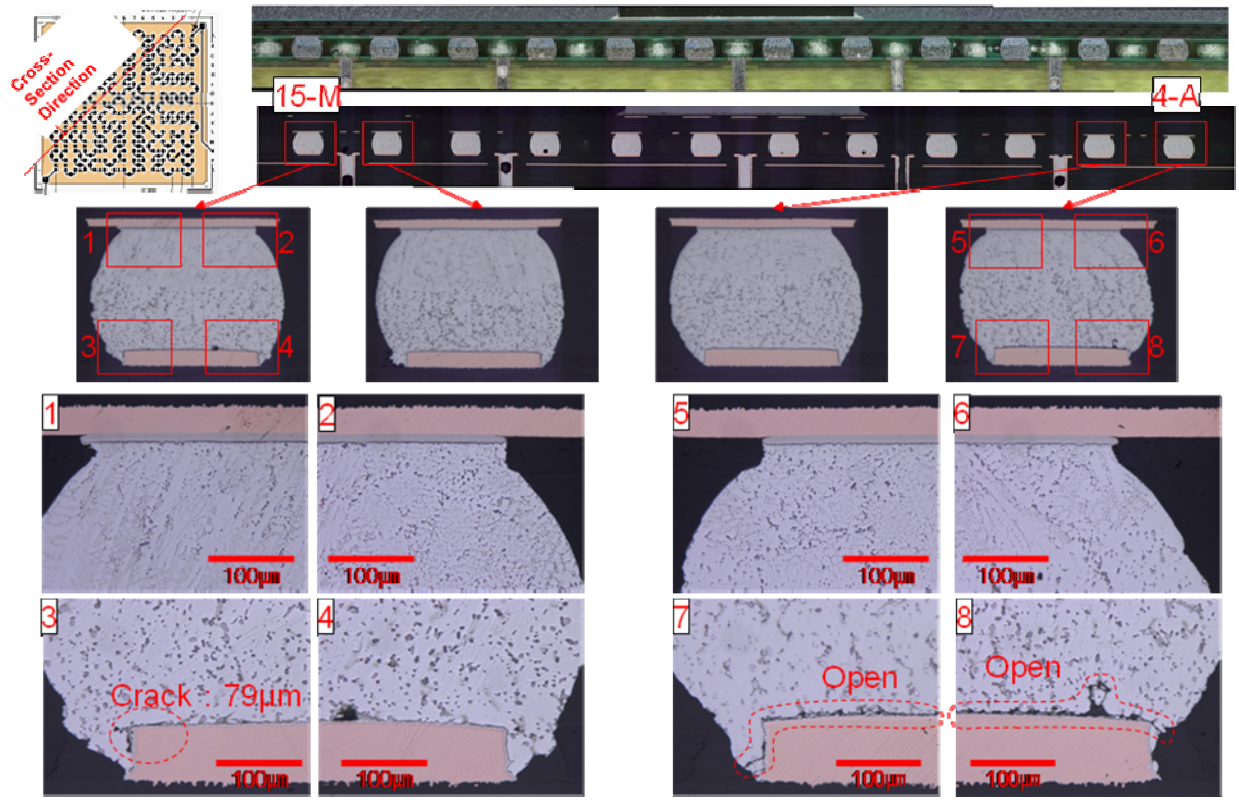

Figure 49 - TV23 U43; Cross-Sectional Micrographs

Cross-sectional micrographs in Figure 50 show different solder structure in lands on board (3, 4) and lands on component (1, 2). Cracking to open along land on board observed at 1-A and 15-Q.

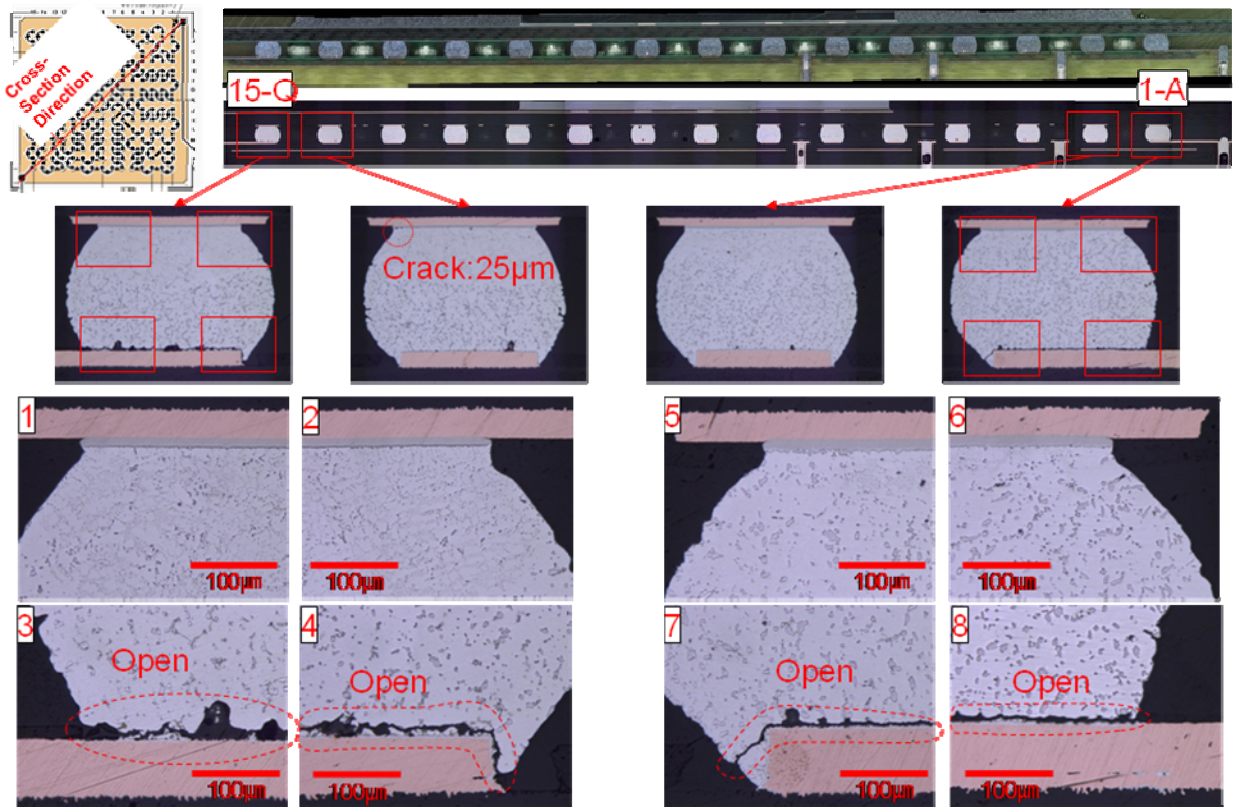

Figure 50 - TV23 U43; Cross-Sectional Micrographs

In Figure 51 SEM mapping shows segregation of Pb around land on board. Cracking found in the part Pb segregated.

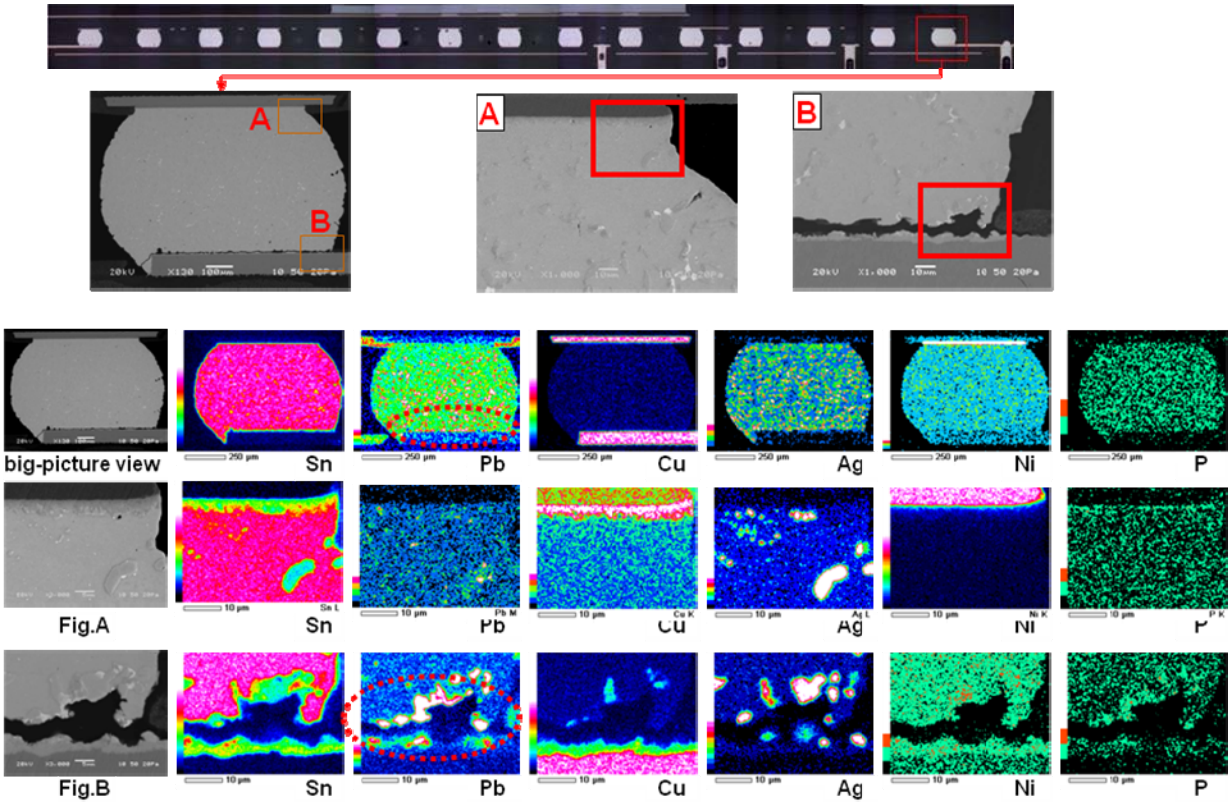

Figure 51 - TV23 U43; SEM Mapping

In Figure 52 the distance between component and board at each sphere is almost the same under the chip in the center. The distance becomes smaller further to the end. Comparing the distance at [1-A] and [15-Q], [1-A] has smaller distance.

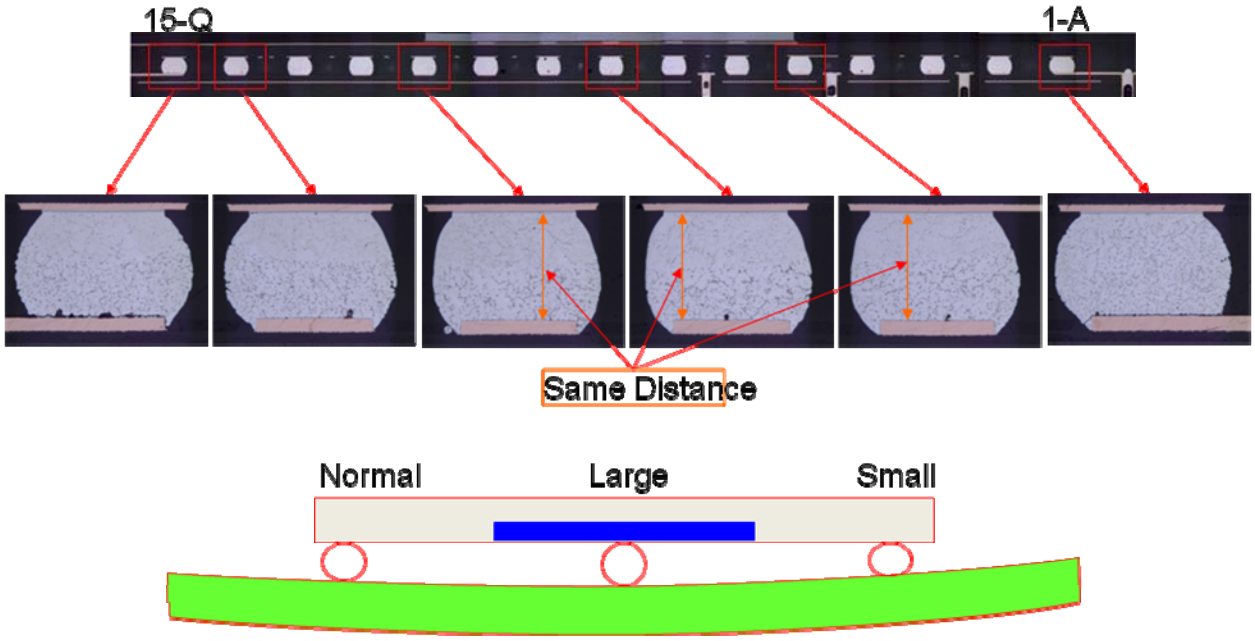

Figure 52 - TV23 U43; Cross-Sectional Micrographs Show Warping

5.3.3.3 Test Vehicle 72, component U29

Component location U29 is a TSOP-50 soldered with SAC305 on SnPb component finish. This component failed at 161 cycles of combined environments testing.

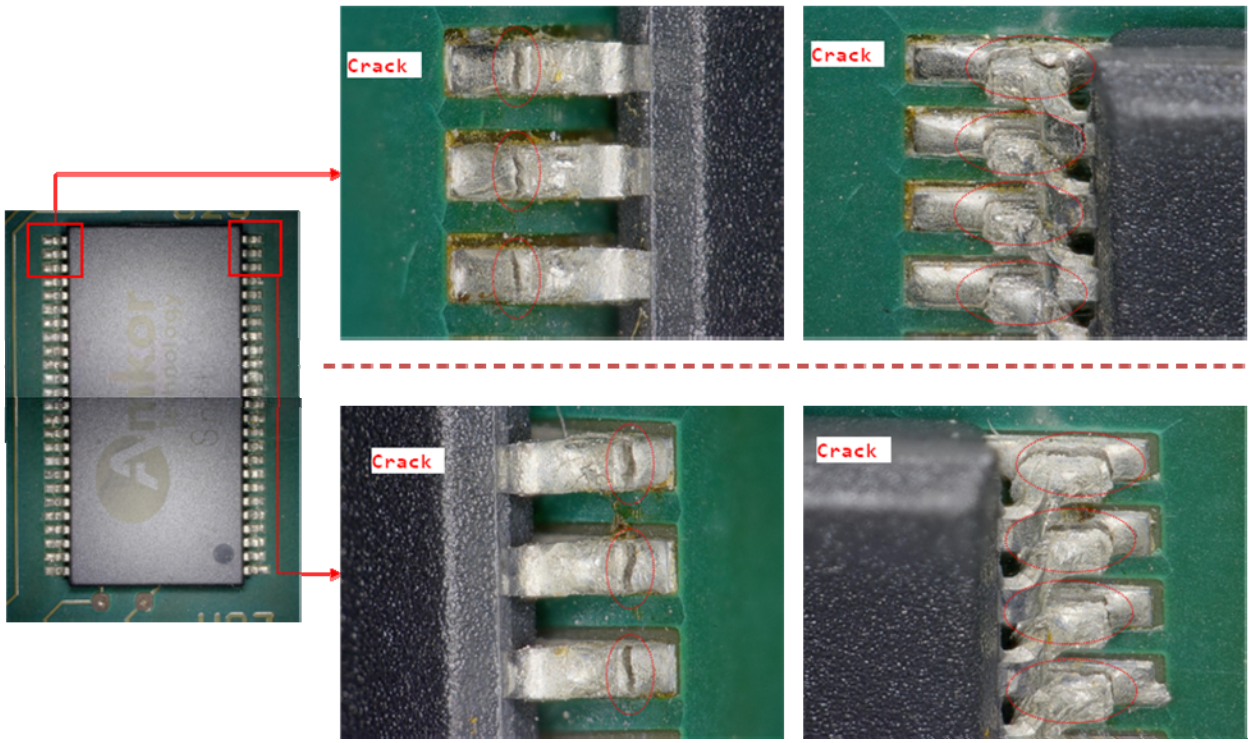

Figure 53 - TV72 U29; Visual Inspection Showing Cracked Solder Joints

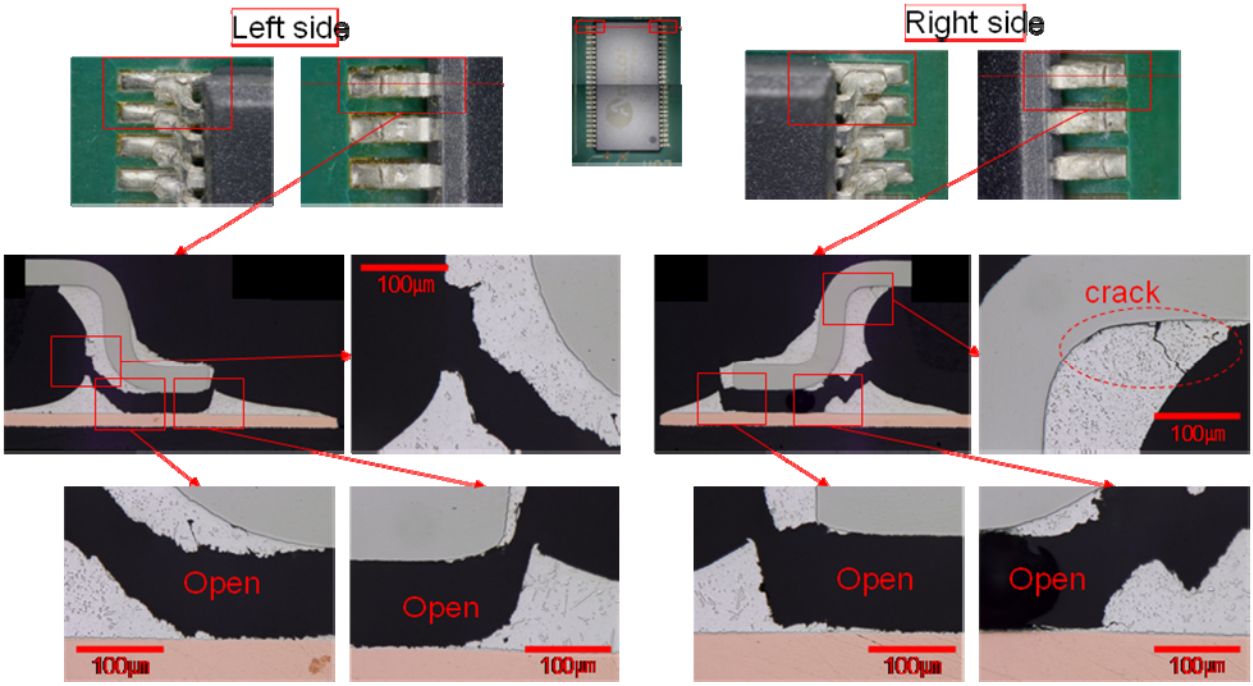

Figure 54 - TV72 U29; Cross-Section Micrographs Showing Open Solder Joints

As observed in Figure 55, more Pb was found from the right lead. Source of Pb is from the lead plating.

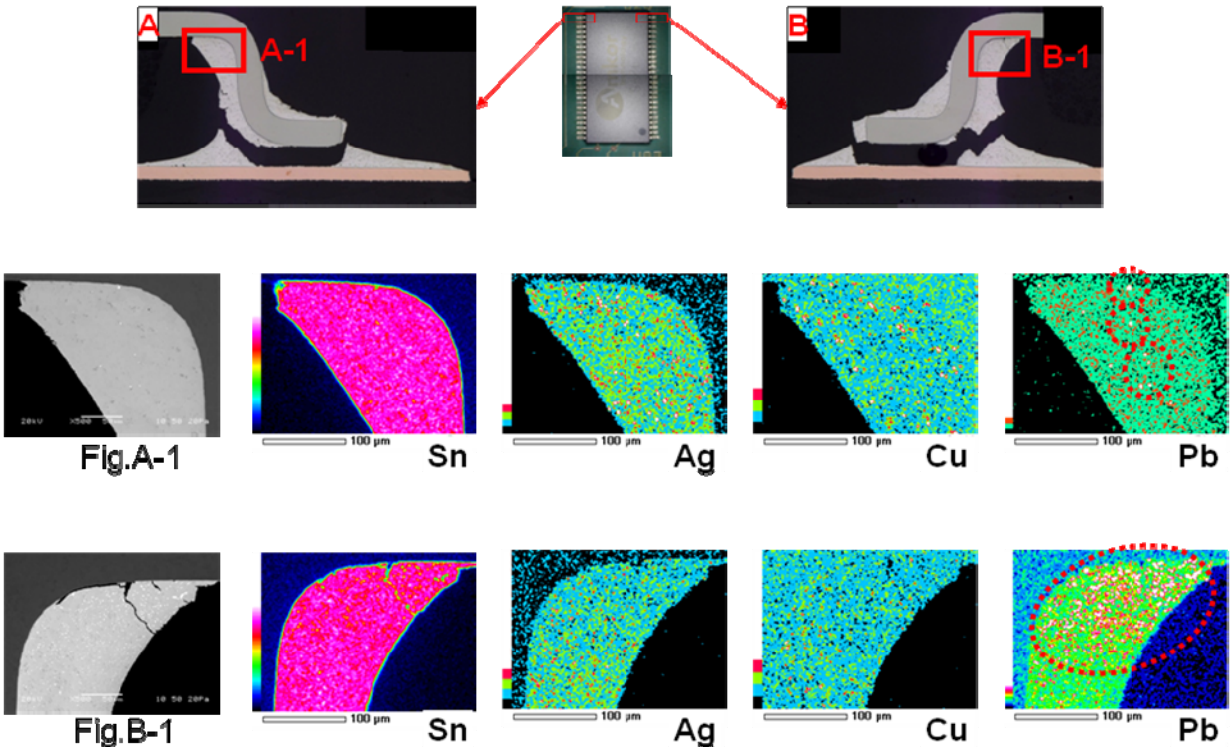

Figure 55 - TV72 U29; SEM Mapping, Pb was Found Around Upper Part of the Both Leads

5.3.3.4 Test Vehicle 117

Component location U4 is a BGA-225 component from lead-free manufactured (Batch G), soldered with SN100C solder paste on SnPb component finish. This component failed after twenty cycles. Figure 56 shows the orientation of the corner solder balls for the cross-sections in Figure 57.

Figure 56 - TV117 U4; Orientation of the Corner Solder Balls

Figure 57 shows cross-sectional micrographs of corner solder balls depicting cracks at component pads on views A, B and C. Crack at the PWB pad detected on view D.

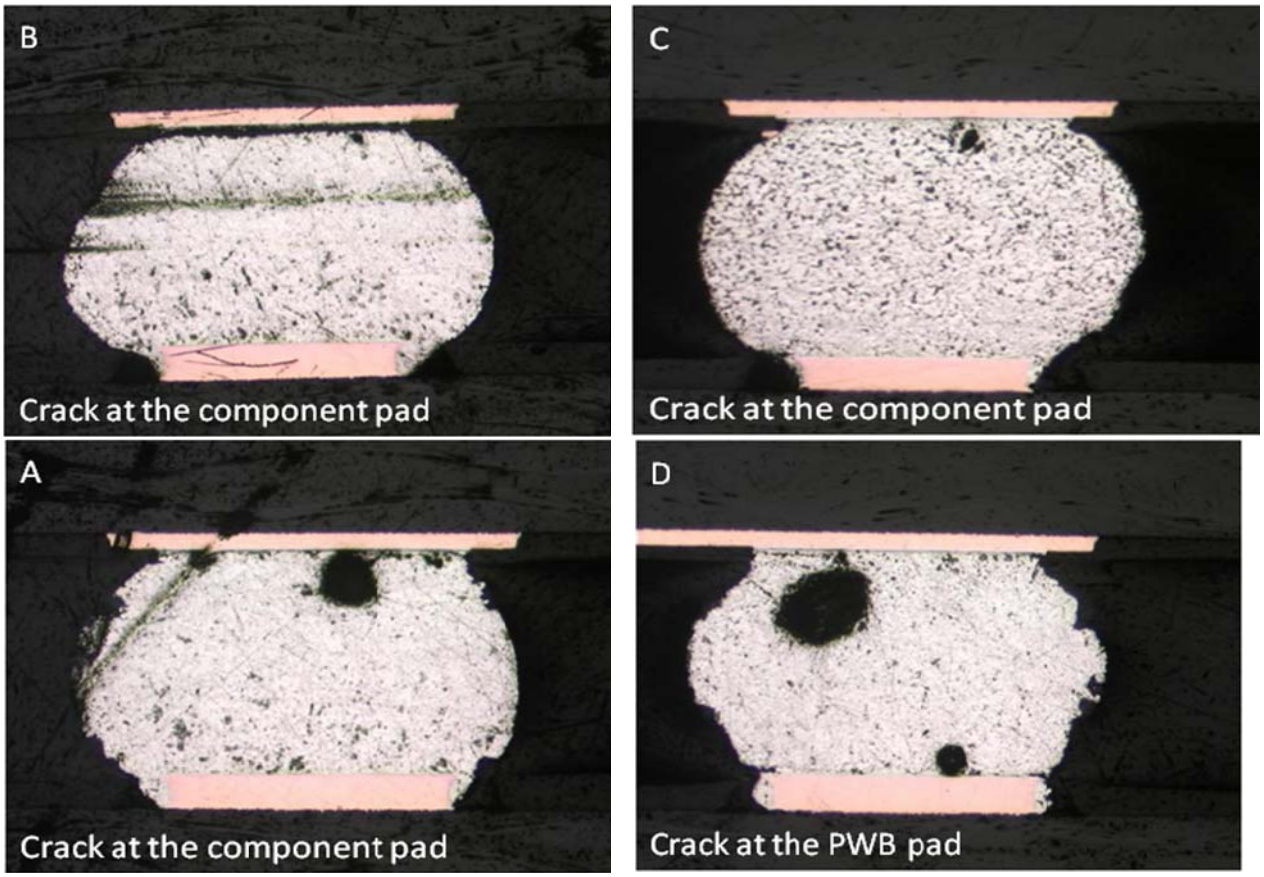

Figure 57 - TV117 U4; Cross-Sectional Micrographs of Corner Solder Balls

There was a progression of cracking between sides A/D and B/C, which can be visually represented in Figure 58. Red on top of the solder ball is cracking observed at the component interface. Red on the bottom of the solder ball is cracking observed at the PWB pad interface. Red on both the top and bottom of the solder ball is cracking observed at both the component and PWB pad interface. No red indicates an intact solder joint.

For this BGA-225 component, cracking was observed on both the second and third rows in from the perimeter row. No cracking was observed on solder balls beneath the component die.

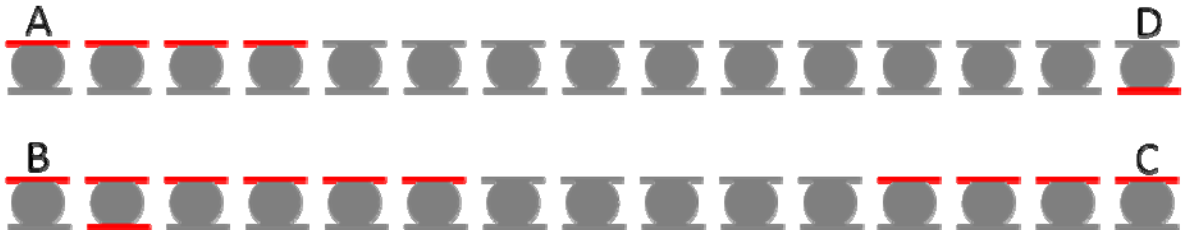

Figure 58 - TV117 U4; Diagram Showing Progression of Cracking in Component

5.3.3.5 Test Vehicle 119

Component location U36 is a CSP-100 component from lead-free manufactured (Batch G), soldered with SN100C solder paste on SAC105 component finish. This component was surrounded by components that fell off during testing and failed after 233 cycles.

Figure 59 is an x-ray image of the center region of the CSP-100 component in location U36. The PCB solder mask has a crack and is not homogeneous.

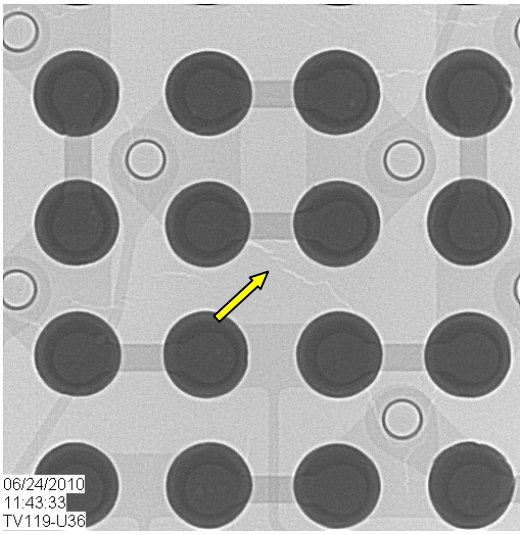

Figure 59 - TV119 U36; X-Ray Image, CSP-100

Figure 60 is an x-ray image for reference of the cross-section analysis in Figure 61. The number '1' and yellow circle indicate the location of pin 1 and the letter 'A' and dotted line indicate the row and level chosen for grinding.

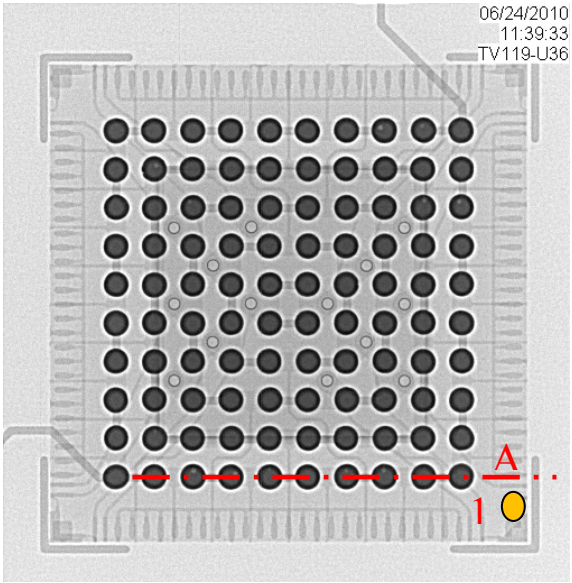

Figure 60 - TV119 U36; X-Ray Image for Reference of the Cross-Section Analysis

In Figure 61, on the left, cross-sectional micrographs of solder ball A1, A2, A9 and A10, at 274X magnification. On the right, the corresponding SEM images for solder ball A1 (300X), A2 (250X), A9 (220X) and A10 (220X).

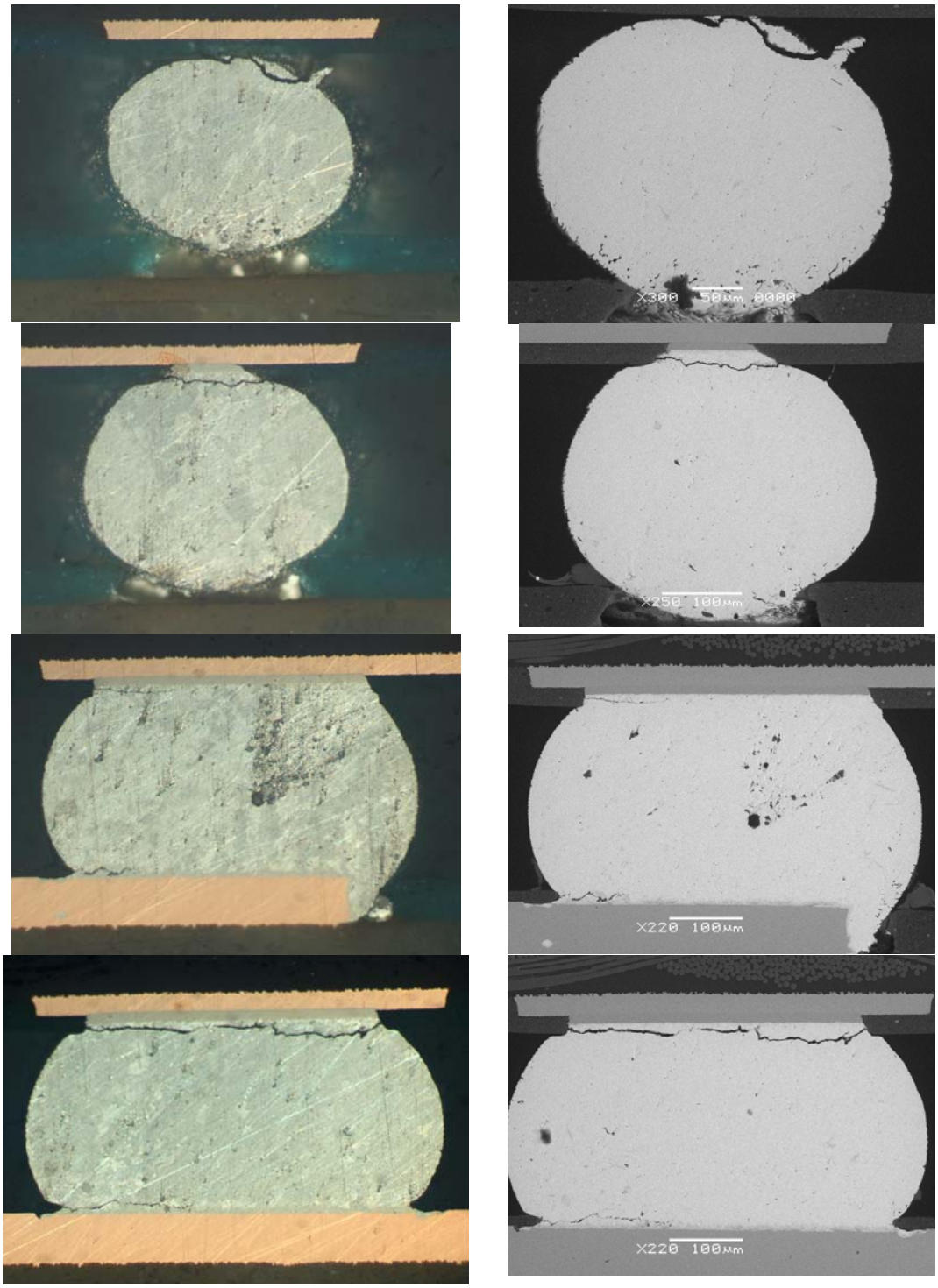

Figure 61 - TV119 U36; Cross-Sectional Micrographs of Solder Balls A1, A2, A9 and A10

Component location U39 is a TSOP-50 component from lead-free manufactured (Batch G), soldered with SN100C solder paste on SnPb component finish. This component was surrounded by components that fell off during testing and failed after 318 cycles.

Figure 62, an optical micrograph at 49X magnification showing cracked solder joints and cracks in the solder mask between leads 47 and 50.

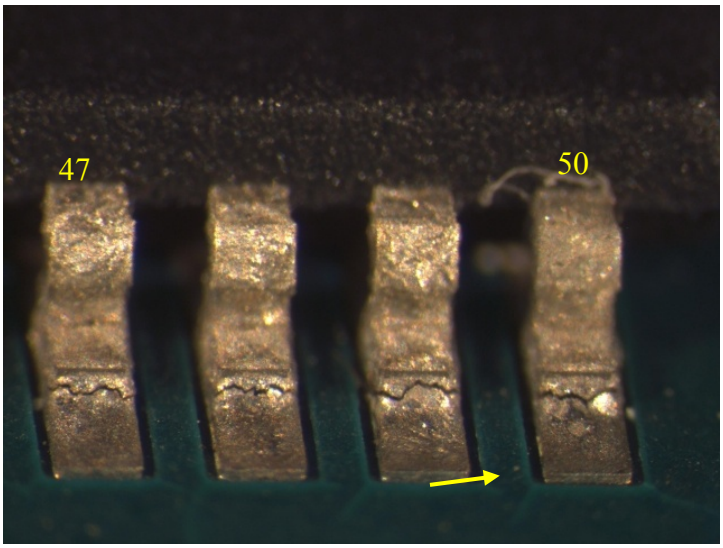

Figure 62 - TV119 U39; Optical Micrograph at 49X Magnification

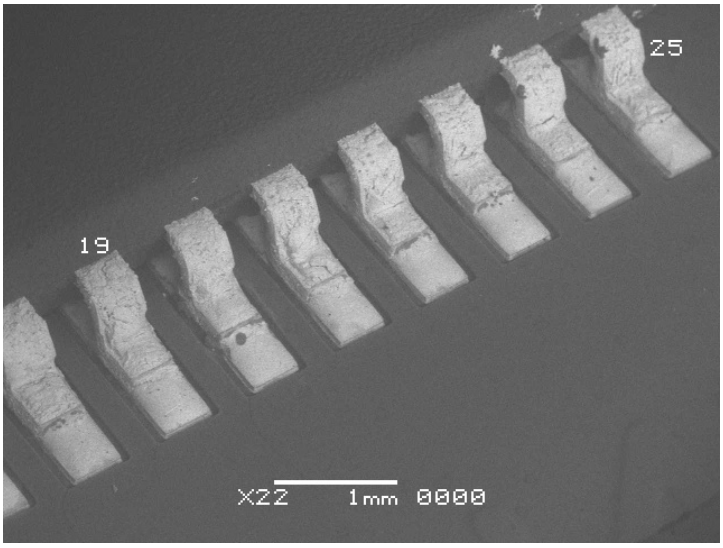

Figure 63 - TV119 U39; SEM Image of Leads 19-25 at 22X Magnification

Figure 64, SEM image, on the left is lead 25 at 70X magnification. SEM image on the right is lead 48-50 at 50X magnification.

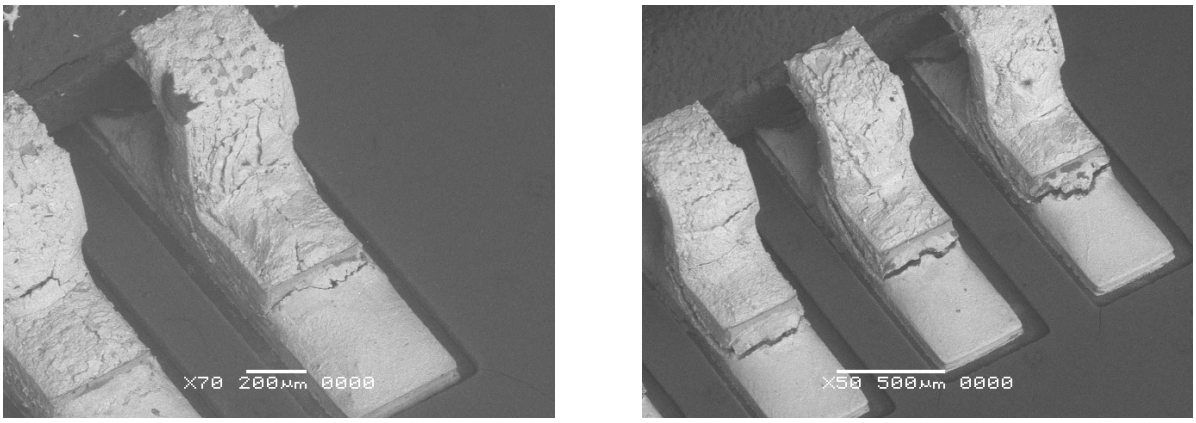

Figure 64 - TV119 U39; SEM Image, Lead 25

Figure 65, cross-sectional micrograph, on the left is lead 1 at 49X magnification. Micrograph on the right is lead 1 at 136X magnification.

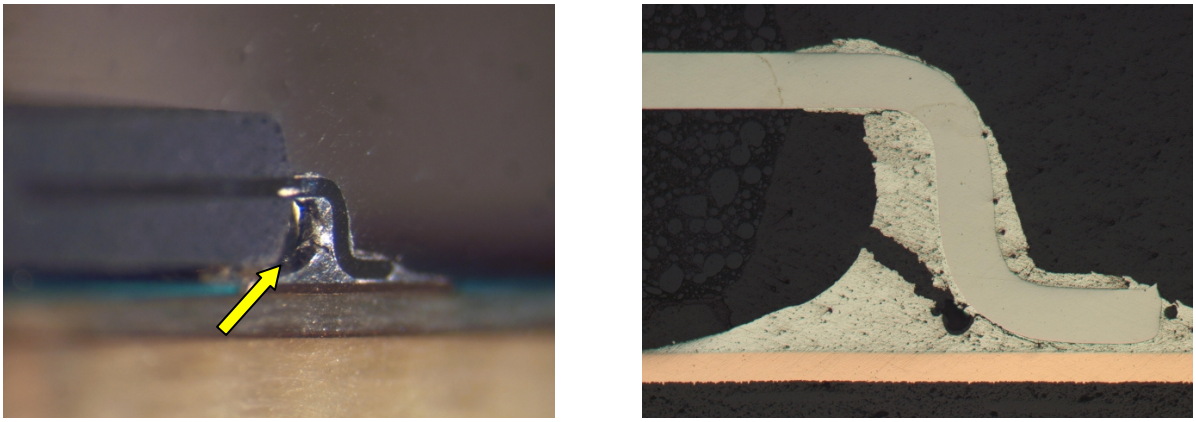

Figure 65 - TV119 U39; Cross-Sectional Micrograph, Lead 1

Figure 66, cross-sectional micrograph, on the left is lead 50 at 49X magnification. Micrograph on the right is lead 50 at 136X magnification.

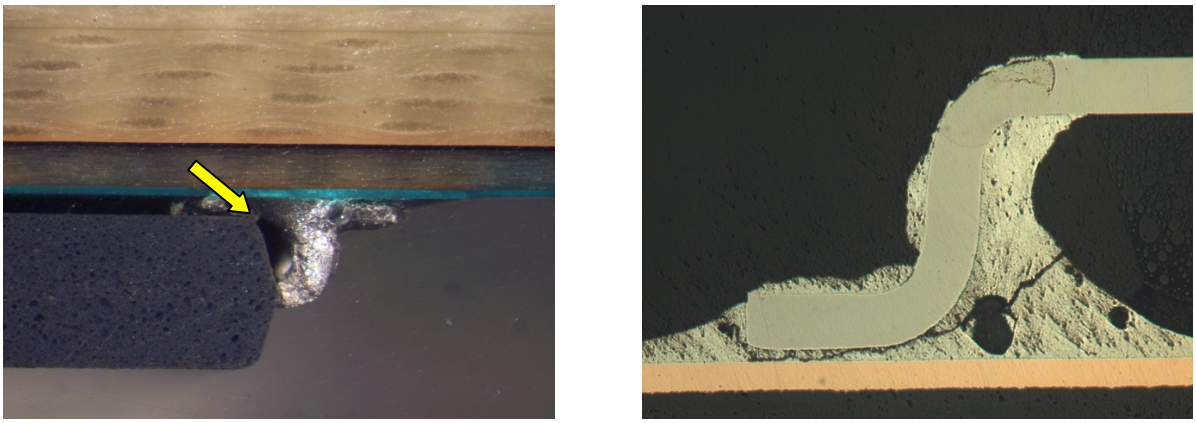

Figure 66 - TV119 U39; Cross-Sectional Micrograph, Lead 50

5.3.3.6 Test Vehicle 140

Component location U11 is a PDIP-20 from SnPb rework (Batch B), soldered with SnPb on SnPb component finish. This component had a damaged pad from the rework process and failed after 398 cycles. For the optical micrograph in Figure 67, on the left shows the suspect lead. Cross-sectional micrograph on the right is the suspect lead.

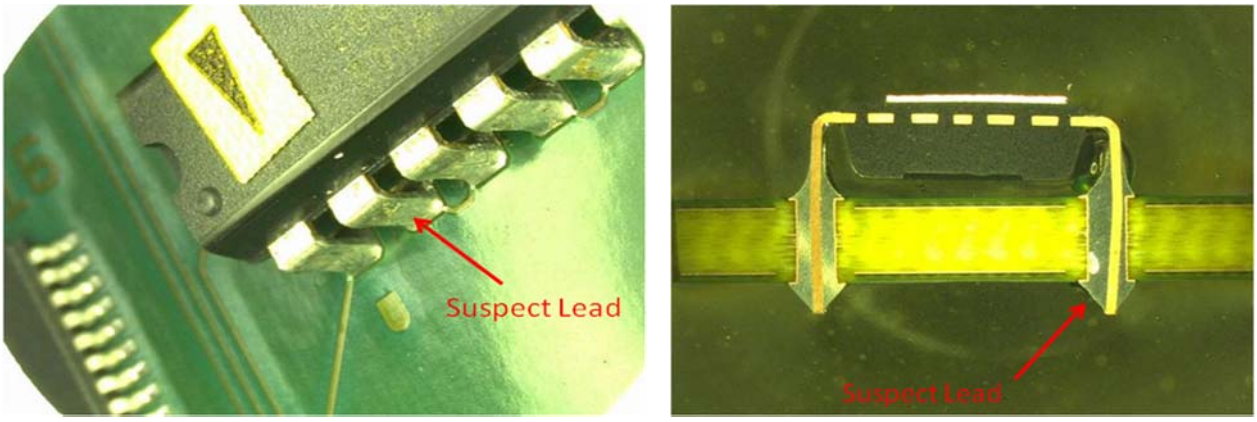

Figure 67 - TV140 U11; Optical Micrograph

Figure 68 shows the cross-sectional micrographs of the suspect lead in the PDIP-20 component showing solder joint crack initiation and lifted land.

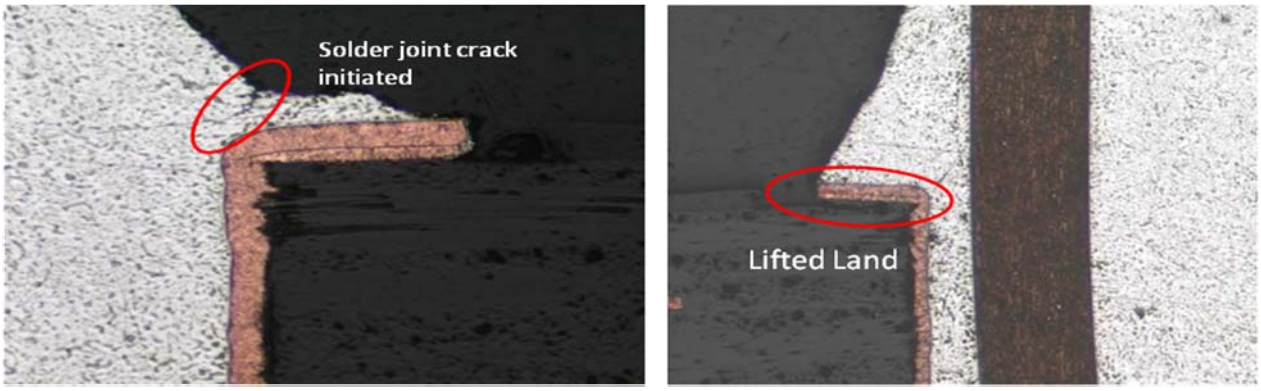

Figure 68 - TV140 U11; Cross-Sectional Micrographs, Suspect PDIP-20 Lead

5.3.3.7 Test Vehicle 142

Component location U13 is a CLCC-20 component from SnPb rework (Batch B), soldered with SnPb on SAC305 component finish. This component was adjacent to reworked components and survived all 650 cycles of testing.

Figure 69, optical micrograph, on the left shows the CLCC package lead numbering. Micrograph on the right shows an improperly sealed lid on the side for leads 1 – 5 where lead 1 is on the left at 19X magnification.

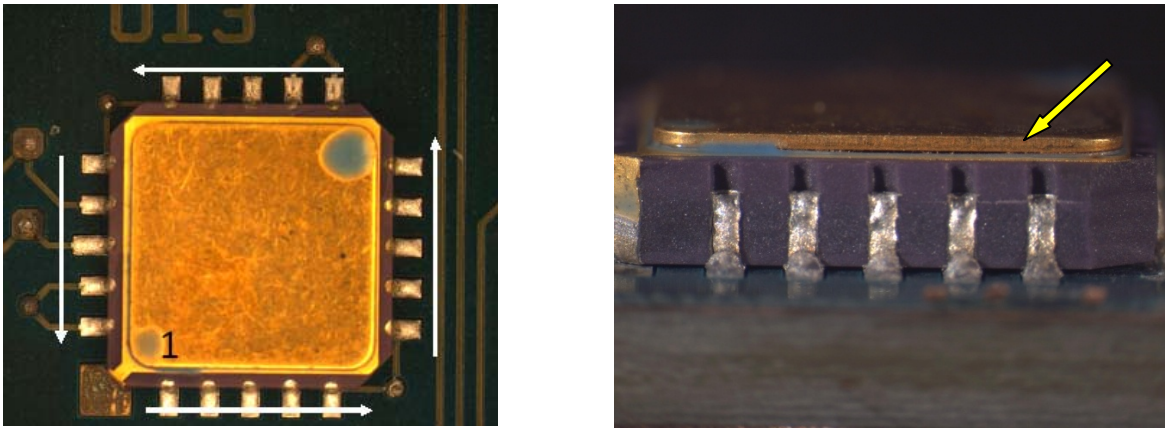

Figure 69 - TV142 U13; Optical Micrograph, CLCC Package Lead

For Figure 70, on the left are leads 6 – 10 starting with lead 6 on the left and on the right are leads 11 – 15 starting with lead 11 on the left. Minor solder cracking is visible.

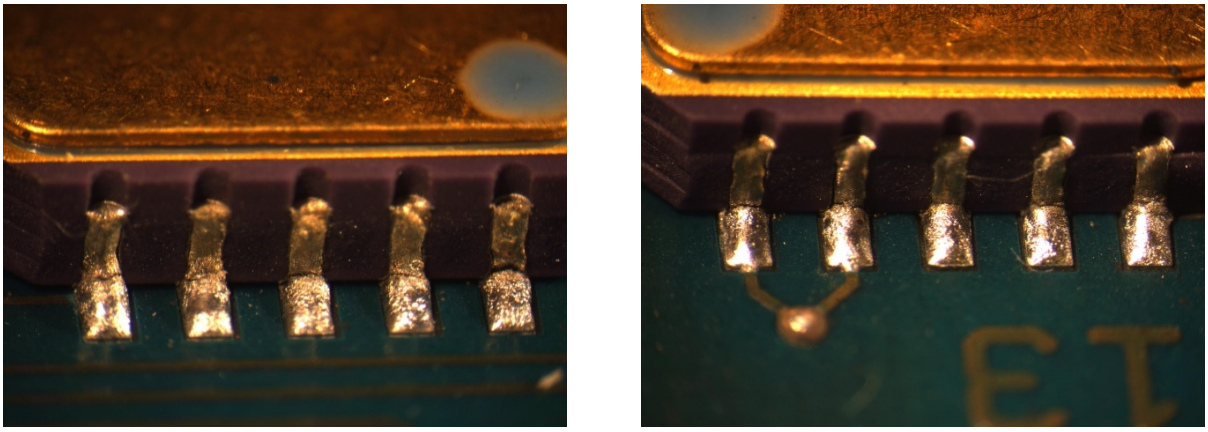

Figure 70 - TV142 U13 Optical Micrographs of CLCC-20 Leads at 24X Magnification

In Figure 71, on the left is the overall x-ray image and on the right is an x-ray of leads 6 – 10 with lead 6 being on the bottom.

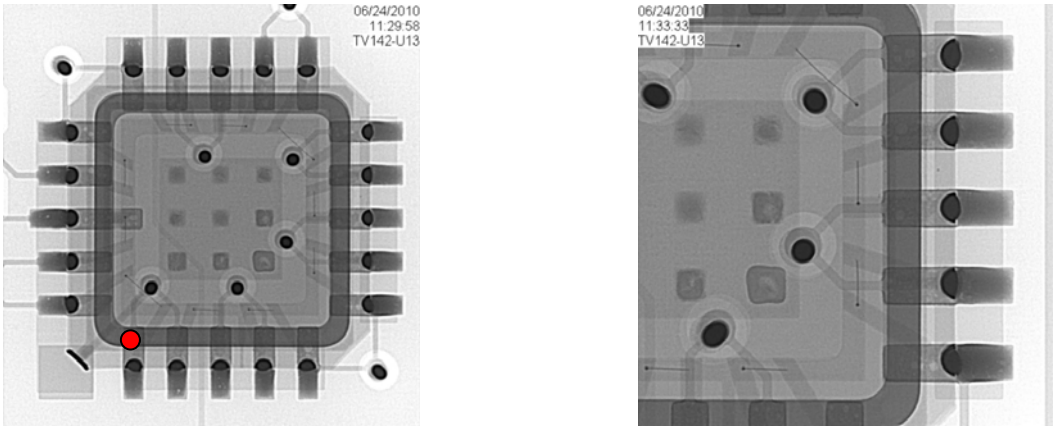

Figure 71 - TV142 U13 X-Ray Inspection of CLCC-20 Component.

In Figure 72 on the left are leads 6 – 10 which have some visible solder cracks and on the right are leads 16 – 20 and do not have solder cracks.

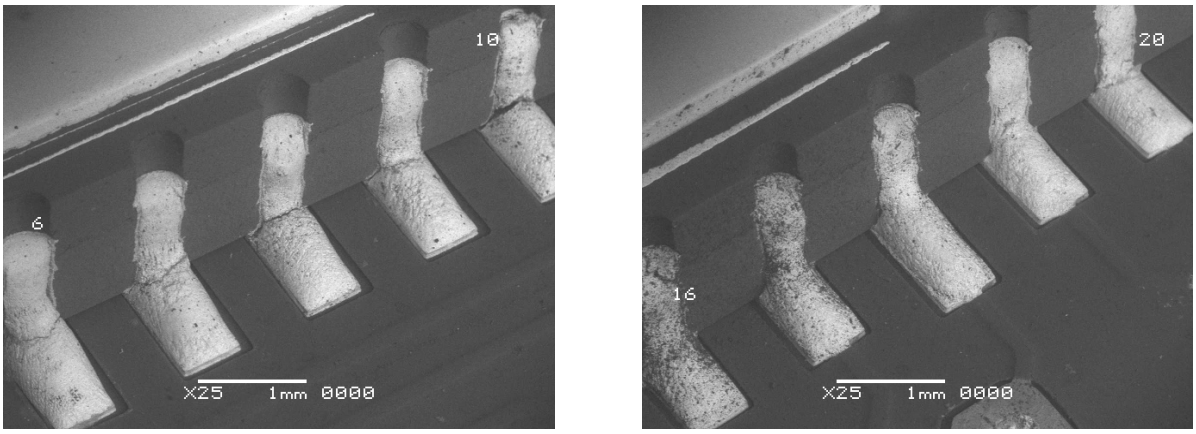

Figure 72 - TV142 U13 SEM Images of Component at 25X Magnification

In Figure 73, the upper left image is lead 8 where the arrow indicates a solder crack. The upper right image is lead 10 where a solder crack is also visible. The lower left image is lead 11 and the lower right image is lead 20.

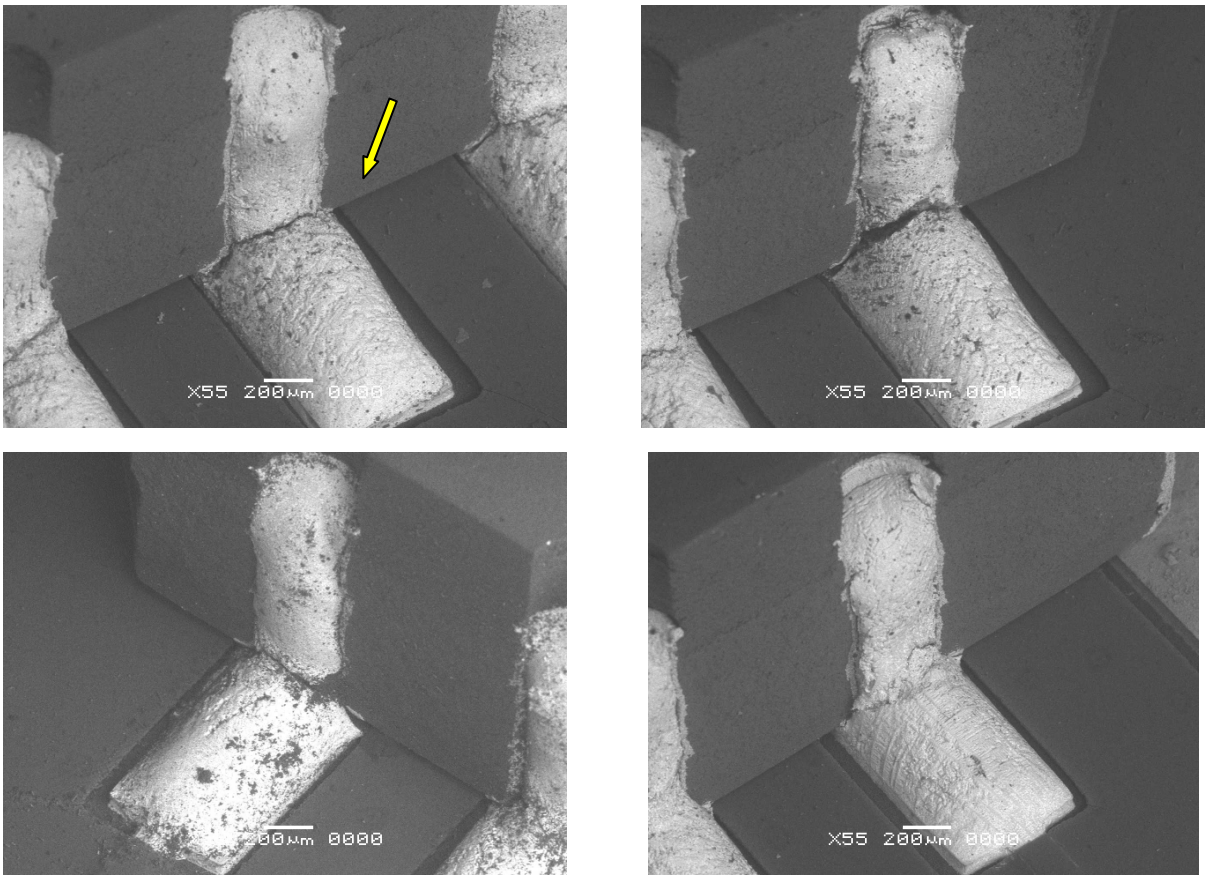

Figure 73 - TV142 U13 SEM Images of Selected Leads at 55X Magnification.

Figure 74 is an optical micrograph indicating the grinding levels of U13 CLCC-20 component.

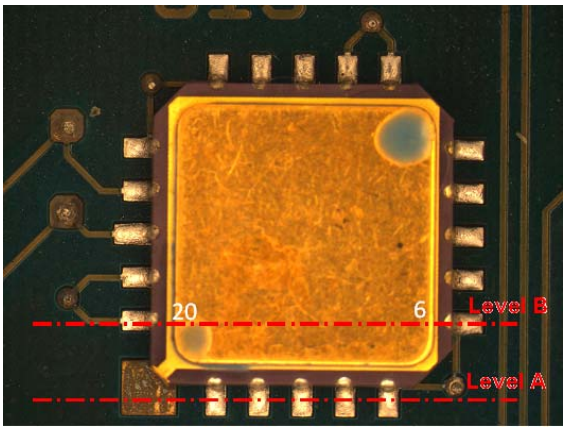

Figure 74 - TV142 U13; CLCC-20 Component

Figure 75, cross-sectional micrographs of lead 1 (left) and lead 5 (right) solder joints, grinding level A, at 136X magnification.

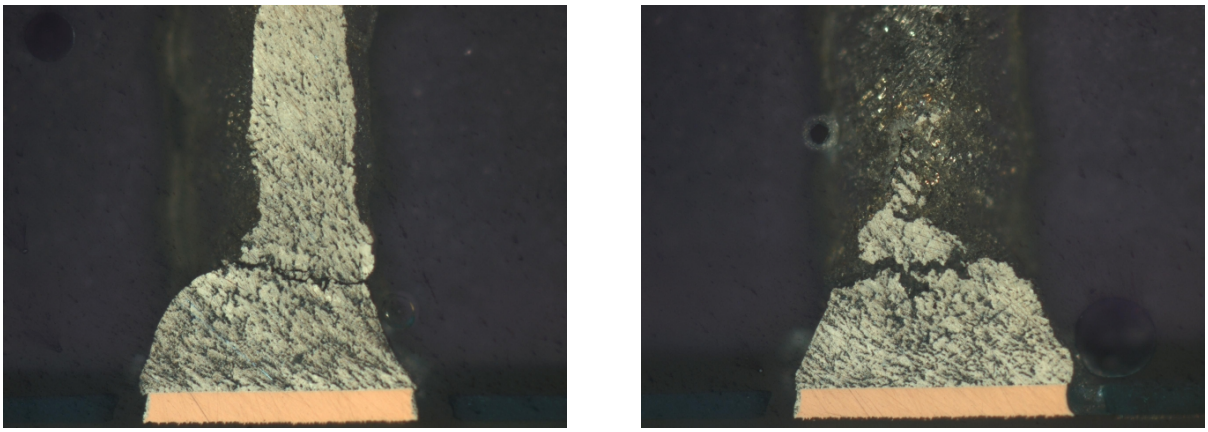

Figure 75 - TV142 U13; Cross-Sectional Micrographs of Lead 1 and Lead 5

Figure 76, cross-sectional micrograph, on the left shows grinding level A of leads 1 – 5 where the arrows indicate separation of the solder joints from the copper pads at 24X magnification. Micrograph on the right is lead 6 at 38X magnification just prior to grinding to level B.

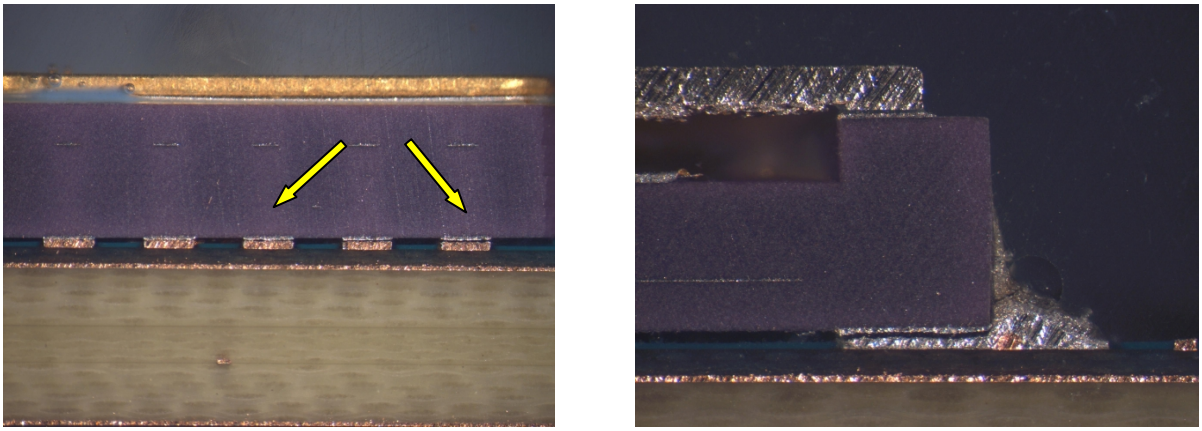

Figure 76 - TV142 U13; Cross-Sectional Micrograph

Figure 77, SEM image, on the left is the cross-section of lead 6 after grinding to level B at a 150X magnification. SEM image on the right is the cross-section of lead 20 after grinding to level B at 55X magnification.

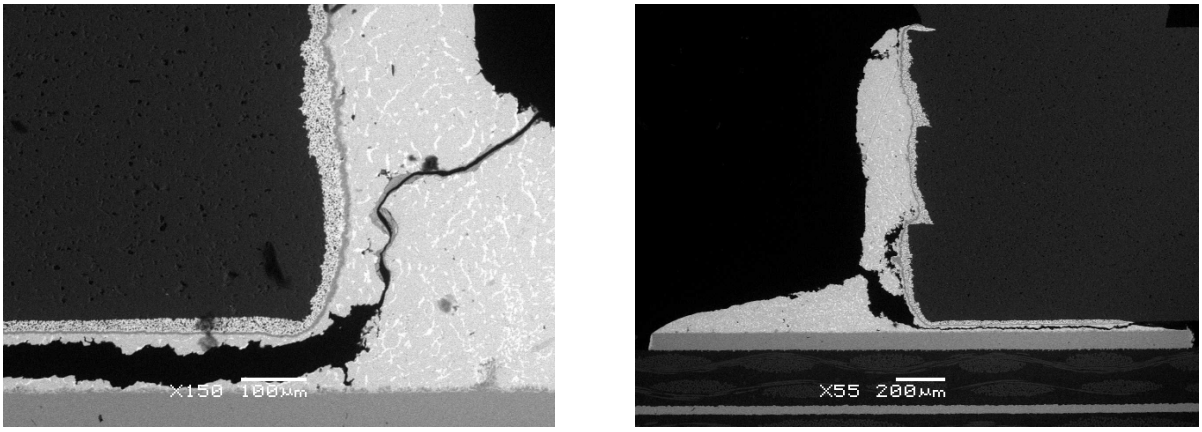

Figure 77 - TV142 U13; SEM Image

5.3.3.8 Test Vehicle 158, U6

Component location U6 is a reworked SnPb BGA-225 component soldered with SnPb solder paste, removed and replaced with a SAC405 BGA-225 component soldered with SnPb solder paste on an ENIG PWB. This component failed during the first cycle.

In Figure 78, the red circles indicate failed solder joints that are open.

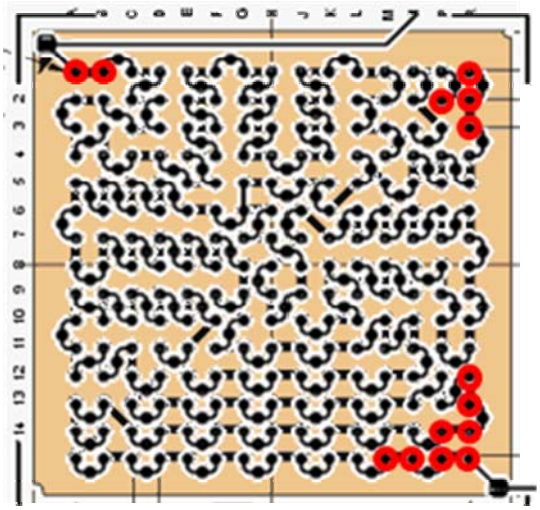

Figure 78 - TV158 U6; FA Results

The cross-sectional micrographs in Figure 79 show different solder structure in lands on board (7, 8) and lands on component (5, 6). Cracking to open along component land observed at 15-N.

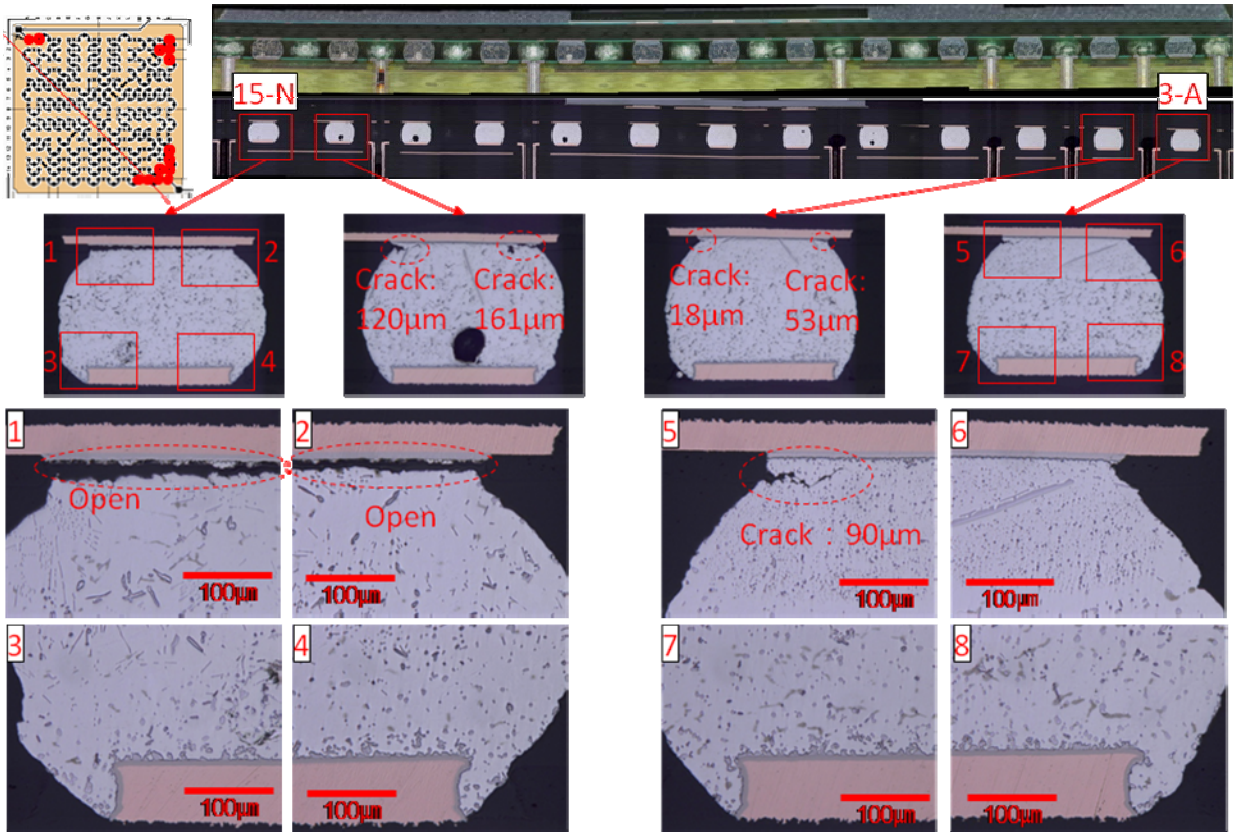

Figure 79 - TV158 U6; Cross-Sectional Micrographs

Figure 80 cross-sectional micrographs show different solder structure in lands on board (1, 2, 7, 8) and lands on component (3, 4, 5, 6). Cracking to open along PWB land found at 15-P.

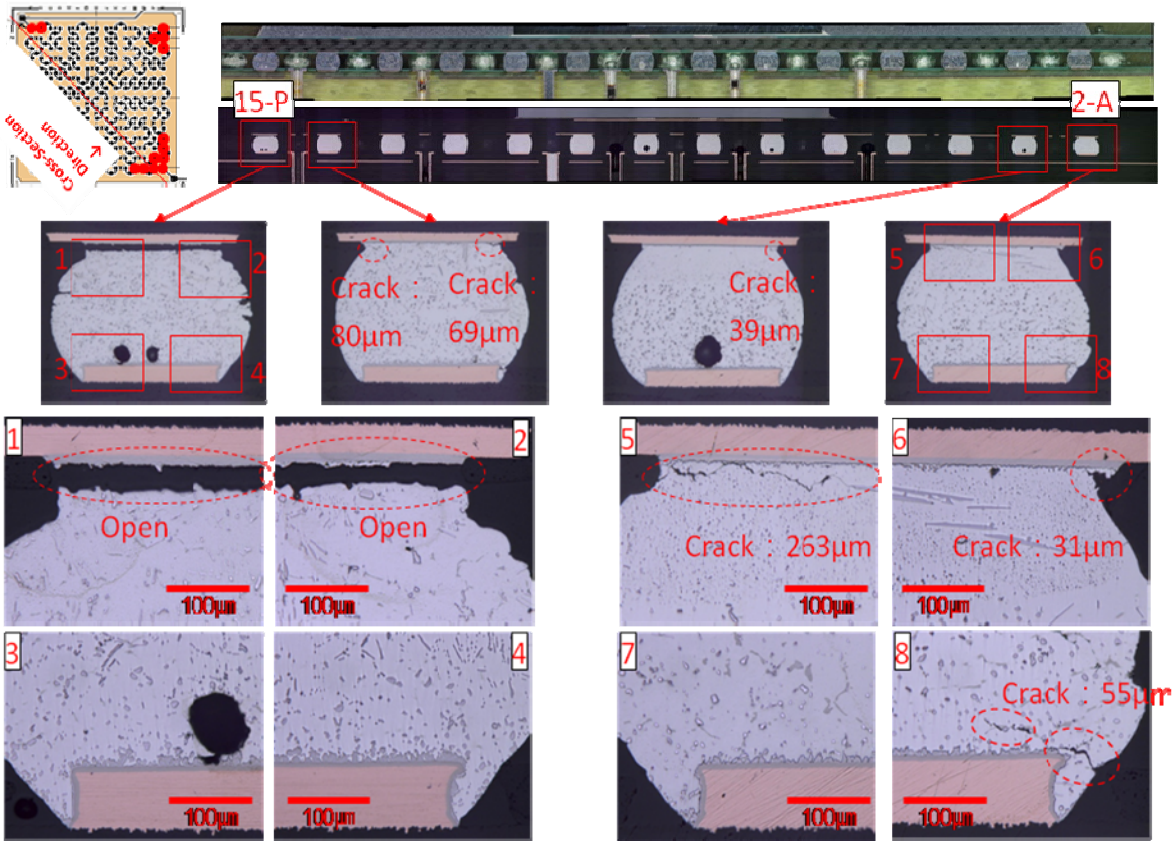

Figure 80 - TV158 U6; Cross-Sectional Micrographs

Cross-sectional micrographs in Figure 81 show different solder structure in lands on board (7, 8) and lands on component (5, 6). Cracking to open inside solder found at 1-A. Open joint along land on component found at 15-N.

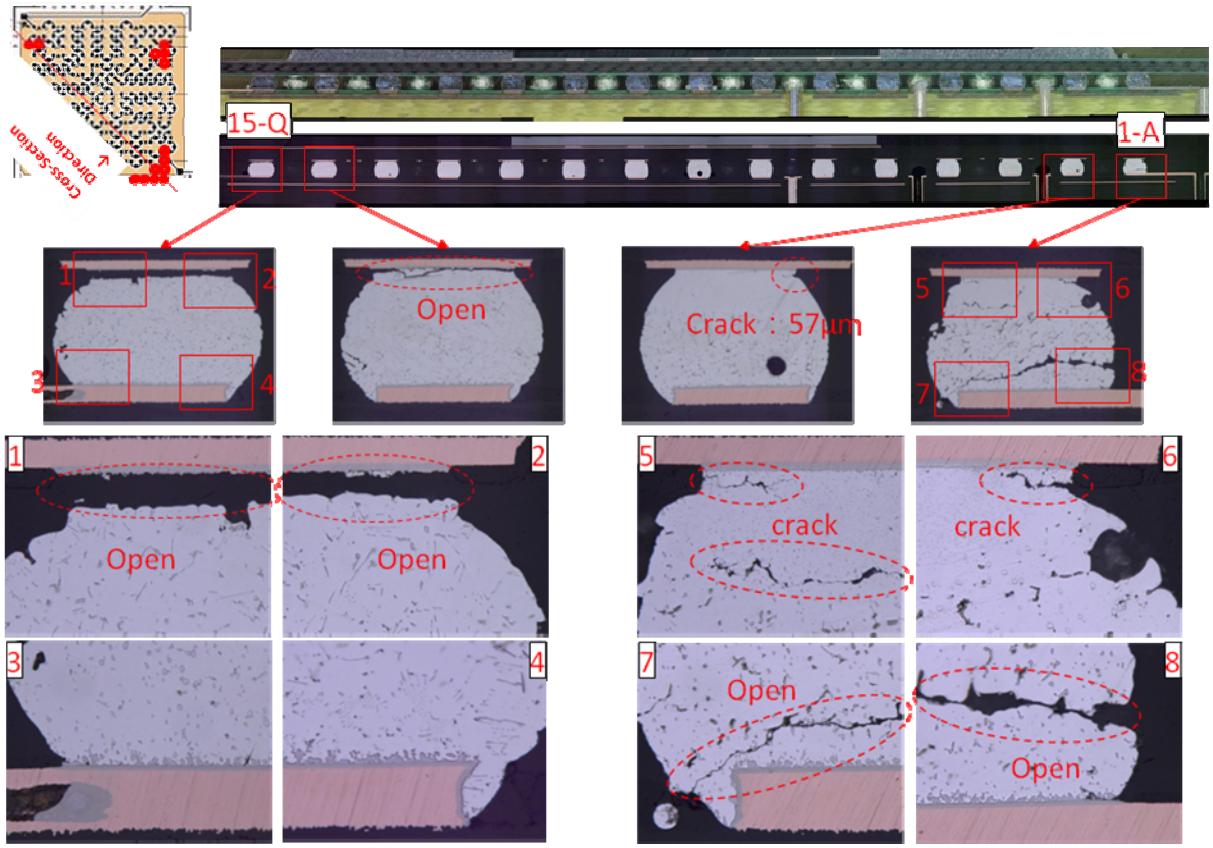

Figure 81 - TV158 U6; Cross-Sectional Micrographs

SEM mapping in Figure 82 shows segregation of Ag around land on component and segregation of Pb around PWB land. Higher concentrations of Pb detected in the cracking / breaking area.

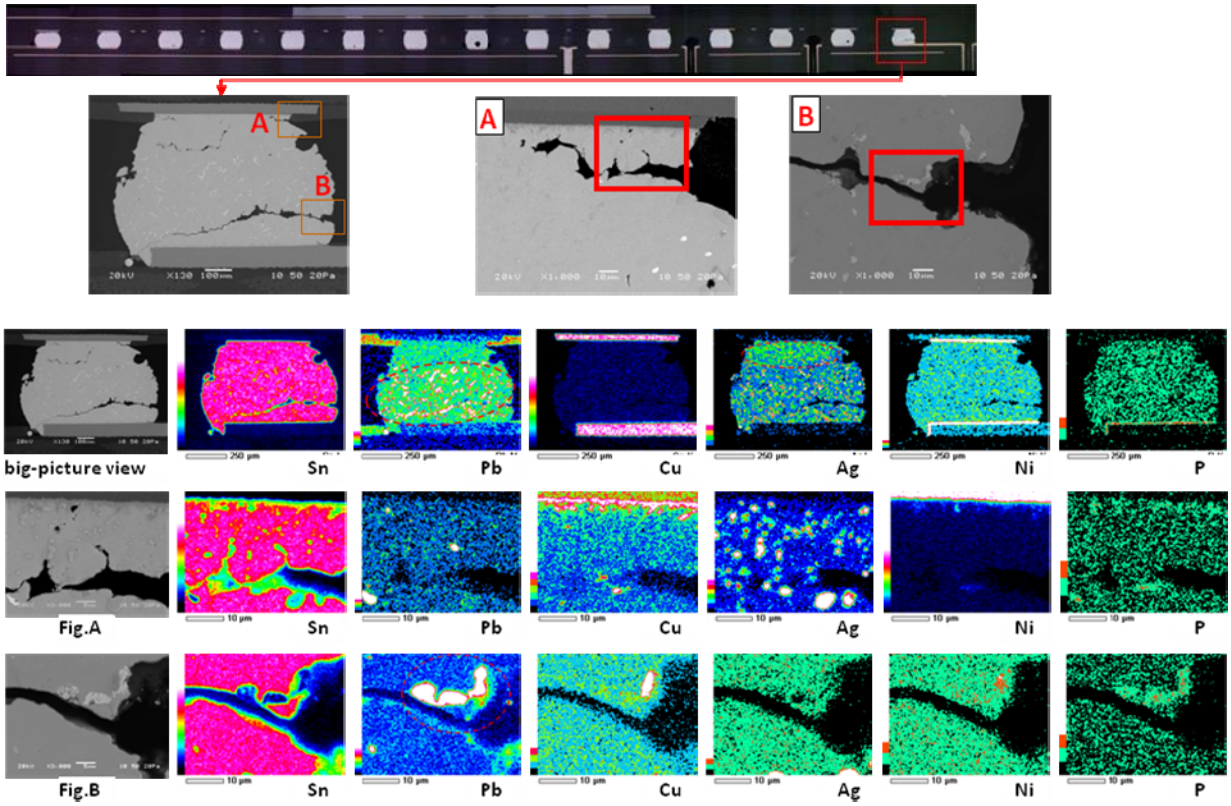

Figure 82 - TV158 U6; SEM Mapping

SEM mapping in Figure 83 shows solder is well blended over all except around component land where higher levels of Pb and cracking were found. Segregation of P from the ENIG board finish, however, no cracking detected.

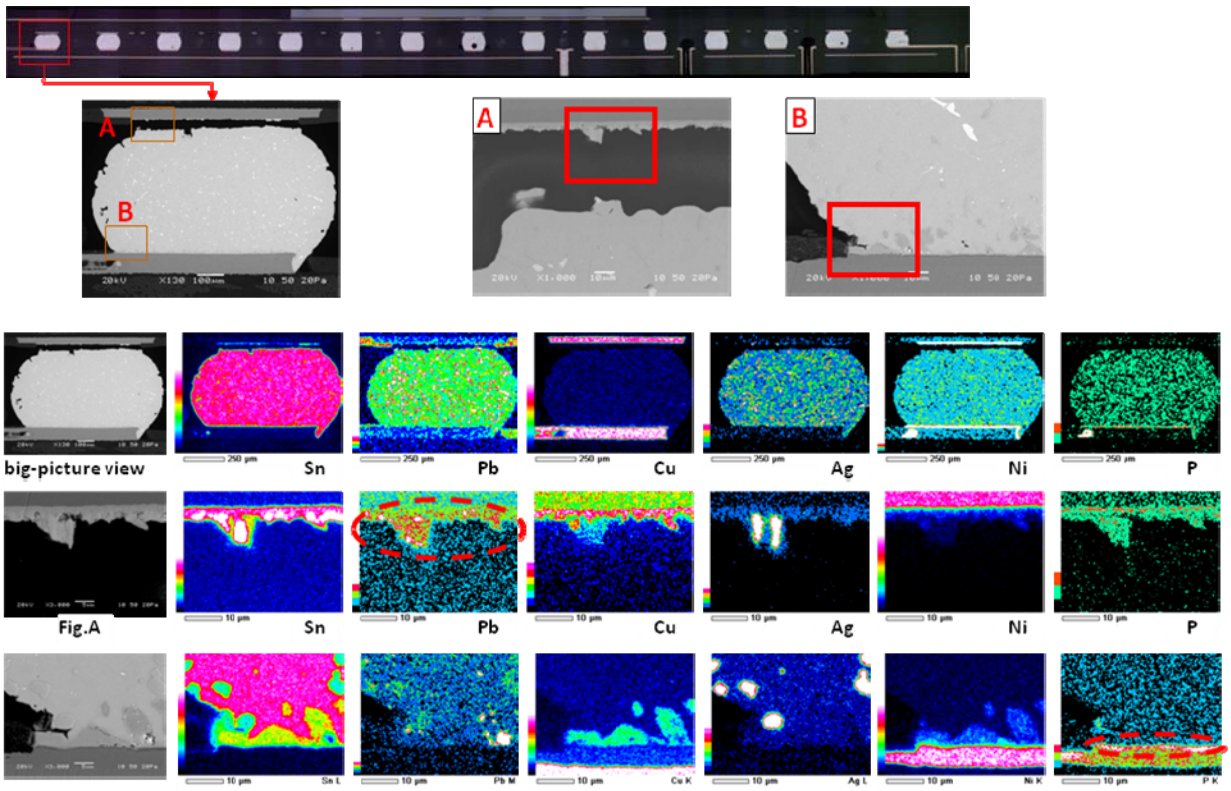

Figure 83 - TV158 U6; SEM Mapping

In Figure 84 the distance between component and board at each sphere is almost the same under the chip in the center. The distance becomes smaller further to the end. Comparing the distance at [1-A] and [15-Q], [1-A] has smaller distance.

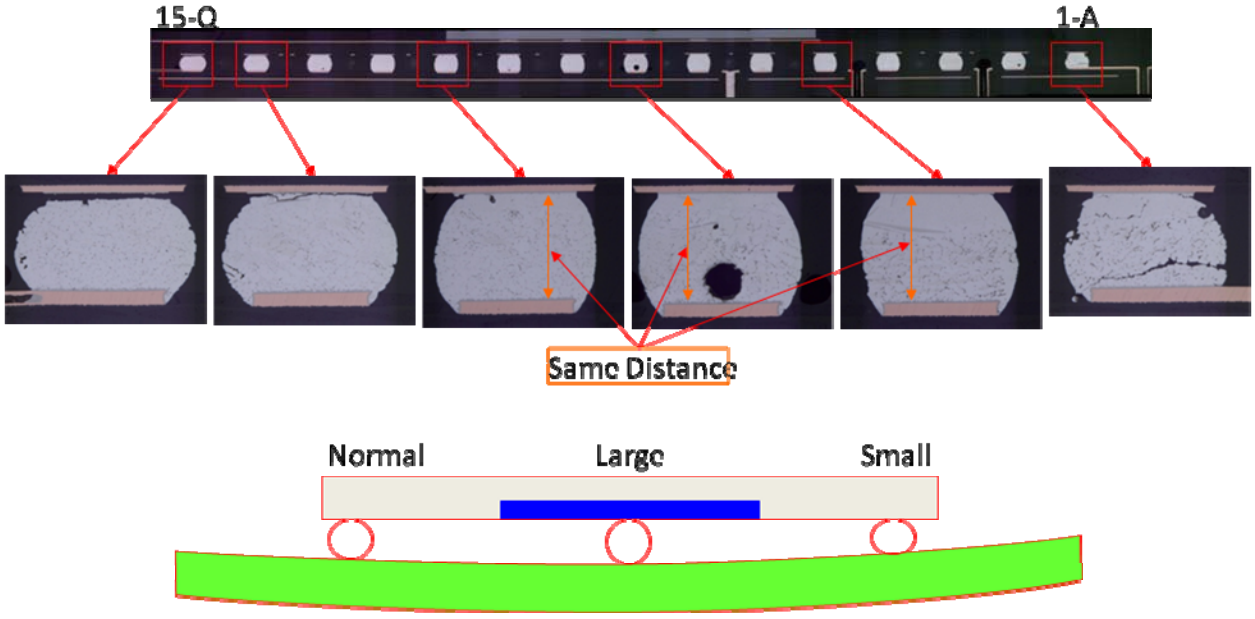

Figure 84 - TV158 U6; Cross-Sectional Micrographs Show Warping on BGA-225

5.3.3.9 Test Vehicle 180

Component location U21 is a reworked BGA-225 soldered with SAC305 on SAC405 component finish and replaced with SAC405 BGA-225 soldered with flux only. This component failed on cycle one and was reworked prior to combine environments testing.

In Figure 85 the yellow circles are solder joints with high resistance and red circles are failed solder joints that are open.

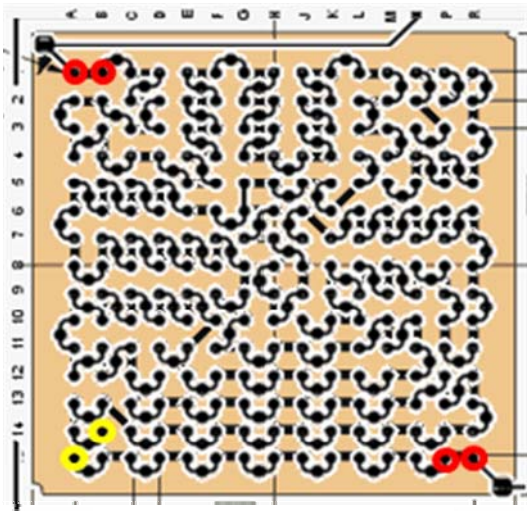

Figure 85 - TV180 U21; FA Results

In Figure 86, the cross-sectional micrographs show cracking to opens on board side (1, 2, 5, 6).

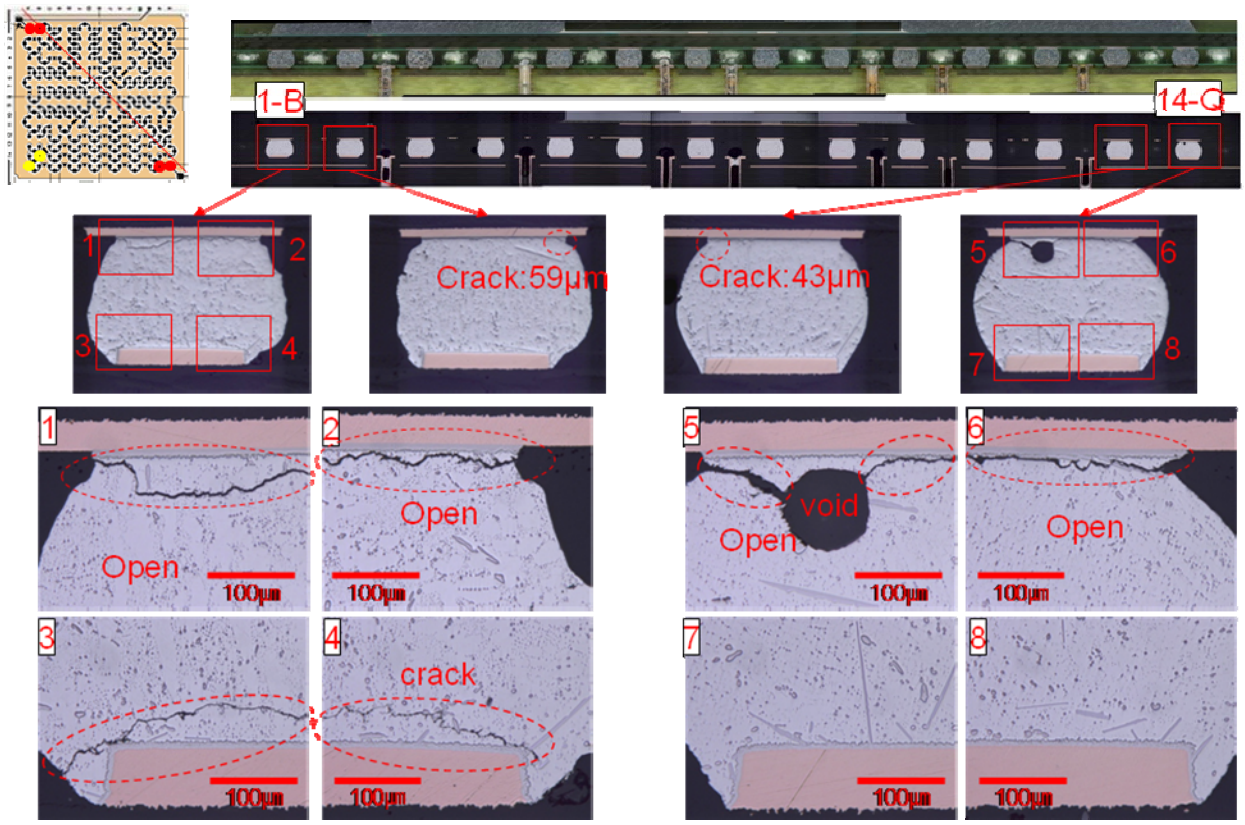

Figure 86 - TV180 U21; Cross-Sectional Micrographs

In Figure 87, the cross-sectional micrographs show cracking to open solder joints around both land on board and component (3, 4, 5, 6). Large intermetallic compounds observed around land on board (3, 4, 7, 8).

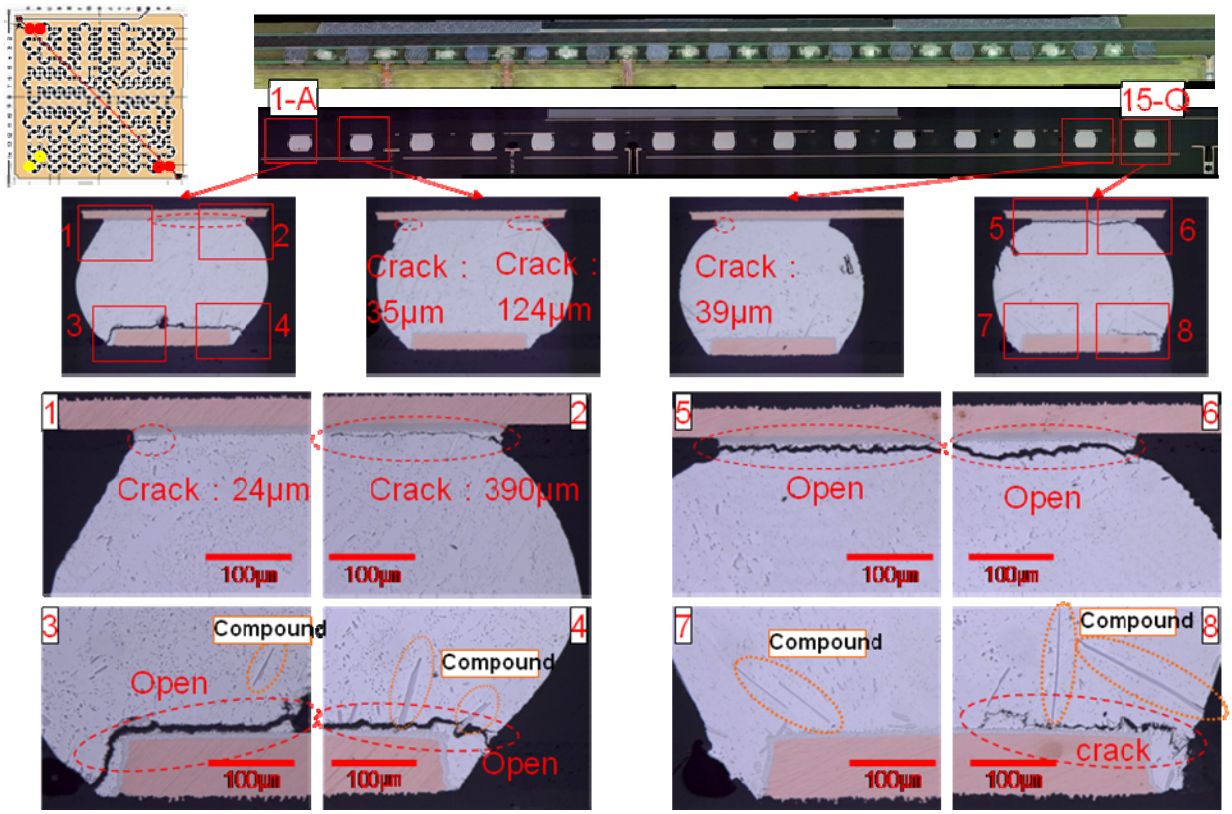

Figure 87 - TV180 U21; Cross-Sectional Micrographs

SEM mapping in Figure 88 shows cracks inside solder as well as cracking to open between IMC and solder, or inside solder.

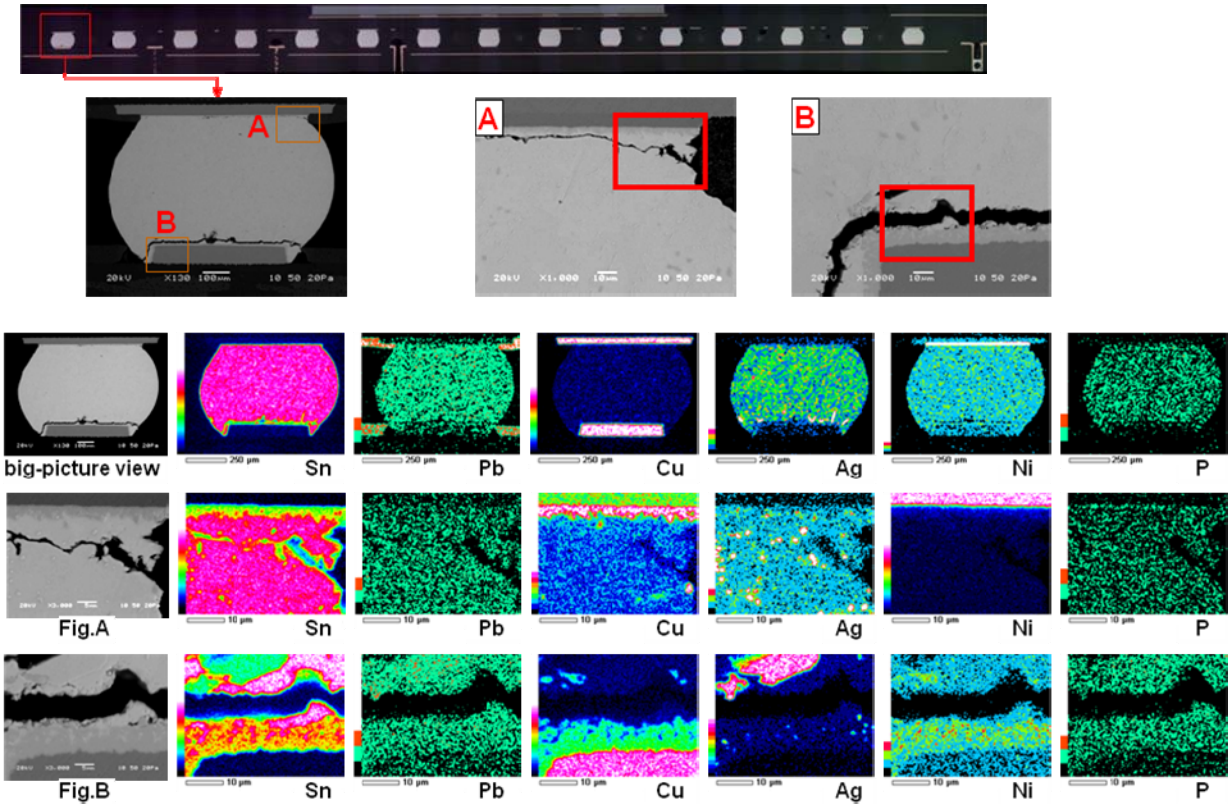

Figure 88 - TV180 U21; SEM Mapping

5.3.3.10 Test Vehicle 181

Component location U56 is a BGA-225 from the lead-free rework (Batch A), soldered with SAC305 on SAC405 component finish. This component failed on cycle one and was reworked prior to combine environments testing.

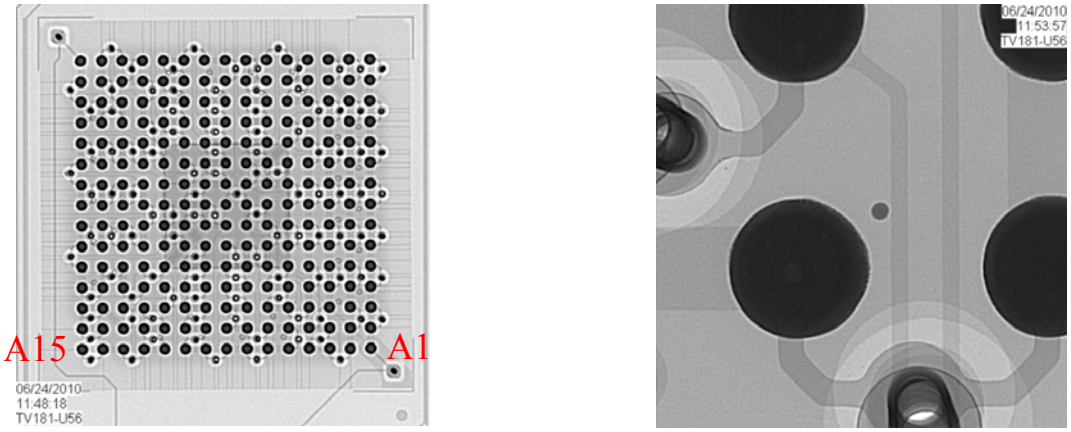

Figure 89 - X-Ray Inspection of TV181 U56 BGA-225

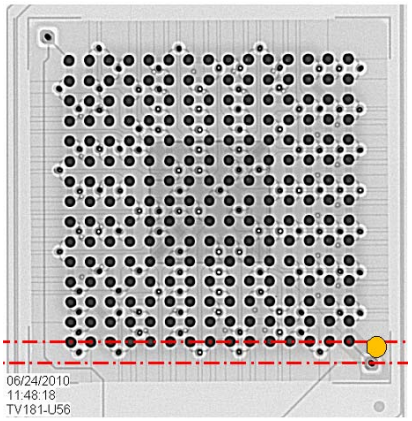

Figure 90 - TV181 U56; X-Ray Image Showing the Grinding Levels

In Figure 91, the image on the left is at 24X magnification and the image on the right is at 136X magnification.

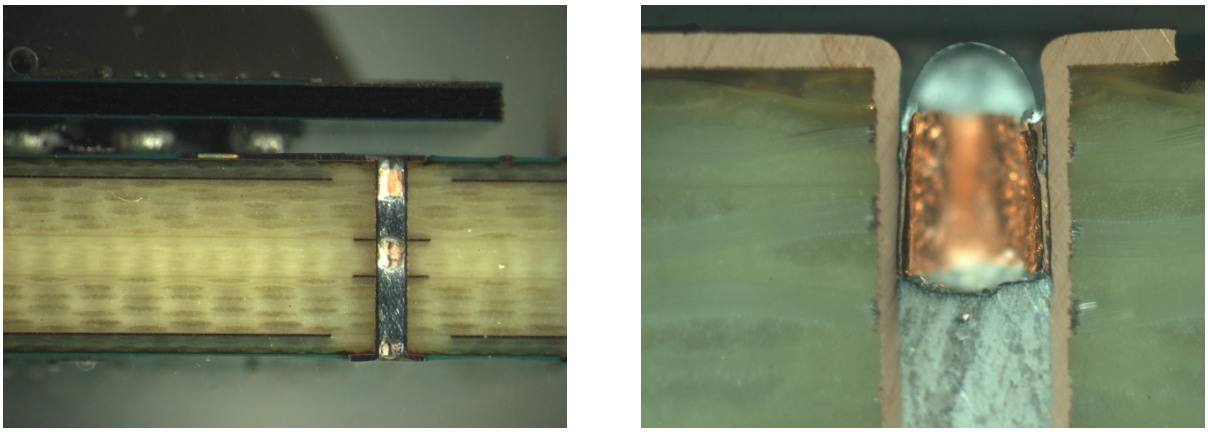

Figure 91 - TV181 U56; Cross-Sectional Micrographs of Via Hole Connected to Ball A1

In Figure 92, the image on the top left is solder ball A1 at 136X magnification. The image on the top right is solder ball A7 at 274X magnification. On the bottom left, is solder ball A9 and on the bottom right is solder ball A11, both at 136X magnification.

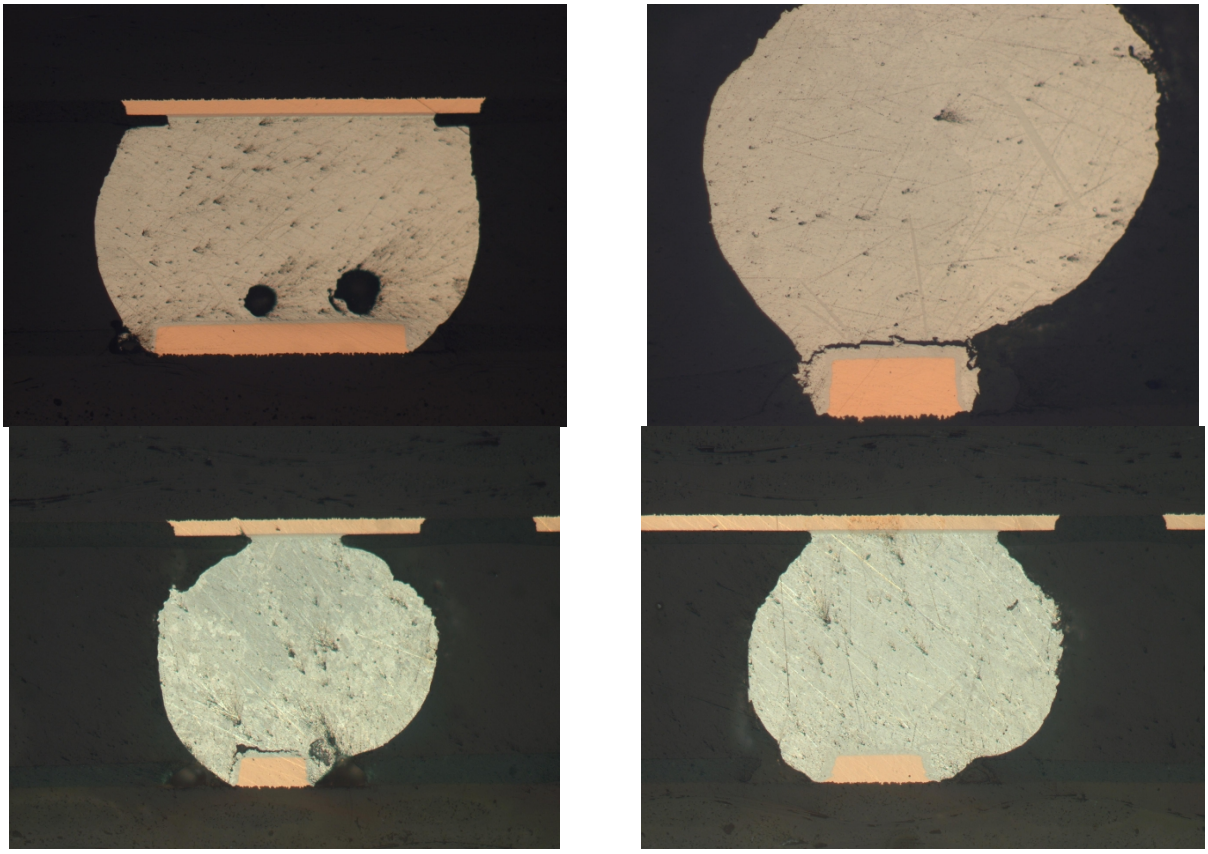

Figure 92 - TV181 U56; Cross-Sectional Micrographs of Solder Balls

In Figure 93, the image on the left is at 140X magnification and the image on the right is at 370X magnification.

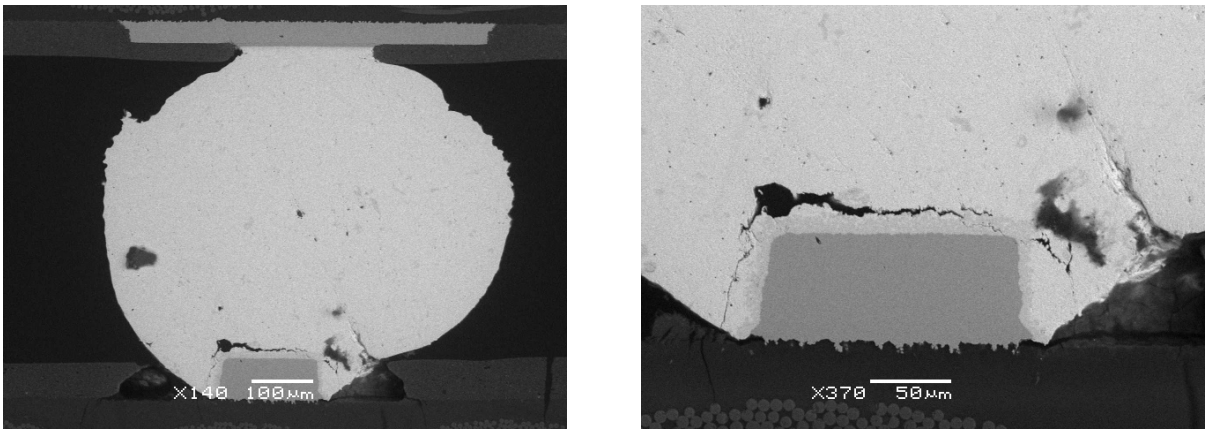

Figure 93 - TV181 U56; SEM Image of Solder Ball A9 Cross-Section

5.3.3.10.1 Component location U25 is a TSOP-50 from the lead-free rework (Batch A), soldered with SAC305 on tin component finish. This component failed on cycle one and was reworked prior to combine environments testing.

In Figure 94, the optical micrograph on the left is the lead numbering and the image on the right is of leads 21-25. The arrows indicate cracked solder mask and the arrow on lead 22 indicates a solder disturbance at 49X magnification.

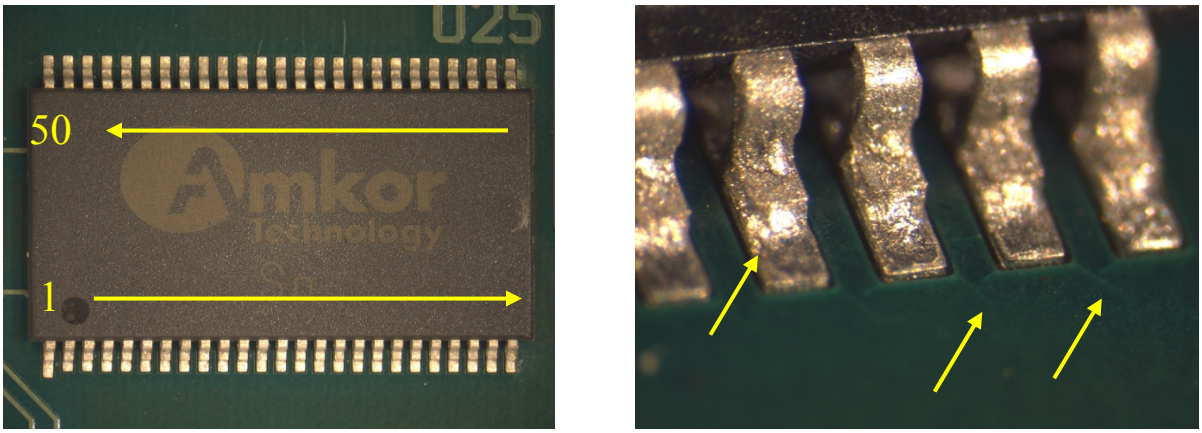

Figure 94 - TV181 U25; Optical Micrographs

In Figure 95, x-ray images of leads 22 -25 on the left and lead 22 on the right.

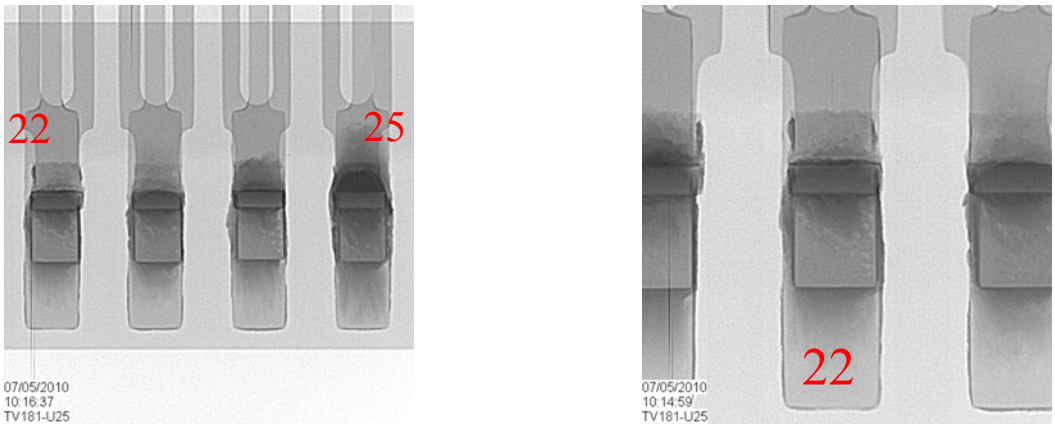

Figure 95 - TV181 U25; X-Ray Images of Component Leads

Figure 96 shows SEM images of leads 19-25 on the left and leads 44-50 on the right at a magnification of 22X.

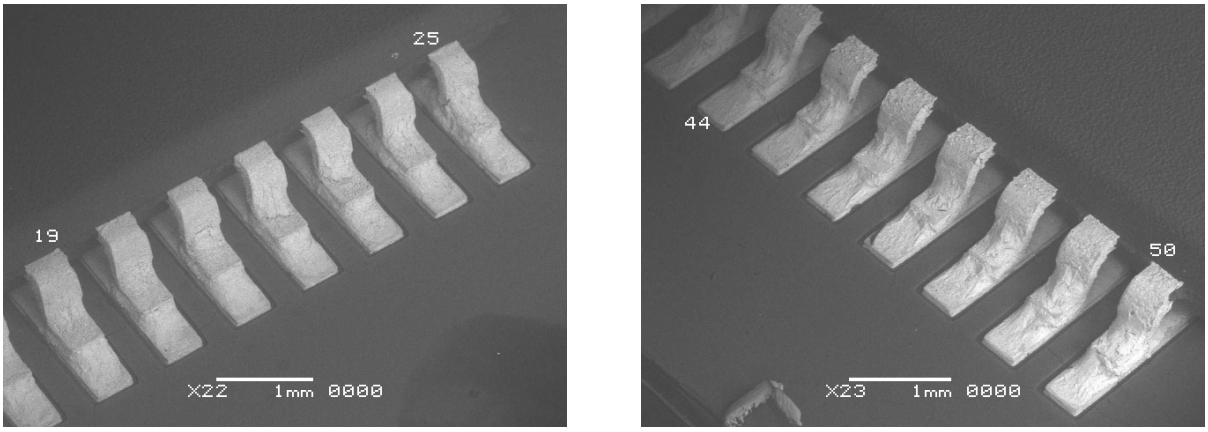

Figure 96 - TV181 U25; SEM Images

Optical micrographs in Figure 97 show grinding levels in the image on the left and a cross-sectional view of lead 1, level 1, at 30X magnification on the right.

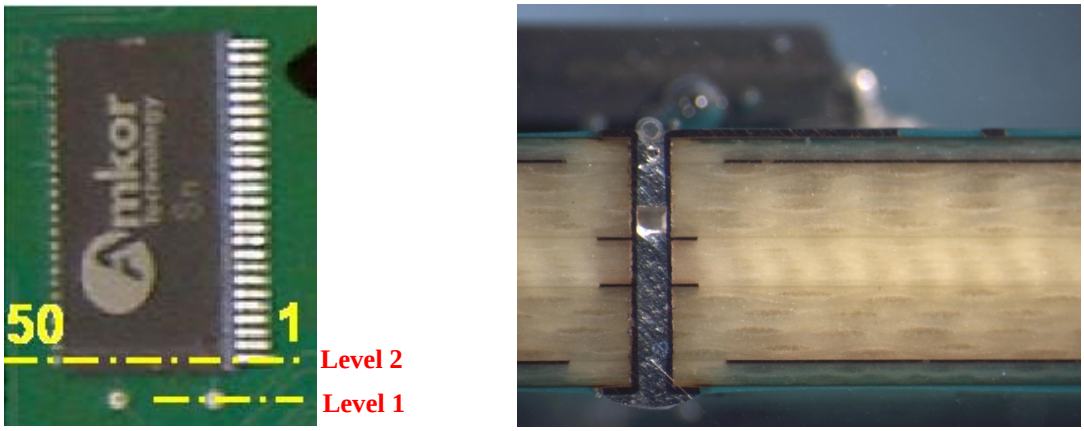

Figure 97 - TV181 U25; Optical Micrographs

Figure 98 shows cross-sectional micrographs of lead 2 (left) and lead 50 (right), level 2 grinding, at 136X magnification.

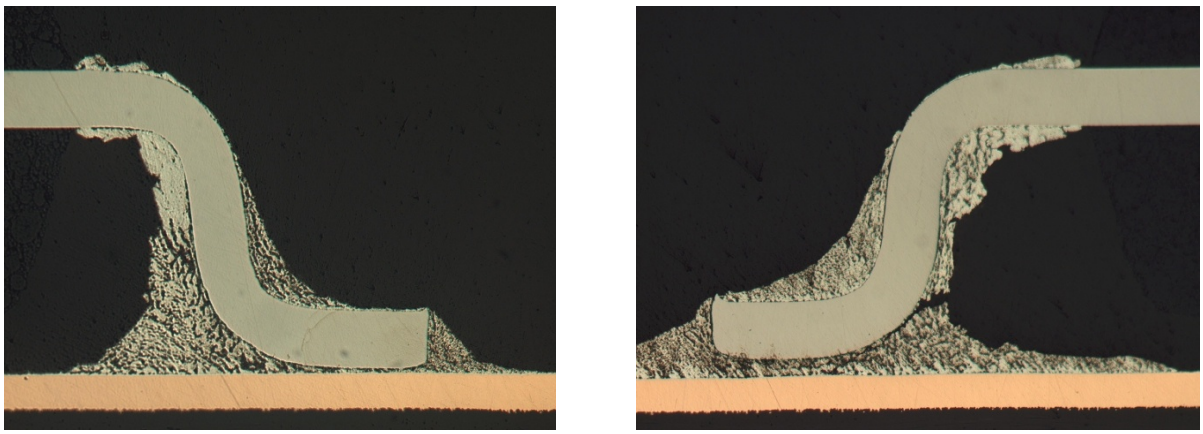

Figure 98 - TV181 U25; Cross-Sectional Micrographs

Figure 99 shows a SEM image of cross-section lead 2, level 2 grinding at 150X magnification.

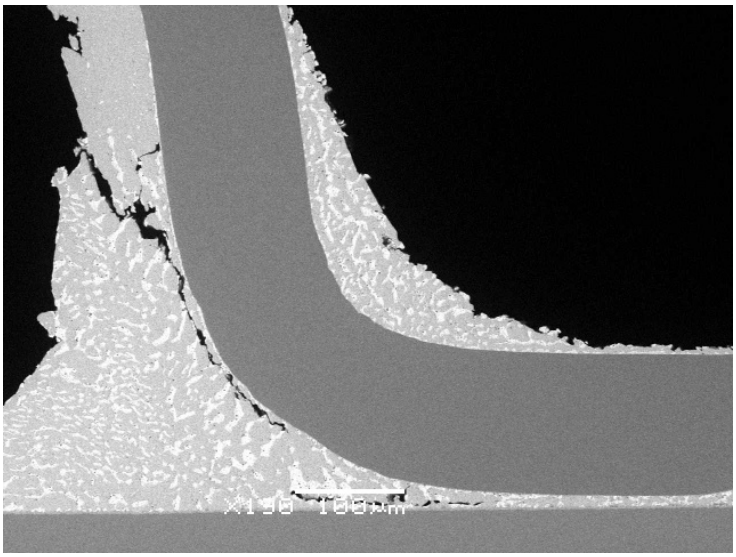

Figure 99 - TV181 U25; SEM Image

5.3.3.11 Test Vehicle 183

Component location U41 is a TQFP-144 from lead-free rework (Batch A), soldered with SAC 305 on SAC305 dip component finish. This component failed on cycle one and was not reworked.

Figure 100 shows inadequate solder joint resulting in no connection between the lead and the pad.

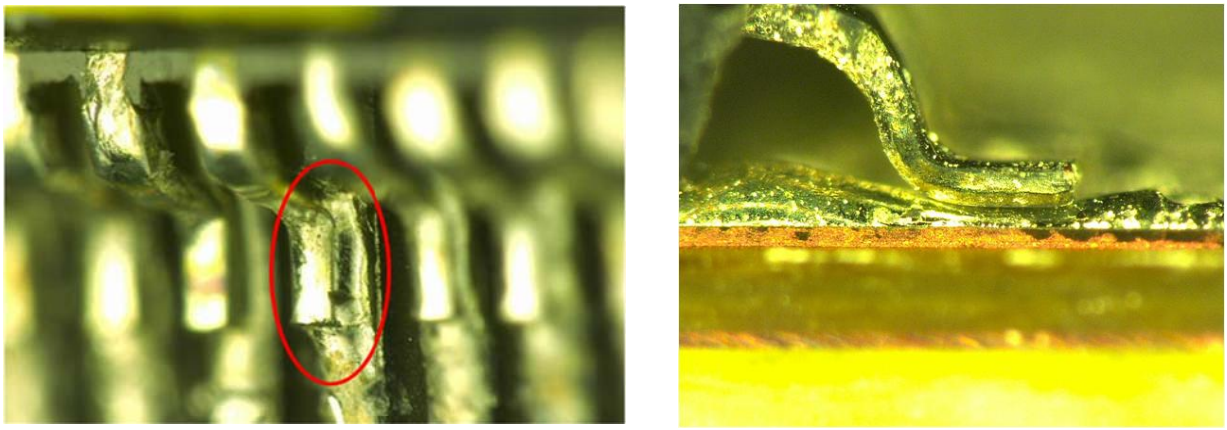

Figure 100 - TV183 U 41; Optical Micrographs of Suspect Lead

Figure 101 shows cross-sectional micrographs of component leads comparing suspect lead to a typical acceptable lead.

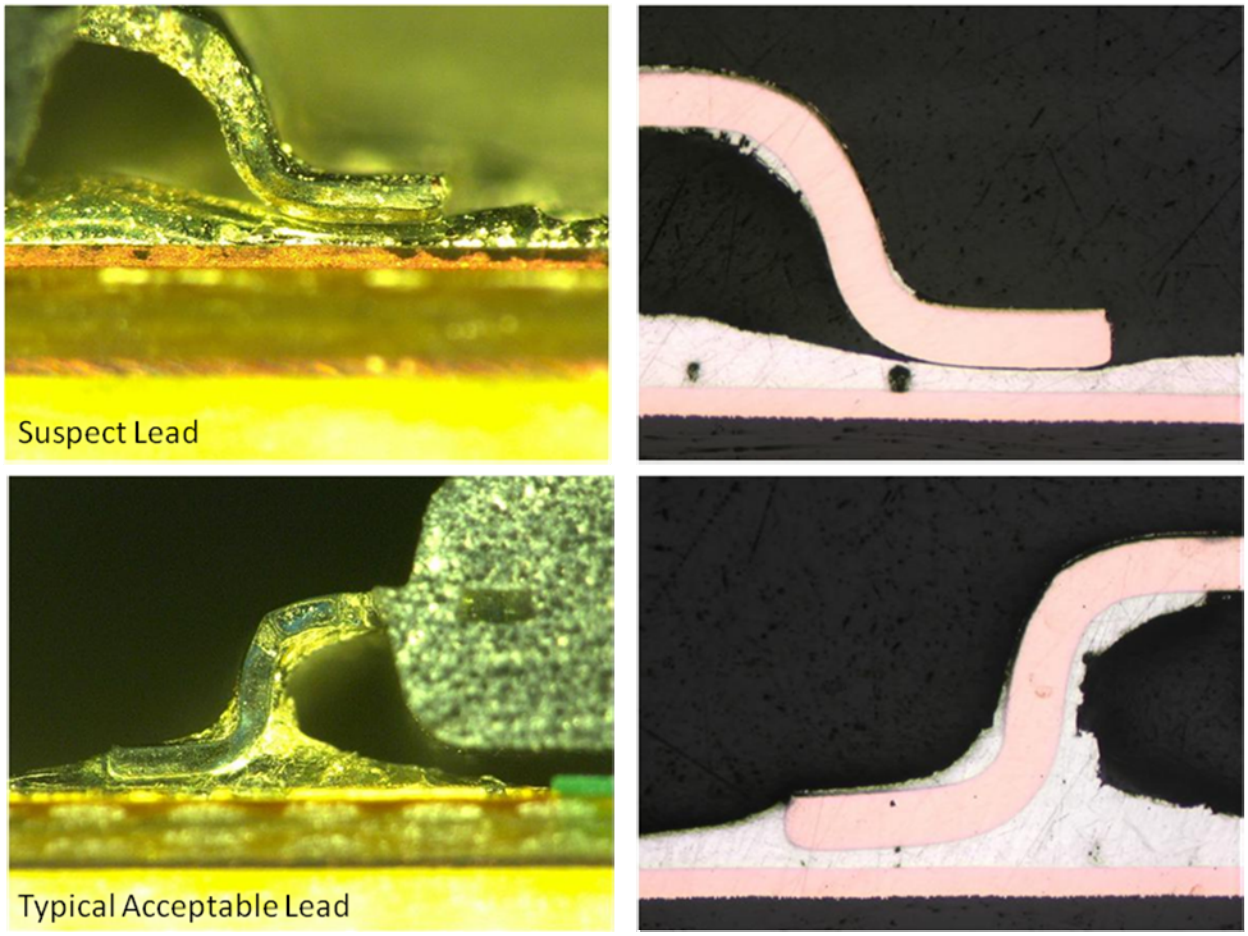

Figure 101 - TV183 U 41; Cross-Sectional Micrographs

5.3.4 Combined Environments Test Summary Tables

Table X and X provide a qualitative comparative summary of the relative performance of the Pb-free solder alloys based on 10 % Weibull failure numbers. Table X is for "Manufactured" test vehicles and Table X is for "Rework" test vehicles. All comparisons are based on a two-parameter Weibull analysis of the data.

Baseline SnPb data and other solder alloy/component finish data which is within 5% of the baseline is denoted with a 0. Single symbols, – or +, denote data that is 5% to 20% above (+) or below (-) the baseline. Double symbols, -- or ++, denote data that is more than 20% above (++) or below (--) the baseline. Green cells denote performance better than the SnPb baseline. Yellow cells denote performance worse than the SnPb baseline. Red cells denote data that is grossly worse than the SnPb baseline. Numerical values can be found in the "Weibull Numbers" Tables. Testing still in-progress is denoted with a P. Data that is not available or where there were not enough failures to rank the solders is denoted with a NA. Some test vehicles did not undergo certain tests which is denoted by an NT (not tested).

Table 17 – Combined Environments Test; Relative Solder Performance, Manufactured Test Vehicles

Board Finish	Component	Alloy	Finish	Nf (1%)	Nf (10%)	Nf (63.2%)
ImAg	BGA-225	SAC305	SAC405	+	0	-
ImAg	BGA-225	SN100C	SAC405	-	-	--
ImAg	BGA-225	SnPb	SAC405	--	--	--
ImAg	BGA-225	SAC305	SnPb	--	--	--
ImAg	BGA-225	SN100C	SnPb	--	--	--
ImAg	BGA-225	SnPb	SnPb	0	0	0
ImAg	CLCC-20	SAC305	SAC305	--	--	-
ImAg	CLCC-20	SN100C	SAC305	--	--	-
ImAg	CLCC-20	SnPb	SAC305	--	--	-
ImAg	CLCC-20	SAC305	SnPb	--	--	--
ImAg	CLCC-20	SN100C	SnPb	--	--	-
ImAg	CLCC-20	SnPb	SnPb	0	0	0
ImAg	CSP-100	SAC305	SAC105	-	0	+
ImAg	CSP-100	SN100C	SAC105	--	--	--
ImAg	CSP-100	SnPb	SAC105	--	--	0
ImAg	CSP-100	SAC305	SnPb	0	0	0
ImAg	CSP-100	SN100C	SnPb	--	-	+
ImAg	CSP-100	SnPb	SnPb	0	0	0
ImAg	TSOP-50	SAC305	SnBi	++	0	--
ImAg	TSOP-50	SN100C	SnBi	--	--	--
ImAg	TSOP-50	SnPb	SnBi	++	+	-
ImAg	TSOP-50	SAC305	SnPb	0	0	0
ImAg	TSOP-50	SN100C	SnPb	--	--	--
ImAg	TSOP-50	SnPb	SnPb	0	0	0

5.4 Thermal Cycle -55°C to +125°C Test

5.4.1 Thermal Cycle -55°C to +125°C Test Method

This test determines a test specimen's resistance to degradation from thermal cycling. The limits identified in thermal cycle testing were used to compare performance differences in the Pb-free test alloys and mixed solder joints vs. the baseline standard SnPb (63/37) alloy.

This test was performed in accordance with IPC-SM-785 *(Guidelines for Accelerated Reliability Testing of Surface Mount Solder Attachments)* and the following procedure:

- Continuously monitor the electrical continuity of the solder joints during the test. It is desirable to continue thermal cycling until 63% of each component type fails.

Table 18 - Thermal Cycling Test Methodology; -55°C to +125°C

Parameters	▪ -55°C to +125°C ▪ Cycles: The project consortia will review the data and determine when the test is complete ▪ Decision point at 2,000 and 4,000 cycles ▪ 5 to 10°C/minute ramp ▪ 30 minute high temperature dwell ▪ 10 minute low temperature dwell		
Number of Test Vehicles Required			
Mfg. SnPb = 5	Mfg. LF = 5	Mfg. LF {SN100C} = 5	Mfg. LF {ENIG} = 1
Rwk. SnPb = 5	Rwk. SnPb {ENIG} = 1	Rwk. LF = 5	
Trials per Specimen	1		

5.4.2 Thermal Cycle -55°C to +125°C Testing Results Summary (3600 cycles)

The -55ºC to +125ºC thermal cycle testing was not completed at the time this report was being drafted. However, nearly all of the components had reached an N63 statistical value (i.e. most of the population had reached at least 63% failure rate) thus allowing for a preliminary graphical analysis of the compiled failure data. The Manufactured test vehicle failure rates are shown in Table 19 and Reworked test vehicle failure rates are shown in Table 20.

Table 19 - Manufactured Test Vehicle Component Population Failure Rates after 3600 Thermal Cycles

Component Type	Total Failures	Population	Percent Failed
CLCC-20	232	311	74.6%
QFN-20	70	134	52.2%
QFP-144	228	309	73.8%
PBGA-225	156	279	56.0%
PDIP-20	160	220	72.7%
CSP-100	175	281	62.3%
TSOP-50	178	249	71.5%

Table 20 - Reworked Test Vehicle Component Population Failure Rates after 3600 Thermal Cycles

Component Type	Total Failures	Population	Percent Failed
PBGA-225	**27**	**66**	**40.9%**
PDIP-20	**41**	**60**	**68.3%**
CSP-100	**31**	**67**	**46.3%**
TSOP-50	**62**	**99**	**62.6%**

5.4.2.1 Ceramic Leadless Chip Carriers (CLCC-20)

The CLCC-20 components had accumulated 74.6% population failure after the completion of 3600 thermal cycles. The CLCC-20 components were included on the test vehicles because of their poor reliability track record on electronic assemblies used in harsh environments. Industry data[3] has demonstrated that the CLCC component style undergoes solder joint integrity degradation under IPC Class 3 use environments due to coefficient of thermal expansion (CTE) mismatch with the printed wiring assembly. CLCC-20 components had six different combinations (SAC/SAC, SAC/SnPb, SnPb/SAC, SnPb/SnPb, SNIC/SAC, SNIC/SnPb) tested and the results showed statistically significant differences in thermal cycle reliability. The completely Pb-free combinations (SAC/SAC and SNIC/SAC) were outperformed by solder/finish combinations that contained SnPb. The Weibull plot in Figure 102 summarizes the CLCC-20 thermal cycle test results.

[3] J. Lau and Y. Pao, Solder Joint Reliability of BGA, CSP, Flip Chip, and Fine Pitch SMT Assemblies, McGraw Hill, ISBN 0-07-036648-9.

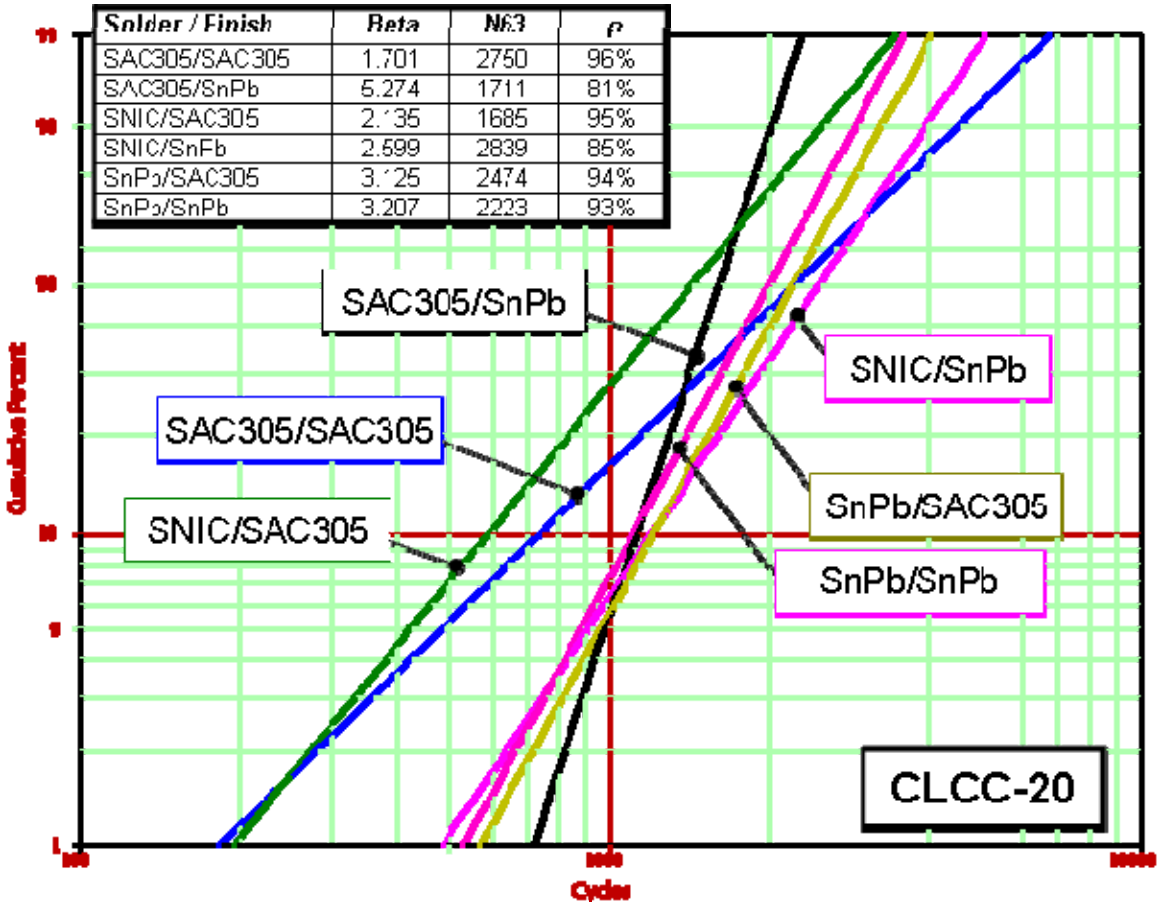

Figure 102 - CLCC-20 Weibull Plot

5.4.2.2 Quad Flatpack No-Lead (QFN-20)

The QFN-20 components had accumulated 52.2% population failure after the completion of 3600 thermal cycles and were the most robust component type in the investigation. QFN-20 components had three different combinations (SAC/Sn, SNIC/Sn, SnPb/Sn) tested and the results showed statistically significant differences in thermal cycle reliability. The SnPb/Sn combination has the best thermal cycle performance. The Weibull plot in Figure 103 summarizes the QFN-20 thermal cycle test results.

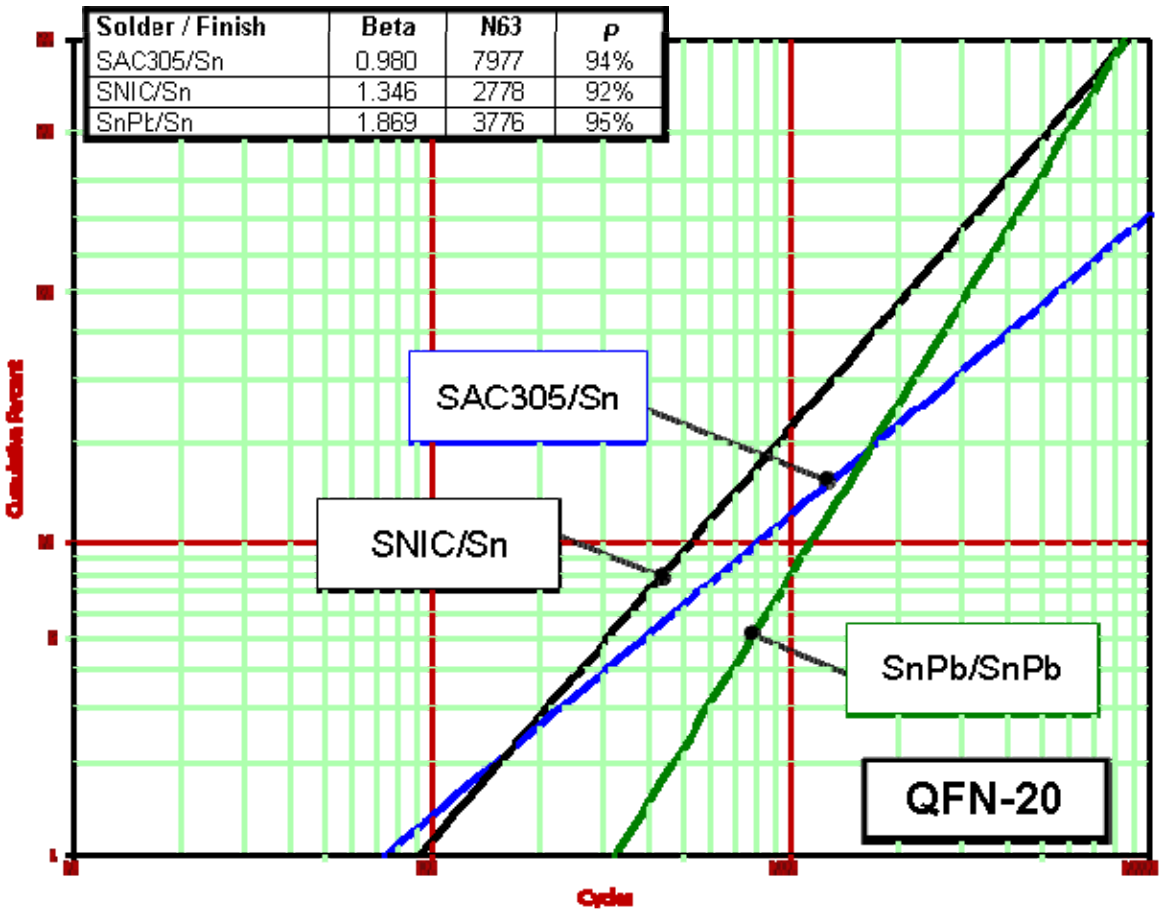

Figure 103 - QFN-20 Weibull Plot

5.4.2.3 Quad Flatpack Package (QFP-144) Results

The TQFP-144 components had accumulated 73.4% population failure after the completion of 3600 thermal cycles. TQFP-144 components had eight different combinations (SAC/Sn, SAC/SnPb, SAC/SAC, SnPb/NiPdAu, SnPb/SnPb, SnPb/Sn, SNIC/Sn, SNIC/SnPb) tested for thermal cycle reliability. The SnPb/SnPb Dip combination had the best thermal cycle performance with all other combinations having similar performances. The Weibull plot in Figure 104 summarizes the TQFP-144 thermal cycle test results.

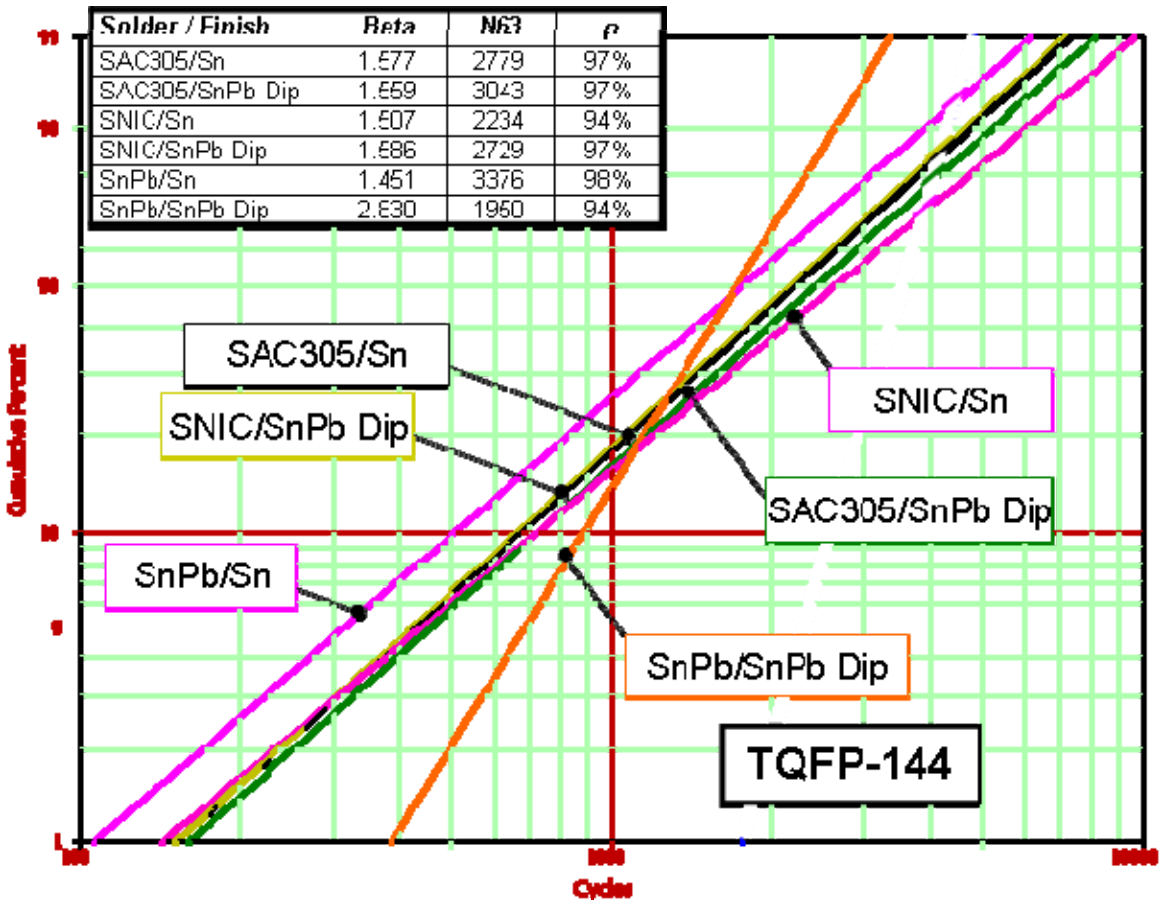

Figure 104 - TQFP-144 Weibull Plot

5.4.2.4 Ball Grid Array (PBGA-225) Results

The PBGA-225 components had accumulated 56% population failure after the completion of 3600 thermal cycles. PBGA-225 components had six different combinations (SAC/SAC, SAC/SnPb, SNIC/SAC, SNIC/SnPb, SnPb/SAC, SnPb/SnPb) tested and the results showed statistically significant differences in thermal cycle reliability. The SnPb/SAC405 and the SAC305/SnPb had the best performance compared to the other combinations as shown in Figure 105. As shown in Figure 106, BGA components that were reworked, i.e. “1 RWK” exhibited similar reliability to their counterparts on the Reworked test vehicles that were not reworked.

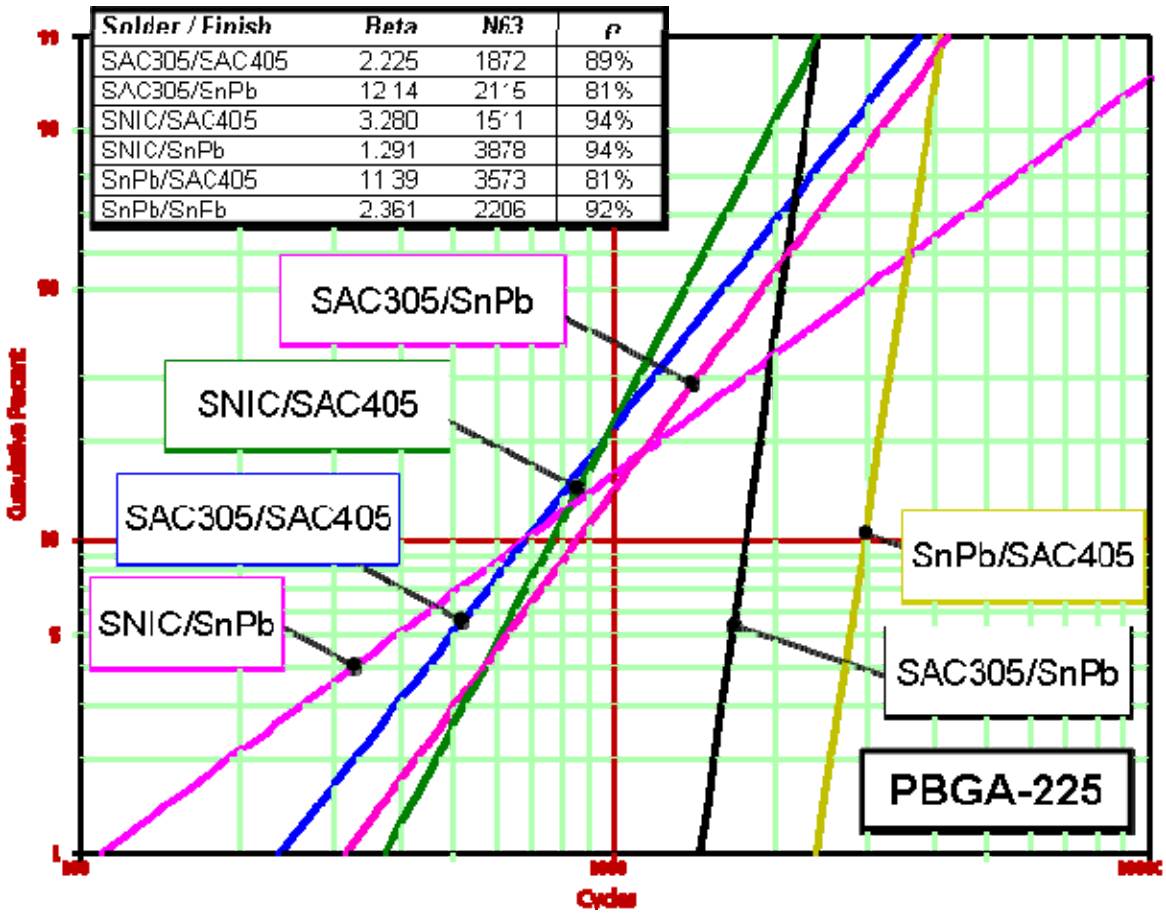

Figure 105 - PBGA-225 Weibull Plot

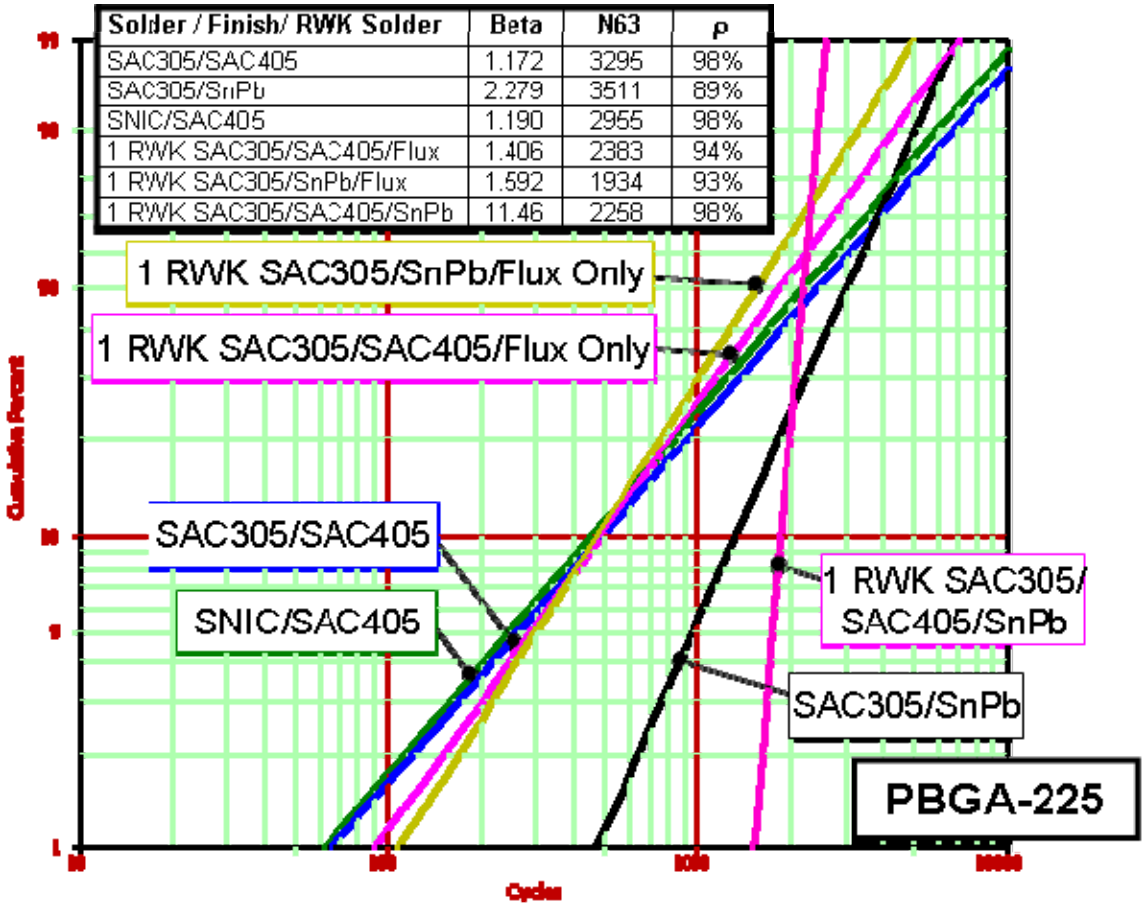

Figure 106 - Reworked PBGA-225 Weibull Plot

5.4.2.5 Chip Scale Package (CSP-100) Results

The CSP-100 components had accumulated 62.3% population failure after the completion of 3600 thermal cycles. CSP-100 components had seven different combinations (SAC/SAC105, SAC/SnPb, SNIC/SAC105, SNIC/SNIC, SNIC/SnPb, SnPb/SAC105, SnPb/SnPb) tested and the results showed statistically significant differences in thermal cycle reliability as shown in Figure 107. The SnPb/SAC105 had the best performance and the SNIC/SAC105 had the poorest performance of the combinations tested. The reworked CSP-100 components (Figure 108) generally showed higher reliability than the manufactured components not reworked on the same test vehicle.

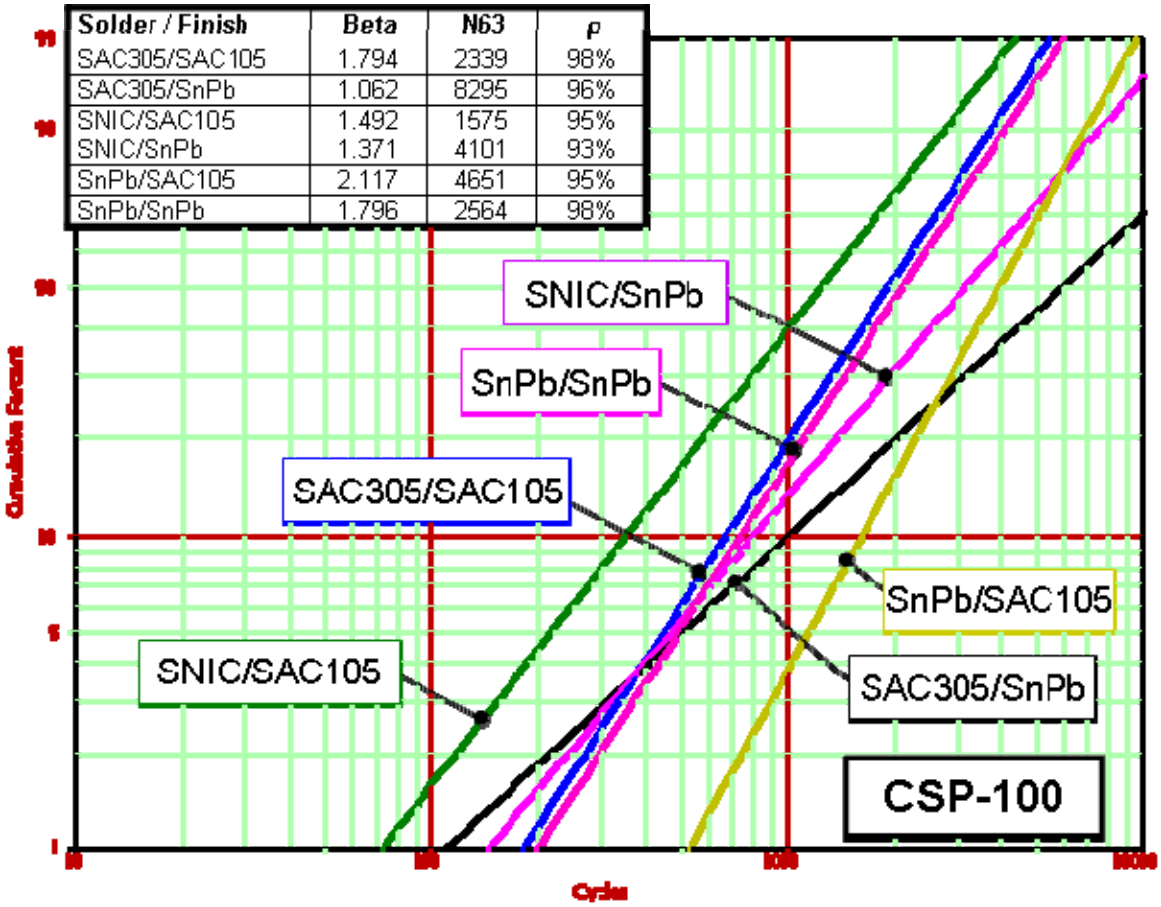

Figure 107 - CSP-100 Weibull Plot

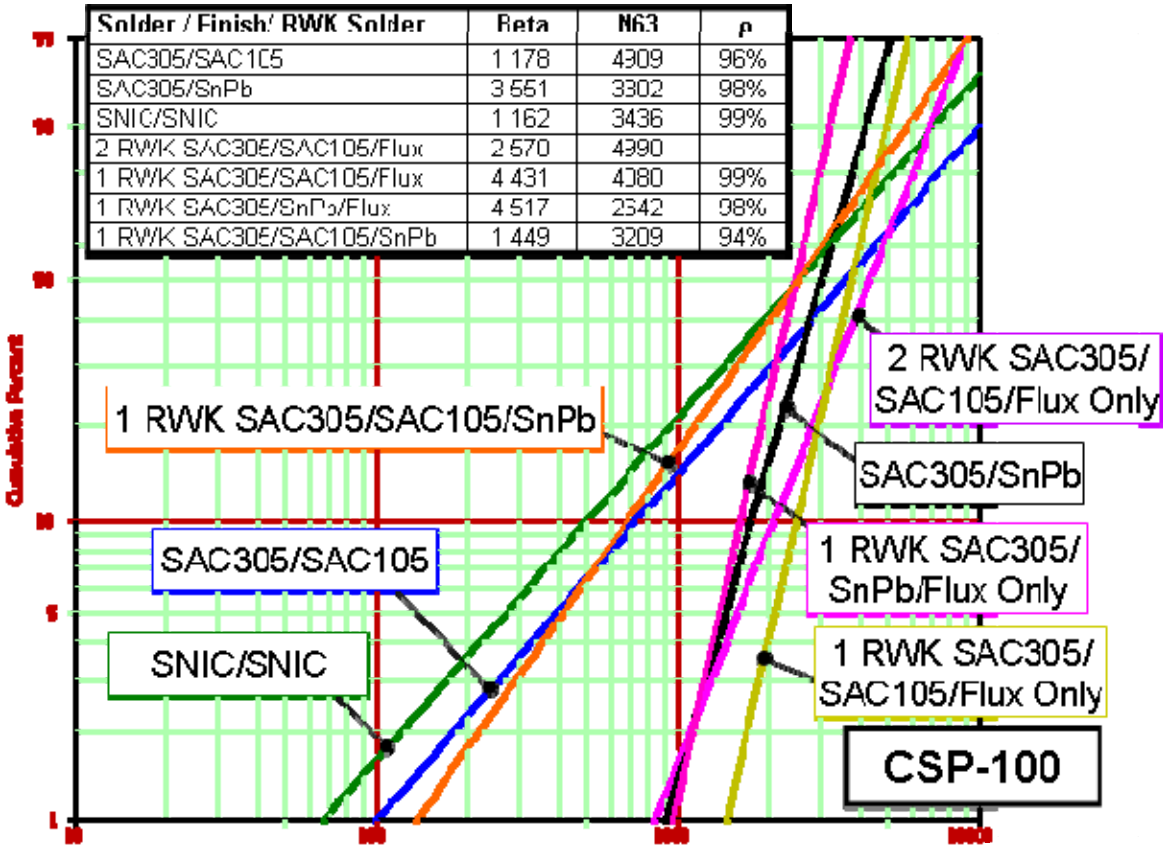

Figure 108 - Reworked CSP-100 Weibull Plot

5.4.2.6 Thin Small Outline Package (TSOP-50) Results

The TSOP-50 components had accumulated 71.5% population failure after the completion of 3600 thermal cycles. TSOP-50 components had nine different combinations (SAC/SnPb, SAC/SnBi, SAC/Sn, SNIC/SnPb, SNIC/SnBi, SNIC/Sn, SnPb/SnBi, SnPb/Sn, SnPb/SnPb) tested. The lead (Pb) containing combinations slightly out performed the Pb-free combinations tested. The rework TSOP-50 components exhibited significantly different trends compared to those on the manufactured test vehicle. These results require further statistical review before drawing any conclusions. The Weibull plots in Figure 109 and Figure 110 summarize the TSOP-50 thermal cycle test results.

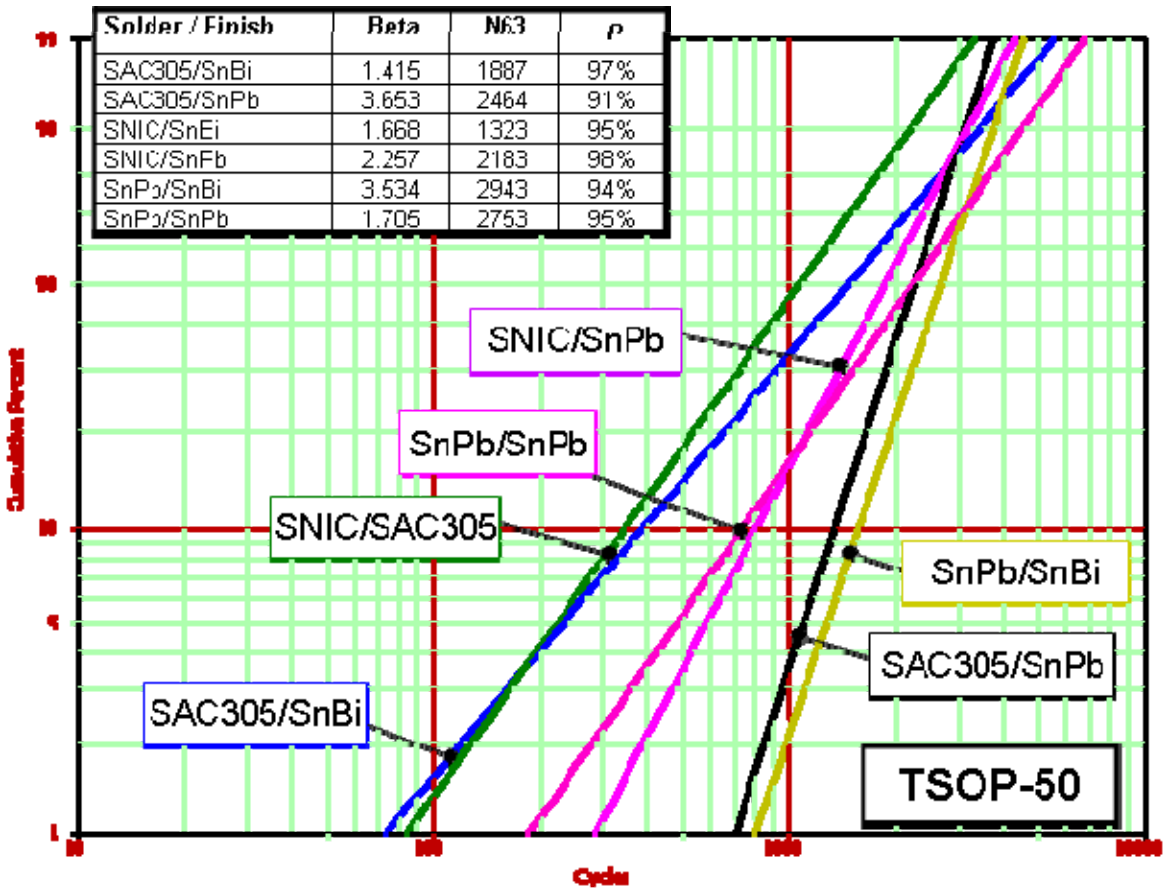

Figure 109 - TSOP-50 Weibull Plot

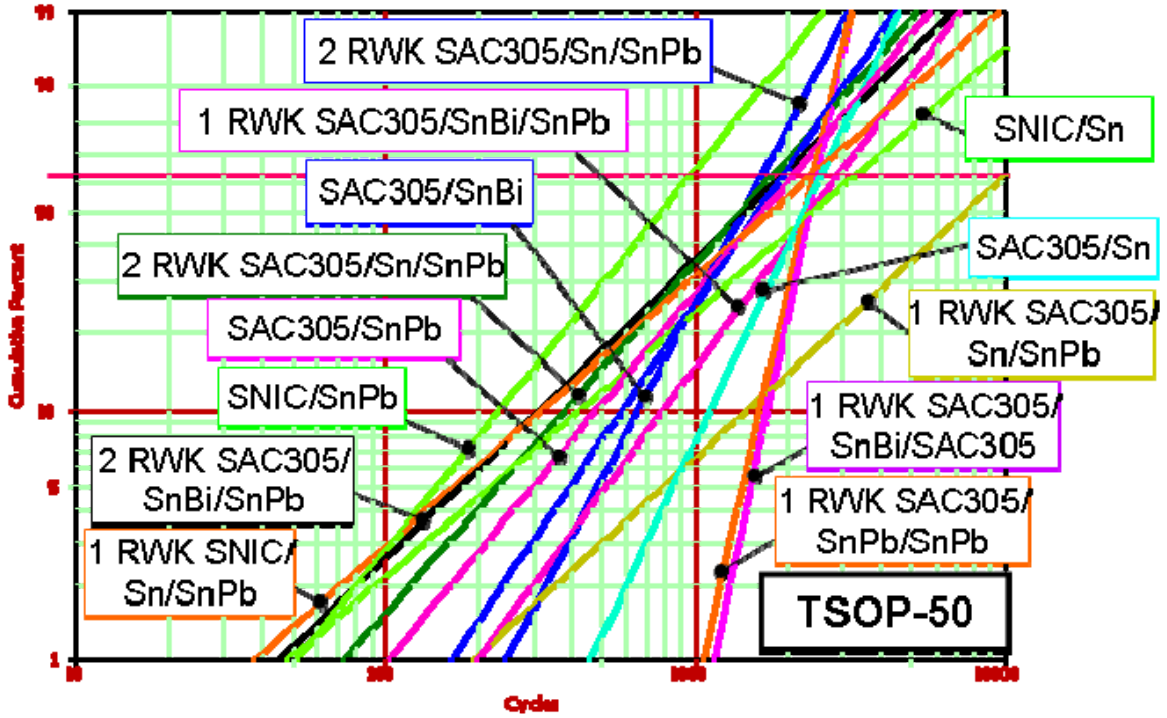

Figure 110 - Reworked TSOP-50 Weibull Plot

5.4.2.7 Dual In-Line Package (PDIP-20) Results

The PDIP-20 components had accumulated 72.7% population failure after the completion of 3600 thermal cycles. The solder joint failure behavior of the PDIP-20 components was a surprise to the consortia team as the PDIP-20 failure rate documented in the JCAA/JGPP investigation results was only 8% after 4743 total thermal cycles. PDIP-20 components had four different combinations (SNIC/Sn, SNIC/NiPdAu, SnPb/NiPdAu, SnPb/Sn) tested and the results showed statistically significant differences in thermal cycle reliability. The SnPb/Sn combination registered the best performance. The reworked PDIP-20 component thermal cycle performance was not statistically different than a non-reworked PDIP-20 component. Additional resources will be focused on determining the exact root cause of the unexpected PDIP-20 failure rates. The Weibull plots in Figure 111 and Figure 112 summarize the PDIP-20 thermal cycle test results.

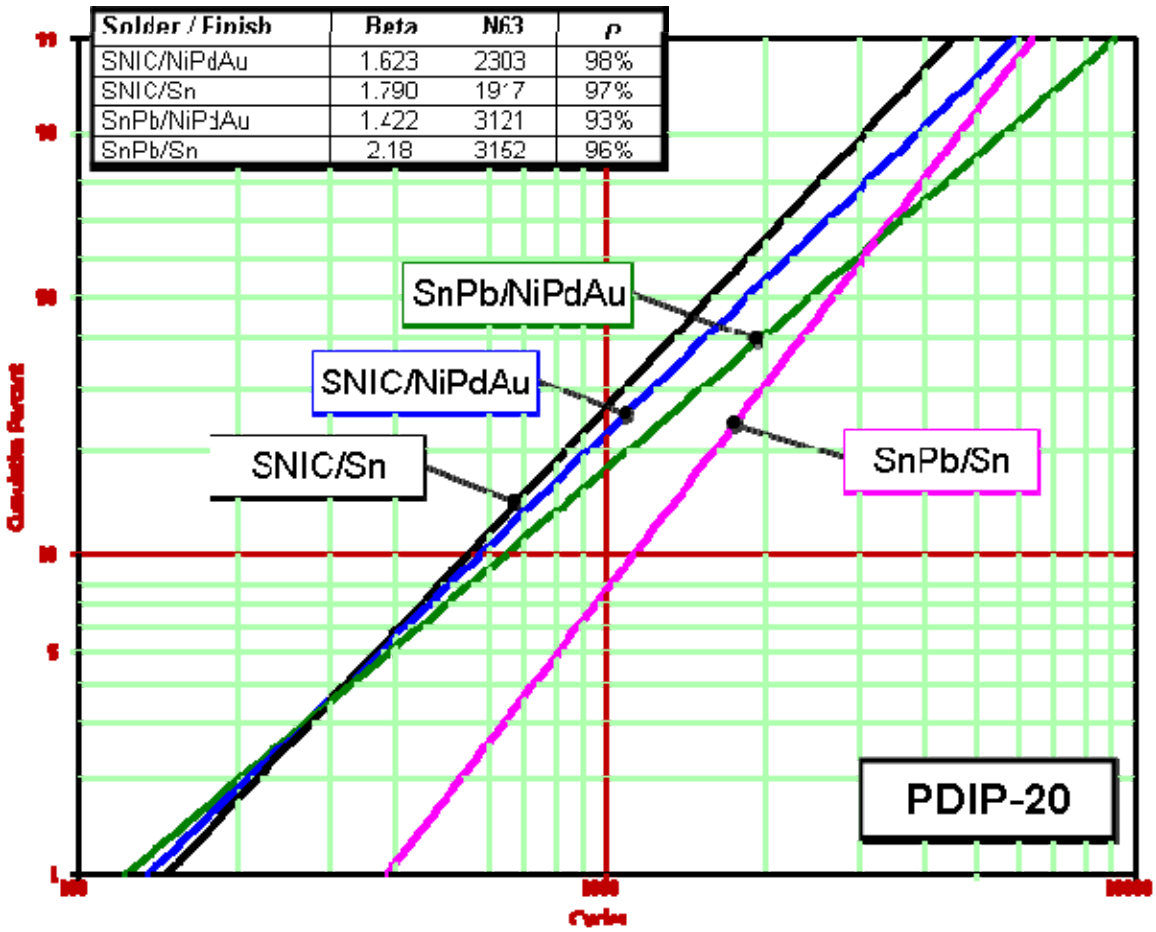

Figure 111 - PDIP-20 Weibull Plot

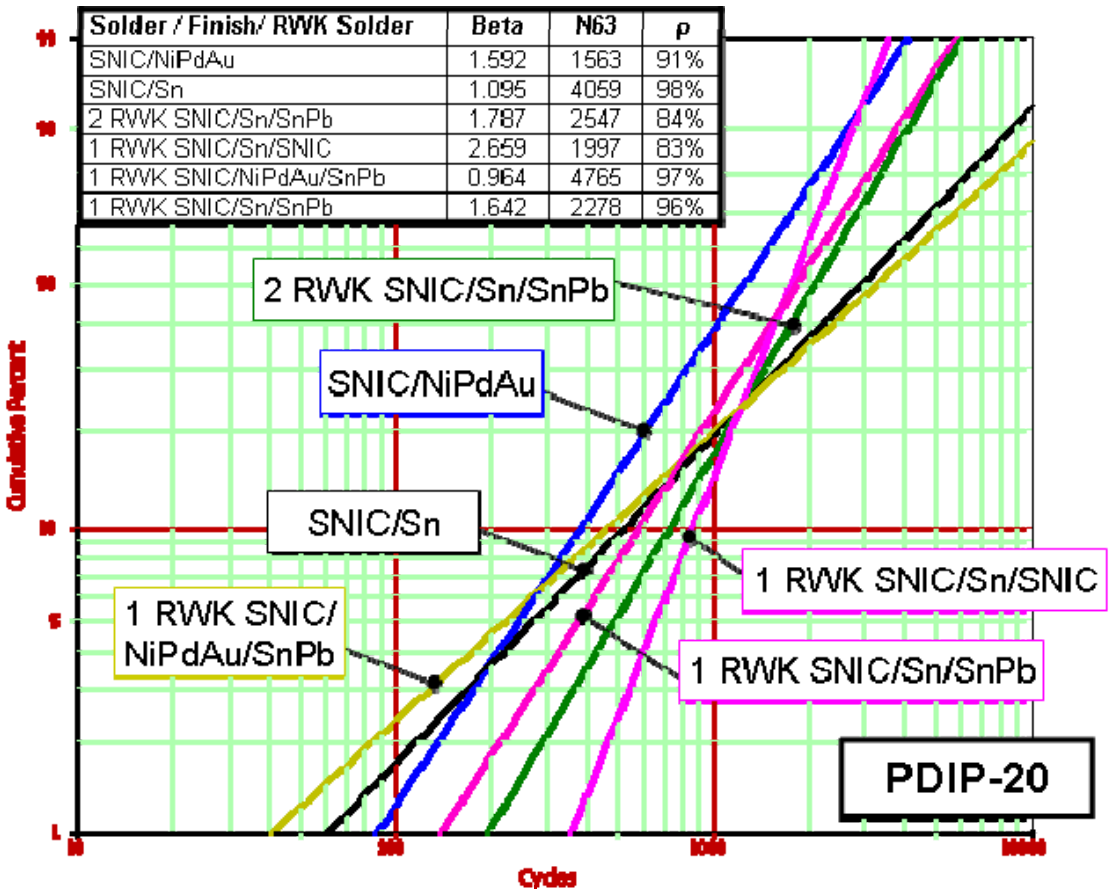

Figure 112 - Reworked PDIP-20 Weibull Plot

Due to the large number of multiple combinations of solder paste alloys and component surface finishes, significant statistical analysis with comparison to physical failure analysis efforts will be required to fully understand the results once thermal cycle testing is completed. In general, the preliminary results show that the SnPb solder alloy outperformed the two Pb-free solder alloys. Test result outliers will be investigated to determine if they have a root cause due to non thermal cycle conditioning factors such as a component, test vehicle fabrication or manufacturing process defect. Statistical analysis of the reviewed test results will be conducted a second time in order to present a more concise picture of the solder joint root cause failure.

5.5 Thermal Cycle -20°C to +80°C Test

5.5.1 Thermal Cycle -20°C to +80°C Test Method

This test determines a test specimen's resistance to degradation from thermal cycling. The limits identified in thermal cycle testing were used to compare performance differences in the Pb-free test alloys and mixed solder joints vs. the baseline standard SnPb (63/37) alloy.

Perform this test in accordance with IPC-SM-785 *(Guidelines for Accelerated Reliability Testing of Surface Mount Solder Attachments)* and the following procedure.

- Continuously monitor the electrical continuity of the solder joints during the test. It is desirable to continue thermal cycling until 63% of each component type fails.

Table 21 - Thermal Cycling Test Methodology; -20°C to +80°C

Parameters	▪ -20°C to +80°C ▪ Cycles: The project consortia will review the data and determine when the test is complete ▪ Decision point at 10,000 cycles ▪ 5 to 10°C/minute ramp ▪ 30 minute high temperature dwell ▪ 10 minute low temperature dwell	
Number of Test Vehicles Required		
Mfg. SnPb = 5	Mfg. LF = 5	
Rwk. SnPb = 5	Rwk. SnPb {ENIG} = 1	Rwk. LF = 5
Trials per Specimen	1	

5.5.2 Thermal Cycle -20°C to +80°C Testing Results Summary

Testing in progress

5.6 Drop Testing

5.6.1 Drop Test Method

This test determines the resistance of board level interconnects to board strain induced by dynamic bending as a result of drop testing. Boards tested using this method typically fail either as interfacial fractures in the solder joint (most common with ENIG) or as pad cratering in the component substrate and/or board laminate (Figure 113). These failure modes commonly occur during manufacturing, electrical testing (especially in-circuit test), card handling and field installation. The root cause of these types of failures are typically a combination of excessive applied strain due to process issues and/or weak interconnects due to process issues and/or the quality of incoming components and/or boards.

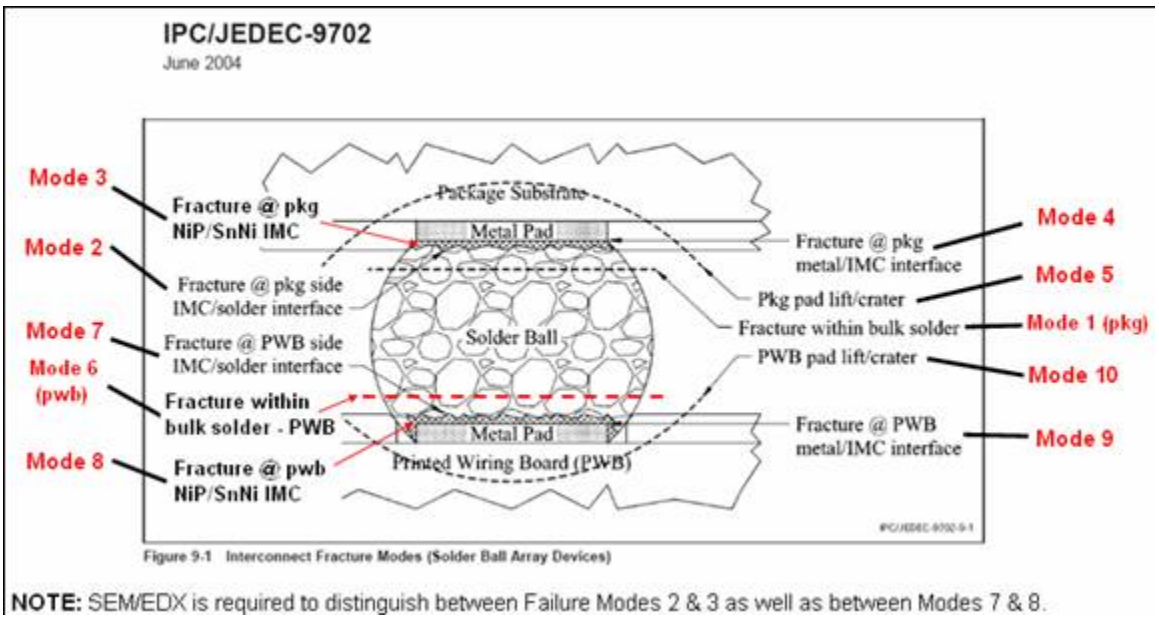

Figure 113 - Interconnect Fracture Modes (Solder Ball Array Device) IPC 9702

This board-level drop test is based on the JEDEC Standard JESD22-B110A known as Subassembly Mechanical Shock as well as insight gained by Celestica after performing numerous drop tests.

The drop test process can identify design, process, and raw material related problems in a much shorter time frame than other development tests. For this project, the drop test will determine the operation and strain endurance limits of the solder alloys and interconnects by subjecting the test vehicles to accelerated environments. The limits identified in drop testing were used to compare performance differences in the Pb-free test alloys and mixed solder joints vs. the baseline standard SnPb (63/37) alloy. The primary accelerated environments are strain and strain rate.

Table 22 - NASA-DoD Lead-Free Electronics Test Vehicle Drop Test Methodology

Parameters	▪ Shock testing will be conducted in the -Z direction ▪ 500G pk input, 2ms pulse duration ▪ Test vehicles will be dropped until all monitored components fail or 10 drops have been completed	
Number of Test Vehicles Required		
Mfg. SnPb = 5		Mfg. LF = 5
Rwk. SnPb = 5	Rwk. SnPb {ENIG} = 1	Rwk. LF = 5
Trials per Specimen	A maximum of 10 drops	

Table 23 - NSWC Crane Test Vehicle Drop Test Methodology

Parameters	▪ Shock testing will be conducted in the -Z direction ▪ 340G pk input, 2ms pulse duration for test vehicles 80, 82, 87 for first 10 drops o Following the initial 10 drops, only BGA components had failed. In an attempt to generate additional failure data, the consortium decided to increase the testing to 500G pk input for 10 additional drops. For the remaining 6 test vehicles, all drops were conducted at the 500G pk input. ▪ 500G pk input, 2ms pulse duration for test vehicles 60, 81, 82, 84, 85, and 86 ▪ Test vehicles will be dropped until all monitored components fail or 20 drops have been completed
Number of Test Vehicles Required	
Mfg. LF then Rwk. SnPb = 9 test vehicles	
Trials per Specimen	A maximum of 20 drops

5.6.2 NASA-DoD Test Vehicle Drop Testing Results Summary

The complete test report, "Drop Testing Report for NASA; TOL0702030", can be found on the NASA TEERM website (http://teerm.nasa.gov/NASA_DODLeadFreeElectronics_Proj2.html).

Although there were duplicates of each component type on the test vehicle, every component experienced a unique strain/strain rate condition due to its particular location on the board. As a result each sample depicts a unique data point and these cannot be easily lumped together. Due to the limited number of samples, the absence of physical failure analysis (at this time) and the lack of electrical opens, excluding the BGAs, it is not possible to draw any firm conclusions as to the significance of the electrical failure data.

It is likely that a great deal of the electrically-functional parts on these drop tested boards have hidden mechanical failures. Any future physical failure analysis should include dye and pry mapping of the majority of the components from a sample of the boards. The results of the dye and pry analysis could then be used to determine which of the remaining parts/boards should be

targeted for cross-sectional analysis and possibly scanning electron microscopy to characterize the damage.

The only component type to show a significant number of electrical failures during this test were the plastic ball grid array (PBGA) components. The PBGA component electrical failures mostly occurred at or near the corner joints. Twenty-eight out of the 176 PBGA components survived all 10 drops. The surviving parts were located near the outer edge of the board where the strain was found to be minimal. On average, most reworked parts failed after a fewer number of drops than compared to non-reworked PBGA components. There was no significant difference in the number of drops until failure between PBGA components reworked 1 time versus 2 times, versus 3 times. SnPb and SAC305 PBGA components on immersion Ag boards had similar failure rates, possibly due to the predominance of pad cratering. PBGA components reflowed on ENIG boards typically failed after fewer drops than those on immersion Ag boards.

There were no electrical failures for the chip-array ball grid array (CABGA), quad flat no leads (QFN) or thin small outline package (TSOP) components during the 10 drops. Future physical failure analysis however may reveal hidden mechanical damage which could be a reliability concern. Only three of the 60 ceramic leadless chip carrier (CLCC) components showed electrical fails (all failed during the 4th drop). The physical failure mechanism of these outliers is unknown at this time. One of the thin quad flat pack (TQFP) components showed an electrical fail during drop 3. Note, however, that this part was marked as a “touch-up” by the assembly team.

5.6.3 NASA-DoD Test Vehicle Drop Test Failure Analysis

After the drop testing was completed, several boards were selected for destructive failure analysis. Both dye-and-pry and cross sectioning were performed, each of which was designed to determine the location, mode and mechanism of the failure. The samples selected for dye-and-pry were examined using an optical microscope after the parts were pried from the board and the results were further mapped. The cross sectioned samples were examined using optical and scanning electron microscopy (SEM) as well as analyzed by energy dispersive x-ray (EDX). The focus was to compare the quality of the solder joints of components that were reworked once using SnPb solder (therefore consisting of a mixed metallurgy of Pb and Pb-free solder), those that were reworked twice using SnPb solder (consisting of leaded solder), and those which were not reworked at all- therefore Pb-free. Table 24 shows which components were selected by Celestica for failure analysis.

Table 24 - Components that Celestica Performed Failure Analysis On

Test Vehicle	Component	Solder	Rework	Finish	Location	Failure Cycle	Cross-section	Dye-and-Pry	Selection Criteria	Failure mode
144	LF	SnPb	N/A	ImmAg	U4	1	+		Electrical failure, row Q	#4 - Ni/IMC brittle
25	SnPb	SnPb	SnPb	ImmAg	U4	5	+		Electrical failure, row A	#10 – Pad Cratering
27	SnPb	SnPb	N/A	ImmAg	U5	3	+		Electrical failure, row Q	No failure confirmed
29	SnPb	SnPb	N/A	ImmAg	U6	3		+	Electrical failure, row A and row Q	All failure are Pad Cratering
26	SnPb	SnPb	N/A	ImmAg	U56	No failure	+		Comparison	Pad Cratering
77	LF	LF	N/A	ImmAg	U4	5	+		Electrical failure, row A	#10 – Pad Cratering
187	SnPb	LF	N/A	ImmAg	U4	2	+		Electrical failure, row Q	#2 – IMC/Solder ? #10 – Pad Cratering
92	LF	LF	N/A	ImmA	U5	3	+		Electrical failure, row A	#10 – Pad Cratering
59	LF	LF	N/A	ImmA	U6	3		+	Electrical failure, row Q	All failure are Pad Cratering
58	LF	LF	N/A	ImmAg	U56	No failure	+		Comparison	No failure
159	LF	SnPb	N/A	ENIG	U4	2	+		Electrical failure, row A, row B, and row 15	#8 – NiP/IMC brittle
159	LF	SnPb	N/A	ENIG	U44	2	+		Electrical failure, row A and row Q	#8 – NiP/IMC brittle
159	SnPb	LF	SnPb	ENIG	U6	2	+		Electrical failure, row A and row 15	#8 – NiP/IMC brittle
159	SnPb	SnPb	SnPb	ENIG	U56	4	+		Electrical failure, row A and row B	#8 – NiP/IMC brittle #10 – Pad Createring

The main focus of the NASA drop test failure analysis was the 225 I/O plastic BGAs. This was because the vast majority of electrical failures on the test vehicle were these larger PBGAs. All CSPs electrically passed drop testing. For the PBGAs there was a wide range in number of drops until failure: 40% failed electrically within less than 6 drops and 99% failed electrically by 20 drops. Less than 1% of non-BGA components electrically failed after 20 drops. Pad cratering was the predominant failure mode for all samples destructively analyzed. Dye-and-pry and cross-sections of failed joints are shown below; Figure 114 and Figure 115.

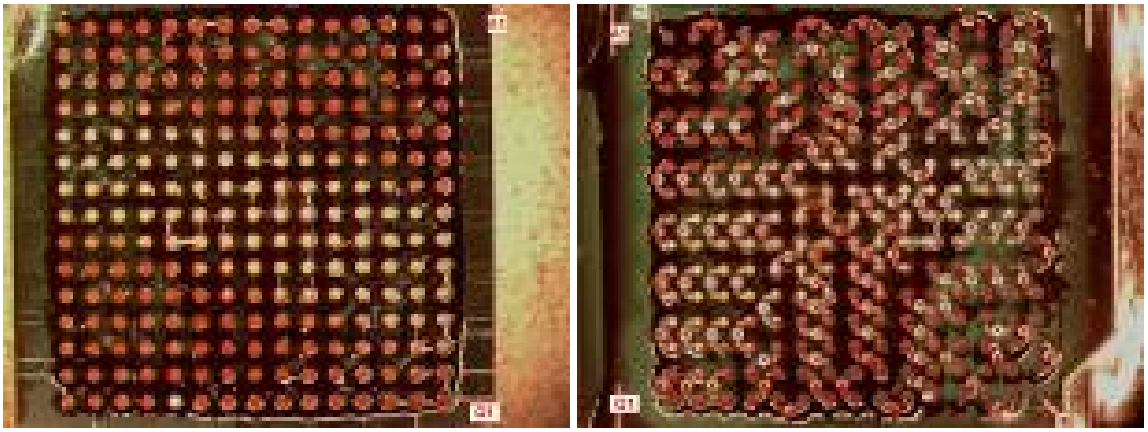

Component side *Board side*

Figure 114 - Typical Pad Cratering seen on BGA225 after Dye-and-Pry

SnPb ball/SnPb solder after rework *Pb-free ball/Pb-free solder as-assembled*

Figure 115 - Typical Pad Cratering seen on BGA225 after cross-section

An Additional mechanism that caused electrical failure in mixed solder joints was crack propagation through a low melting Sn+Pb+Ag_3Sn ternary and/or Sn+Pb+Ag_3Sn +Cu_6Sn_5 quaternary eutectic accumulation layer at the board or component interface depending on sample history. In as-assembled condition the crack grew between the intermetallic layer and the bulk solder at the board side and after rework the more susceptible location was the interface between the intermetallic layer and the bulk solder at the component side; Figure 116. For the ENIG finished boards the predominant failure modes were brittle intermetallic cracking on both board and component sides.

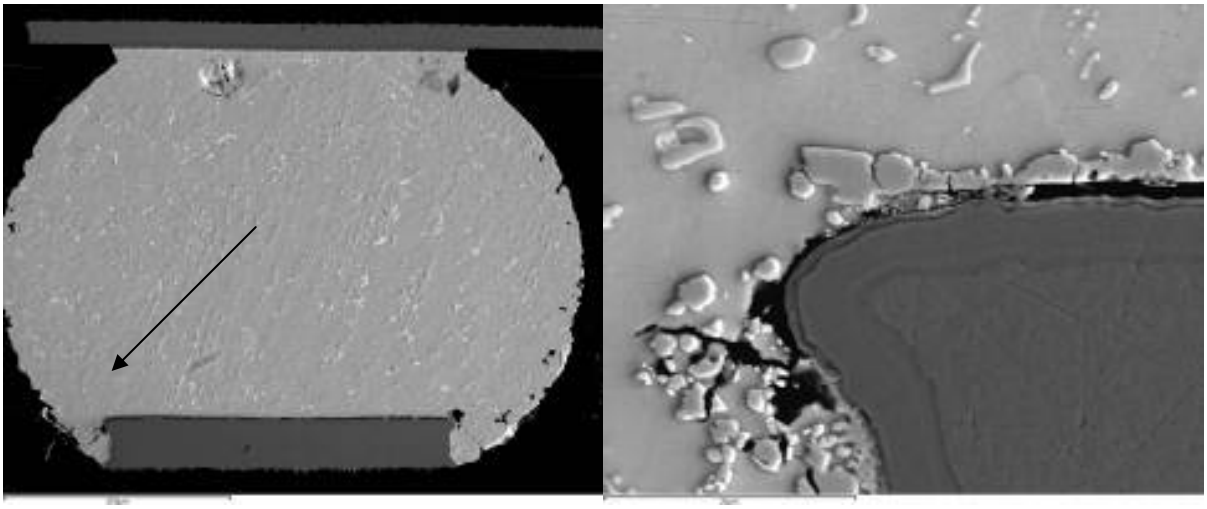

General view *High magnification*

Figure 116 - SEM of Brittle Intermetallic Failure on BGA225

One of the cards tested, which had no electrically failing leaded parts, was chosen for dye & pry of all 63 parts in order to map the mechanical damage. Figure 117 summarizes the mechanical failure (red overlay) of one board after 20 drops at 500G. In-situ electrical data on BGAs showed that some PBGAs failed after as little as 5 drops – this implies that mechanical failure may have occurred after even fewer drops. Interesting to note that the board was held by posts in the 4 corners and as such the strain is not symmetrical across the card.

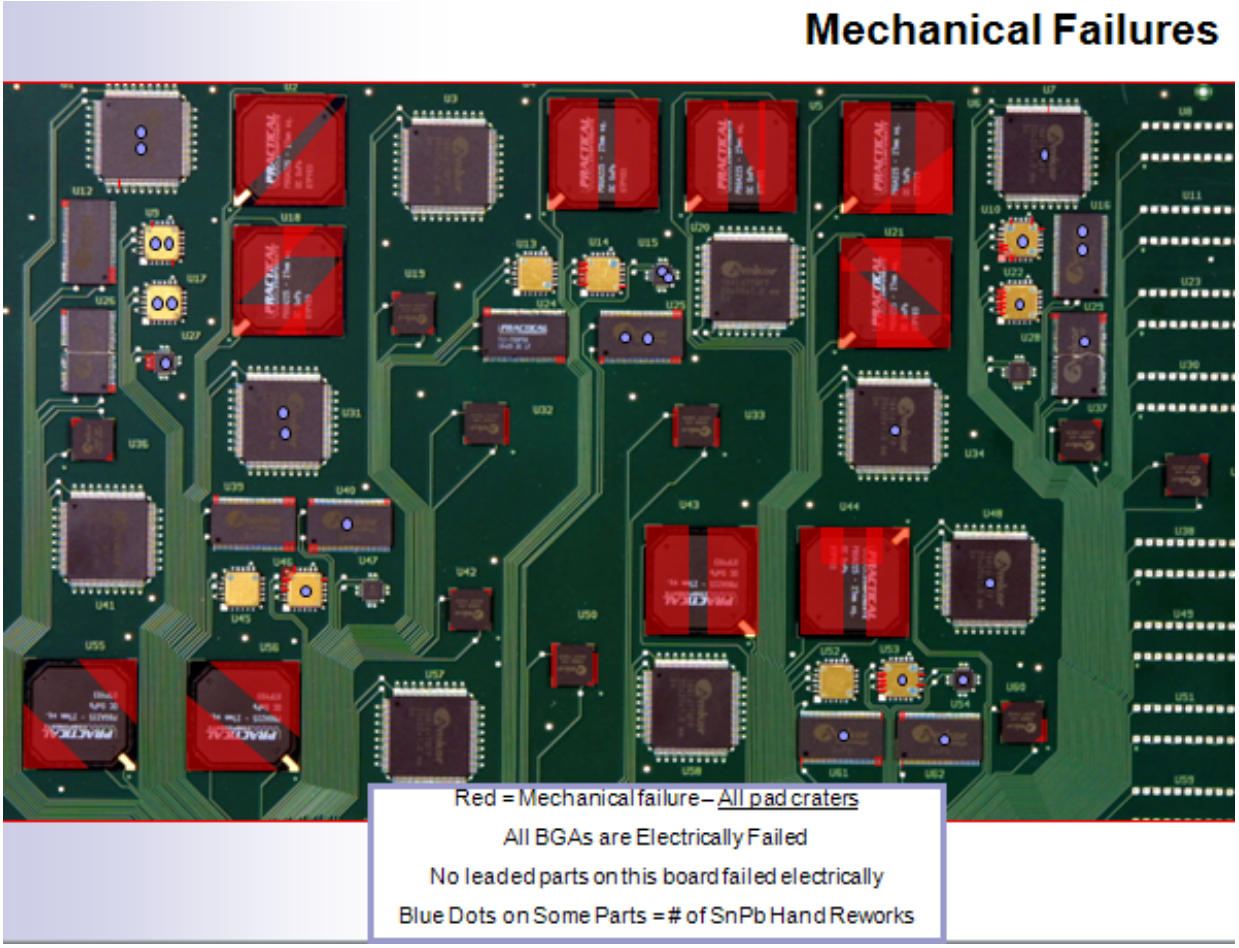

Figure 117 – Mechanical Failure Mapping

5.6.4 NSWC Crane Test Vehicle Drop Testing Results Summary

The complete test report, "Drop Testing Report for Crane; TOL0801002", can be found on the NASA TEERM website (http://teerm.nasa.gov/NASA_DODLeadFreeElectronics_Proj2.html).

Although there were duplicates of each component type on the test vehicle, every component experienced a unique strain/strain rate condition due to its particular location on the board. As a result each sample depicts a unique data point and these cannot be easily lumped together.

After drop testing only three of the leaded components had electrical failures:

- SN 85, TQFP 144, U57; reworked once
- SN 85, PDIP-20, U8; reworked once
- SN 84, CLCC-20, U14; not reworked

One of the quad flat no leads (QFN-20) components had an electrical failure after drop testing:

- SN 86, QFN-20, U15; reworked twice

99 percent (89 out of 90) of the plastic ball grid array (PBGA) components had an electrical failure following drop testing. All of the Pb-free PBGAs (non-reworked) electrically failed by 20 drops at 500G.

Twenty-three leaded components from various cards were selected for failure analysis and subjected to dye & pry testing. None of the components selected for dye & pry testing had electrical failures. Ten out of the 23 components that were selected for dye & pry testing showed signs of mechanical fracture. All except 2 mechanical fractures inspected were in the laminate under the pad; pad cratering. Only two out of the 23 components showed signs of solder joint fractures. Based on the 23 components selected for dye & pry, there is no correlation between the number of reworks and the amount of mechanical damage. This selection of components shows no difference in drop test performance between SnPb and Pb-free solder.

Fifteen components were also selected for cross-sectioning, three of which were electrical failures after drop testing {SN 85, TQFP 144, U57; reworked once, SN 85, PDIP-20, U8; reworked once, SN 84, CLCC-20, U14; not reworked}. Five out of the 15 cross-sectioned joints were found to have some level of mechanical damage, or pad cratering. For two of the electrically failing parts the root cause of the electrical failure was a trace break due to pad cratering. The other part failed due to solder fatigue fracture. The remaining 2 samples had pad cratering which did not sever the copper trace.

5.6.5 NSWC Crane Test Vehicle Drop Test Failure Analysis

After the drop testing was complete, several boards were selected for destructive failure analysis. Both dye-and-pry and cross sectioning were performed, each of which was designed to determine the location, mode and mechanism of the failure. The samples selected for dye-and-pry were examined using an optical microscope after the parts were pried from the board and the results were further mapped. The cross sectioned samples were examined using optical and scanning electron microscopy (SEM) as well as analyzed by energy dispersive x-ray (EDX). The focus was to compare the quality of the solder joints of components that were reworked once using SnPb solder (therefore consisting of a mixed metallurgy of Pb and Pb-free solder), those that were reworked twice using SnPb solder (consisting of leaded solder), and those which were not reworked at all- therefore Pb-free. Only non-BGA components are described in detail in this project.

Pad cratering was the predominant failure mechanism in all components, as observed through both dye-and-pry and cross sectioning; Figure 118. In two cases the pad cratering was significant enough to break the trace and cause an electrical failure. However in most cases the trace remained intact and therefore no electrical failure was detected.

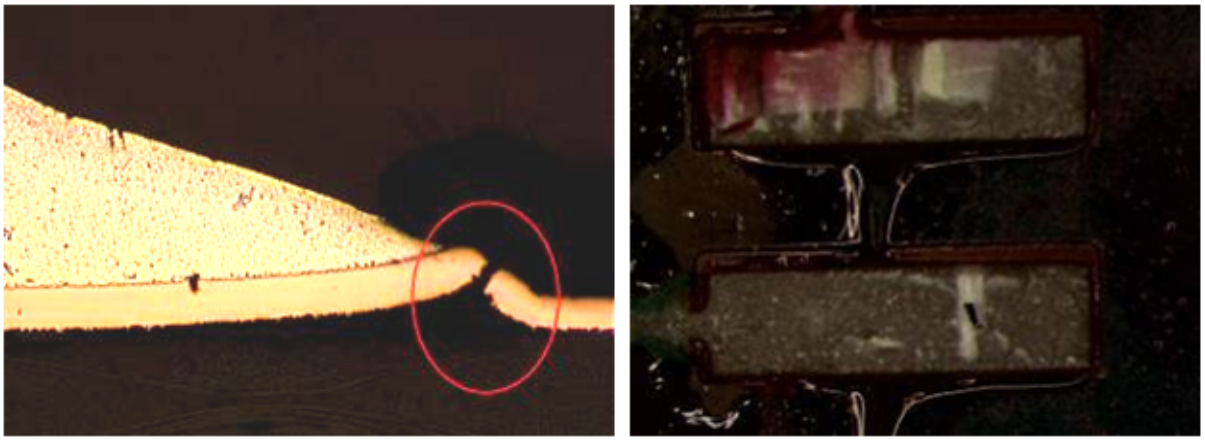

Cross-sectioning *Dye and pry*

Figure 118 - Pad Cratering seen on CLCC-20

A small number of the analyzed solder joints had signs of solder fracture; however only in one case did this lead to an electrical failure; Figure 119. This indicates that, for the most part, the solder fractures did not penetrate through the entire solder joint.

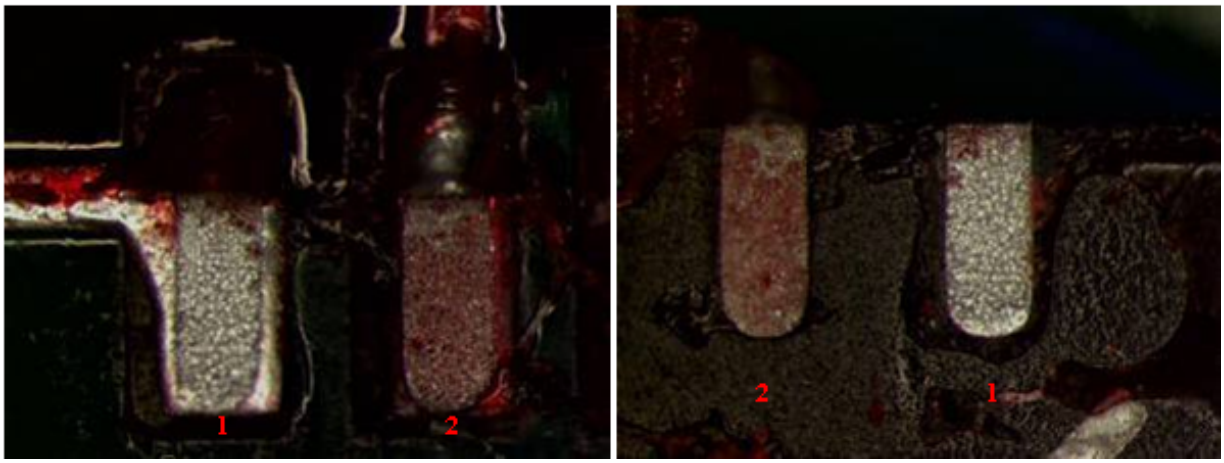

Board side *Component side*

Figure 119 - Dye and Pry of a QFN-20 showing dye penetration through the bulk solder

Pad cratering occurred in all package types (CLCC-20, QFN-20, TQFP-144, TSOP-50) but was less prevalent in the TQFP-144 in which pad cratering was observed on only one out of nine dye-and-pry samples. This is likely due to the structure of the part which has compliant copper leads on all four sides, ensuring efficient stress distribution. However, in one part, the interconnect failure was through the bulk solder in a fatigue failure mode; Figure 120.

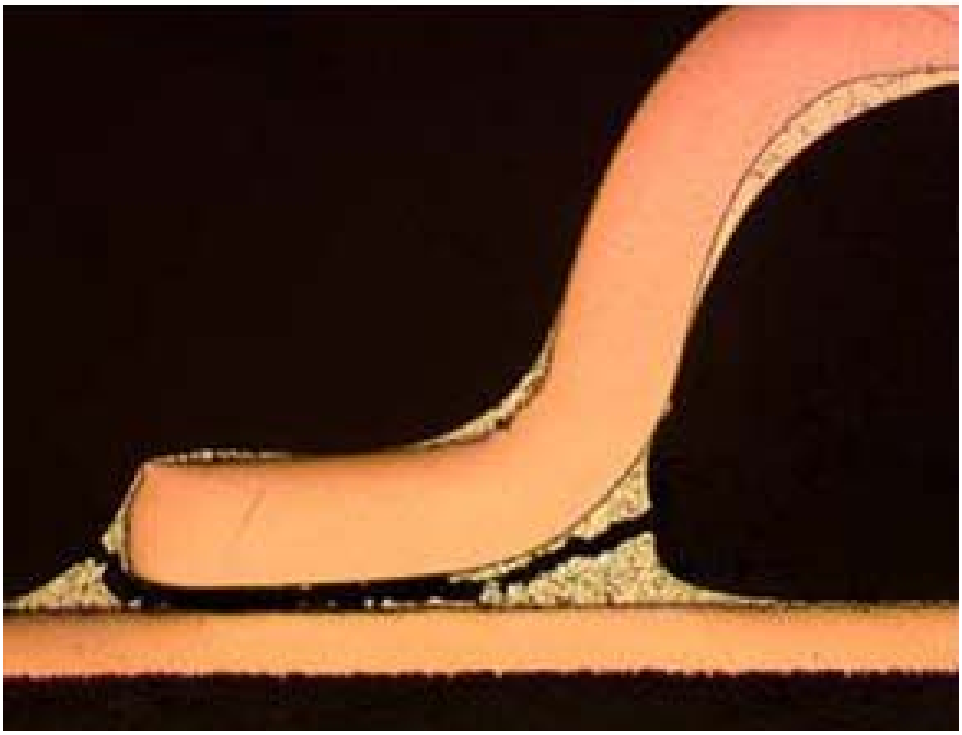

Figure 120 – Fatigue Failure of TQFP-144 with 1x Rework as seen through cross sectioning

6 Summary Tables

7 Conclusions

7.1 Assembly Conclusions

7.2 Reliability Conclusions

7.3 PDIP Discussion

8 Recommendations